/
Article / Book Information

( )	FePt/AlN
Title(English)	Magnetic Anisotropy Transition in FePt/AlN Layered Structure
( )	,,,,
Author(English)	Cong Zhang,Sannomiya, T.,Muraishi, S.,Shi, J.,YOSHIO NAKAMURA
( )	: ( ), : , : 9426 , :2014 3 26 , : , : , , , ,
Citation(English)	Degree:Doctor (Engineering), Conferring organization: Tokyo Institute of Technology, Report number: 9426 , Conferred date:2014/3/26, Degree Type:Course doctor, Examiner:,,,,
( )	
Type(English)	Doctoral Thesis

Magnetic Anisotropy Transition in FePt/AlN Layered Structure

Cong Zhang

Directed by: Professor Ji Shi

Professor Yoshio Nakamura

Department of Metallurgy and Ceramics Science

Tokyo Institute of Technology

December, 2013

Abstract

Hard disk drives (HDDs) is currently the dominant digital data storage device and are expected to remain this position due to predicted continuing advantages in recording capacity and price of per storage unit, comparing to solid-state drives (SSDs). Among magnetic recording technologies for HDDs, perpendicular magnetic recording is considered to be advantageous for overcoming superparamagnetic limitation and achieving high areal recording density. Therefore, recording media with perpendicular magnetic anisotropy have attracted much research interest in the past decades. For example, metallic layered structures (such as Co/Pt, Co/Pd) and $L1_0$-FePt/CoPt alloy films have been intensively studied as promising materials for ultrahigh density magnetic recording.

In this work, magnetic anisotropy of metal/ceramic-FePt/AlN layered structures has been systematically studied. By using nitride layer, the interface diffusion which often occurs in metallic layered structure can be effectively avoided. It is found that FePt/AlN layered structure shows unconventional magnetic anisotropy transition after thermal annealing comparing to the well-studied metallic layered structures. The interface anisotropy and magnetoelastic effect introduced by layered structure are also unique in the past studies of FePt alloy. Microstructures, residual stress and interface quality are investigated to disclose the origin of perpendicular magnetic anisotropy in FePt/AlN layered structure and the mechanism of magnetic anisotropy transition.

Contents

Chapter 1 Introduction

The origin of and the possibility to control magnetic anisotropy have been a hot issue for a long time.[1–3] Especially, the perpendicular magnetic anisotropy (PMA) has drawn much research interest for its application in hard disk drives (HDDs). Firstly introduced by IBM in 1956, HDDs became the dominant digital data storage device since the early 1960s and are expected to remain this position for general purpose computers due to predicted continuing advantages in recording capacity and price of per storage unit, comparing to solid-state drives (SSDs).[4-6] Among magnetic recording technologies for HDDs, perpendicular magnetic recording is considered as a promising technology to realize these advantages on account of high magnetization stability which can overcome the thermal effects appearing as increases areal recording density.[7] So as a core element of such technology, perpendicular recording media with PMA have been extensively studied in the past decades.[8-10] The study of candidate for future perpendicular recording media will accelerate the evolution of HDDs.

In this chapter, a summary on the fundamental of magnetic anisotropy and magnetic recording technology will be shown firstly. Then the objectives and organization of this thesis will be given.

1.1 Magnetic anisotropy

The directional dependence of a material's magnetic properties is called magnetic anisotropy. Simply speaking, there are easy and hard axes for magnetization in a magnetically anisotropic material. An easy axis is an energetically favorable direction of spontaneous magnetization and hard axis means the energies required to magnetize will be maximum along that direction. The two opposite directions along an easy axis

are usually equivalent, and the actual direction of magnetization can be along either of them. Basing on the number of easy and hard axes, magnetic anisotropy can be called as uniaxial anisotropy, triaxial anisotropy and cubic anisotropy. There is only one easy axis in uniaxial anisotropic material. For triaxial anisotropy, there is a single easy axis, but it also has a hard axis and an intermediate axis. The magnetic materials with cubic anisotropy have three or four easy axes. The magnetic anisotropy mainly refers to uniaxial anisotropy in this thesis.

The magnetic anisotropy is one of the most important properties of magnetic materials and has different kinds of applications. For example, materials with high, medium and low magnetic anisotropy can be applied to permanent magnets, information storage media and magnetic recording heads respectively.[11]

For thin film materials, if the easy direction of the magnetization is perpendicular to the plane, we can call this perpendicular magnetic anisotropy (PMA). The PMA is currently of great research interest for its important applications in magnetic random access memory (MRAM),[12] and especially in high density magnetic recording technology for HDDs.

1.2 Perpendicular magnetic anisotropy for magnetic recording

Nowadays, huge amount of data is stored in commercial data storage devices. Storage devices can be classified into different types depending on data storage method. For popular ones, there are optical storage devices (CDs, DVDs), semiconductor storage devices (flash memories and SD cards), magnetic-optical storage devices (MO disks) and magnetic storage devices (such as magnetic tapes and HDDs). Among them, HDDs are the dominant storage device for general purpose computers due to the large capacity and low cost.

When invented by IBM in 1957, the areal density of first HDD was only 2 Kb/in^2.

Then HDDs were undergoing a rapid development, and the areal density had reached 200 Gb/in^2 by 2004, about one million times larger.[5] However, accompanying the increasing of areal density, the traditional magnetic recording method, which can be called as longitudinal recording, is facing a serious problem, the thermal effects. The energy required to reverse the magnetization of a magnetic particle can be expressed as $K=K_u V$,[13] where K_u is the uniaxial (effective) anisotropy energy and V is the volume of magnetic particle. So if the size of magnetic particle is too small, the magnetization can be reversed by local thermal fluctuations and the data stored will be lost. Therefore, the thermal effects seriously restrict the raise of areal density. To solve this problem, the perpendicular magnetic recording was proposed by Iwasaki and Takemura in 1975.[14]

Figure 1-1 shows the schematic diagram of the longitudinal recording and perpendicular recording. As seen in this figure, the perpendicular magnetic recording magnetizes the magnetic elements perpendicularly to the surface of disk plane. By this way, the volume of magnetic elements can be maintained by increasing vertical size while decreasing the in-plane size to increase areal density. Since the magnetization is aligned perpendicularly to disk surface, perpendicular magnetic anisotropy is necessary for recording media. After thirty years for exploring suitable recording media, the first commercial HDD was presented by TOSHIBA in 2005. By august 2010, HDDs with areal density of 667 Gb/in^2 were available commercially, and the density is predicted to continue to grow.[15] It is reasonable to consider the needs of HDDs using perpendicular recording technology will go up in future, so the study of perpendicular recording media with PMA is of great significance.

1.3 Sources of magnetic anisotropy

Strong perpendicular magnetic anisotropy is the key point of perpendicular

recording media. It is necessary to know the various sources of magnetic anisotropy for designing new media for perpendicular recording. Basing on the different dependences of magnetic properties, there are several different types of anisotropy which can be called as magnetocrystalline anisotropy, shape anisotropy and magnetoelastic anisotropy. The descriptions of each type of anisotropy will be given in the following.

1.3.1 Magnetocrystalline anisotropy

Dependence on the orientation of the magnetization relative to the crystalline axes is called magnetocrystalline anisotropy. For a simple example, magnetization curves for magnetite are shown in figure 1-2.[16] It can be seen that the curves are different when measuring along different crystal directions. For magnetite, above 130 K, <111> is the easy direction of magnetization and <100> is the hard direction of magnetization.

The magnetocrystalline anisotropy mainly originates from spin–orbit interaction. In a magnetic material, the spins are coupled via the spin–orbit interaction to the orbits which are influenced by the crystal lattice. In principle, also the dipolar interaction could contribute to the magnetocrystalline anisotropy. However, for cubic crystals the sum of the dipole–dipole energy will be zero due to the special symmetry and the contribution can be neglected.[17]

For thin film materials, especially the layered structures (multilayers), the atoms located at surface or interface could show very different magnetocrystalline anisotropy from that of the bulk atoms due to the reduced symmetry. Such anisotropy is called as surface (interface) anisotropy and firstly predicted by N´eel for cubic ferromagnetic crystals in 1954.[18] This interface anisotropy is one of the most important origin of PMA for the layered structures and will be discussed more detailedly in subsequent chapters.

1.3.2 Shape anisotropy

The shape effect on material's magnetic properties is shape (magnetic dipolar) anisotropy. It originates from the long range magnetic dipolar interaction. A magnetized matter will produce magnetic charges or poles at the surface. This surface charges distribute non-uniformly depending on the shape of matter and result in another magnetic field which acts in opposition to the magnetization that produces it, called the demagnetizing field. For example, for matters with elliptic shape, the demagnetizing field will be smaller if the magnetization is along the long axis than that when along the short axis, due to the different distributions of surface charges. This brings about an easy axis of magnetization along the long axis.[19]

For thin films, the strong demagnetizing fields are usually responsible for the commonly observed in-plane anisotropy.

1.3.3 Magnetoelastic (Stress) anisotropy

Before explaining the magnetoelastic anisotropy, I would like to introduce the magnetostriction. Magnetostriction is a phenomenon of ferromagnetic materials that the sample dimensions change during the process of magnetization. This effect is also related to spin-orbit coupling. Upon magnetization, demagnetized crystal will experience a strain that can be measured as a function of applied field along the principal crystallographic axes.[20]

Magnetoelastic is the 'inverse' of magnetostriction. Strain in a ferromagnet can also change the magnetocrystalline anisotropy and may thereby alter the direction of the magnetization. In another word, a uniaxial stress can produce a unique easy axis of magnetization if the stress is sufficient to overcome all other anisotropies.

For layered structures, residual stresses often occur in magnetic layers due to the existences of interface. So the influences from magnetoelastic anisotropy are also significant.

1.4 Thin film recording media for perpendicular recording

Perpendicular recording requires the recording media to have perpendicular magnetic anisotropy, i.e., the easy-magnetization axis is perpendicular to the film plane. According to the equation $K=K_uV$, for a given K which maintains the magnetization stable, the larger the (effective) anisotropy energy K_u is, more further the volume of magnetic grain can be decreased to improve the areal recording density. Therefore large anisotropy energy is required for recording media materials. To pursue such perpendicular recording media, magnetocrystalline anisotropy, magnetoelastic anisotropy and interface anisotropy as introduced above are used to obtain strong PMA. On the other hand, from the applied perspective, the magnetic grains must be isolated by the non-magnetic surroundings to decouple the magnetic grains. In the following, perpendicular recording media popular for now, either applied as the media of commercial HDDs or intensively studied as the candidates for future media, will be introduced.

1.4.1 CoCrPt-SiO$_2$ granular film

Co-Cr alloy has been selected as longitudinal recording media for HDDs since 1980s, due to the high magnetocrystalline anisotropy and the property of magnetically induced phase separation. Then the alloy system extended to the Co-Cr-Pt and Co-Cr-Ta alloys in the 1990s.[21] In 2002, Oikawa added SiO$_2$ to Co-Cr-Pt alloy for perpendicular recording media. The additive of SiO$_2$ formed good amorphous-like boundaries at ambient temperature and enhanced the grain isolation and the CoCrPt was in hexagonal closed packed structure with easy-magnetization direction perpendicular to the film plane.[22] Now the CoCrPt-SiO$_2$ granular media have been widely used in the commercial perpendicular recording HDDs.

1.4.2 Co/metal layered structure

Layered structures or multilayers are periodic stackings of a layer A on a different layer of material B. With few exceptions, these layers are polycrystalline and highly textured along the growth direction. Because of differences in the lattice constant between the two different materials, large strains can develop within individual layers. Also, since the layers of these layered structures are very thin (below 100 Å), the density of interfaces or the ratio of interfacial atoms along the film thickness direction is high. If one layer is magnetic material, then such layered structures can be characterized by the common sources of magnetic anisotropy as introduced above, i.e., magnetocrystalline anisotropy, magnetoelastic anisotropy and interface anisotropy. Therefore, magnetic layered structure should be a vehicle for tailoring perpendicular magnetic anisotropy.[23] Carcia *et al* firstly reported PMA for layered structure in Co/Pd system and attributed it to the interface anisotropy which was predicted by Néel for thin film materials.[24] Later, PMA was also been found in other metal/metal LS, such as Co/Pt, Co/Au, Co/Ru.[25-27]

1.4.3 $L1_0$ FePt and CoPt granular film

Face centered tetragonal ($L1_0$ phase) FePt and CoPt alloys have been extensively studied as future high density recording media due to the high uniaxial magnetocrystalline anisotropy along c-axis. To separate the recording elements, much work has been done on CoPt and FePt granular films with various non-magnetic matrices such as Al_2O_3, B_2O_3, BN.[28-30] However, there still remain problems for practical application. One is the high ordering transformation temperature and the other is that, it is difficult to magnetize such material by the current magnetic head because of the large coercivity. To decrease the ordering temperature, a method of alloying with Ag, B and Pb was proposed.[31-33] On the other hand, to solve the writing problem, a new recording technology called heat assisted magnetic recording is also

found to be effective.[34]

1.5 Objectives of this work

In the search for candidate recording media, layered structure (or multilayered) thin films have drawn much research interest because that, owing to the abundance of interfaces, the anisotropy could be dominated by the interface anisotropy which was firstly predicted by N´eel. For experiments on layered structures, PMA was first observed in the metallic layered structure Co/Pd system in 1985 and then in several other Co-based layered structures: Co/Pt, Co/Au, Co/Ru and Co/Ir.[35] The PMA was attributed to interface anisotropy due to the broken crystal symmetry at interface as introduced above. Later, subsequent research found that the magnetoelastic anisotropy, originates from stresses stored in magnetic layer owing to the lattice mismatch at the interface, can also contribute to PMA for such metallic layered structures.[36-37] However, the problem is that, interfacial diffusion or mixing often occurs between two different metallic layers. This will strongly depress the PMA.

In contrary to the well-studied metallic layered structures, the metal/ceramic layered structure has been seldom studied as recording media. In fact, the metal/ceramics interface is expect to show better thermal stability than the metal/metal layered structures, especially when annealing at high temperatures. Furthermore, the large interface mismatch between metal and ceramic would also introduce comparatively high strain/stress in the relatively soft metal layer and thus induce strong magnetoelastic anisotropy. In 2007, our group firstly reported PMA in metal/ceramics-CoPt/AlN layered structures.[38] The magnetic anisotropy of the films changed from in-plane direction to the direction perpendicular to the film plane after annealing. In subsequent works, the internal stresses were quantificationally studied.[39] It was found that the stresses in CoPt layers undergone a transition from

compressive to tensile as annealing temperature increased. Since the CoPt alloy has a negative magnetostriction constant, such stress transition will introduce positive magnetoelastic anisotropy which favors the perpendicular magnetization. On the other hand, the CoPt/AlN interface quality was found to be improved through annealing. This can also enhance the interface anisotropy. Therefore, we cannot determine the main origin of the PMA in CoPt/AlN layered structures from interface anisotropy and magnetoelastic anisotropy.

To solve this problem, the study of FePt/AlN layered structures is proposed. Because the FePt alloy has positive magnetostriction constant, the contributions from interface anisotropy and magnetoelastic anisotropy are expected to be separated. Moreover, $L1_0$-FePt alloy films, which possess large uniaxial magnetocrystalline anisotropy energy, have been considered as a promising material for ultrahigh density magnetic recording. Recently, much work has been devoted to lowering the ordering temperature of FePt alloy, or finding new ways to promote ordering transformation, such as electromigration induction.[40, 41] However, there has been little work concerning the magnetoelastic effect and interface anisotropy of FePt films. Therefore, the study on the magnetic behavior of FePt/AlN layered structures is of great significance for the research of both metal/ceramics layered structures and FePt alloy.

The objectives of this study are as follows:

(1) To systematically study the magnetic behavior of FePt/AlN layered structures, finding out the influencing factors on the magnetic anisotropy.

(2) To investigate the origin of perpendicular magnetic anisotropy in FePt/AlN layered structures and disclose the mechanism of magnetic anisotropy transition in the layered structures.

1.6 Organization of this thesis

Chapter 1 Introduction: The background, objectives of this study are given. For better understanding, the fundamental of magnetic anisotropy, magnetic recording and perpendicular recording media are introduced.

Chapter 2 Preparation and characterization of FePt/AlN layered structure: The experimental methods of layered structure preparation, microstructure characterization and magnetic property measurement are introduced. Some typical structural results and magnetic properties of FePt/AlN layered structure are also given.

Chapter 3 Magnetic properties of FePt/AlN layered structure: Detail experimental results on the magnetic properties of FePt/AlN layered structures with different annealing temperatures and FePt layer thicknesses are given. The layered structure shows unconventional magnetic anisotropy transition after thermal annealing and perpendicular magnetic anisotropy is realized.

Chapter 4 Mechanism of magnetic anisotropy transition in FePt/AlN layered structure: The origin of the perpendicular magnetic anisotropy and the mechanisms of magnetic anisotropy transition in FePt/AlN layered structure are investigated. The effects of annealing temperature and FePt layer thickness on magnetic anisotropy are studied through residual stress and interface quality analyses.

Chapter 5 Influence of AlN layer thickness on the magnetic anisotropy of FePt/AlN layered structure: The results on the magnetic properties of FePt/AlN layered structures with different AlN layer thicknesses are shown. It is found that the perpendicular magnetic anisotropy of FePt/AlN layered structure can be further enhanced by decreasing the AlN layer thickness. The enhancement in perpendicular magnetic anisotropy is explained by the influencing mechanism discussed in chapter

4.

Chapter 6 Conclusions: The general conclusions of this study are given.

Reference

1. Ch. Kittel, Phys. Rev. 73, 155 (1948).

2. D. Weller, J. Stöhr, R. Nakajima, A. Carl, M. G. Samant, C. Chappert, R. Megy, P. Beauvillain, P. Veillet, and G. A. Held, Phys. Rev. Lett. 75, 3752 (1995).

3. G. Laan, J. Phys.: Condens. Matter 10, 3239 (1998).

4. Y. Nakamura, Magune, 1, (5), 190-196 (2006).

5. G. W. Qin, Y. P. Ren, N. Xiao, B. Yang, L. Zuo, and K. Oikawa, Int. Mater. Rev. 54, 157 (2009).

6. C. D. Mee and E. D. Daniel, Magnetic Storage Handbook (2nd Edition), McGraw-Hill Professional (1990).

7. S. Khizroev, M. Kryder, Y. Ikeda, K. Rubin, P. Arnett, M. Best, D. A. Thompson, IEEE Trans. Magn. 35 (5), 2544-6 (1999).

8. J. P. J. Groenland, C. J. M. Egkel, J. H. J. Flultman, and R. M. de Ridder, Sens. Actuators, A 30, 89 (1992).

9. D. J. Monsma, J. C. Lodder, Th. J. A. Popma, and B. Dieny, Phys. Rev. Lett. 74, 5260 (1995).

10. S. A. Wolf, D. D. Awschalom, R. A. Buhrman, J. M. Daughton, S. Von Molnar, M. L. Rouker, A. Y. Chtchelkanova, and D. M. Treger, Science 294, 1488 (2001).

11. M. T. Johnson, P. J. H. Bloemen, F. J. A. den Broeder, J. J. de Vries, Rep. Prog. Phys. 59, 1409 (1996).

12. R. Sbiaa, H. Meng, and S. N. Piramanayagam, P hys. Status Solidi RRL 5 (12), 413–9 (2011).

13. D. Weller and A. Moser, IEEE Trans. Magn. 35, 4423 (1999).

14. S. Iwasaki and Y. Nakamura, IEEE Transactions on Magnetics 13, 1272-1277 (1977).

15. J. H. Judy, Journal of Magnetism and Magnetic Materials 287, 16-26 (2005).

16. S. K. Banerjee and B. M. Moskowitz, Ferrimagnetic properties of magnetite, in Magnetite Biomineralization and Magnetoreception in Organisms: A New Magnetism, 17-41, Plenum Publishing Corporation (1985).

17. G. H. O. Daalderop, P. J. Kelly and, M. F. H. Schuurmans, Phys. Rev. B 41 (11), 919–37 (1990).

18. L. Néel, J. Phys. Radium 15, 225 (1954).

19. B. D. Cullity, Introduction to Magnetic Minerals, Addison-Wesley, Reading Massachusetts (1972).

20. W. O'Reilly, Rock and Mineral Magnetism, Blackie, Glasgow (1984).

21. D. Weller and M. F. Doerner, Annu. Rev. Mater. Sci. 30, 611-44 (2000).

22. T. Oikawa, M. Nakamura, H. Uwazumi, T. Shimatsu, H. Muraoka, and Y. Nakamura, IEEE

23. S. Iwasaki, K. Ouchi, and N. Honda, IEEE Trans. Magn. MAG-14, 849(1978).

24. P. F. Carcia, A. D. Meinhaldt, A. Suna, Appl. Phys. Lett. 47, 178 (1985).

25. P. F. Carcia, J. Appl. Phys. 63, 5066 (1988).

26. M. Sakurai, T. Takahata, I. Moritani, J. Magn. Soc. Japan. 15, 411 (1991).

27. F. J. A. den Broeder, D. Kuiper, A. P. van de Mosselaer, W. Hoving, Phys. Rev. Lett. 60, 2769 (1988).

28. J. Bai, Z. Yang, F. Wei, M. Matsumoto, A. Morisako. Journal of Magnetism and Magnetic Materials 257, 132-7(2003).

29. M. L. Yan, H. Zeng, N. Powers, D. J. Sellmyer. Journal of Applied Physics 91, 8471-3 (2002).

30. M. Daniil, P. A. Farber, H. Okumura, G. C. Hadjipanayis, D. Weller. Journal of Magnetism and Magnetic Materials 246, 297-302 (2002).

31. C. Chen, O. Kitakami, S. Okamoto and, Y. Shimada, Appl. Phys. Lett. 76, 3218 (2000).

32. H. Yamaguchi, O. Kitakami, S. Okamoto, and Y. Shimada, Appl. Phys. Lett. 79, 2001 (2001).

33. O. Kitakami, T. Shimada, K. Oikawa, H. Daimon, and K. Fukamichi, Appl. Phys. Lett. 78, 1104 (2001).

34. 青井　基　他, 応用磁気学会第144回研究会資料, 55-62 (2005).

35. F. J. A. den Broeder, W. Hoving, and P. J. H. Bloemen, J. Magn. Magn. Mater. 93, 562–70(1991).

36. C. Chappert, P. Bruno, J. Appl. Phys. 64, 5736 (1988).

37. C. H. Lee, H. He, F. J. Lamelas, W. Vavra, C. Uher, R. Clarke, Phys. Rev. B 42, 1066 (1990).

38. Y. Hodumi, J. Shi, Y. Nakamura, Appl. Phys. Lett. 90, 212506 (2007).

39. Y. X. Yu, J. Shi, Y. Nakamura, J. Appl. Phys. 108, 023912 (2010).

40. C. Feng, Q. Zhan, B. Li, J. Teng, M. Li, Y. Jiang, and G. Yu, Appl. Phys. Lett. 93, 152513(2008).

41. C. Feng, X. Li, M. Yang, K. Gong, Y. Zhu, Q. Zhan, L. Sun, B. Li, Y. Jiang, and G. Yu, Appl. Phys. Lett. 102, 022411(2013).

Magnetic head

Disk plane

Longitudinal recording

Data are recorded longitudinally.

Disk plane

Magnetic head

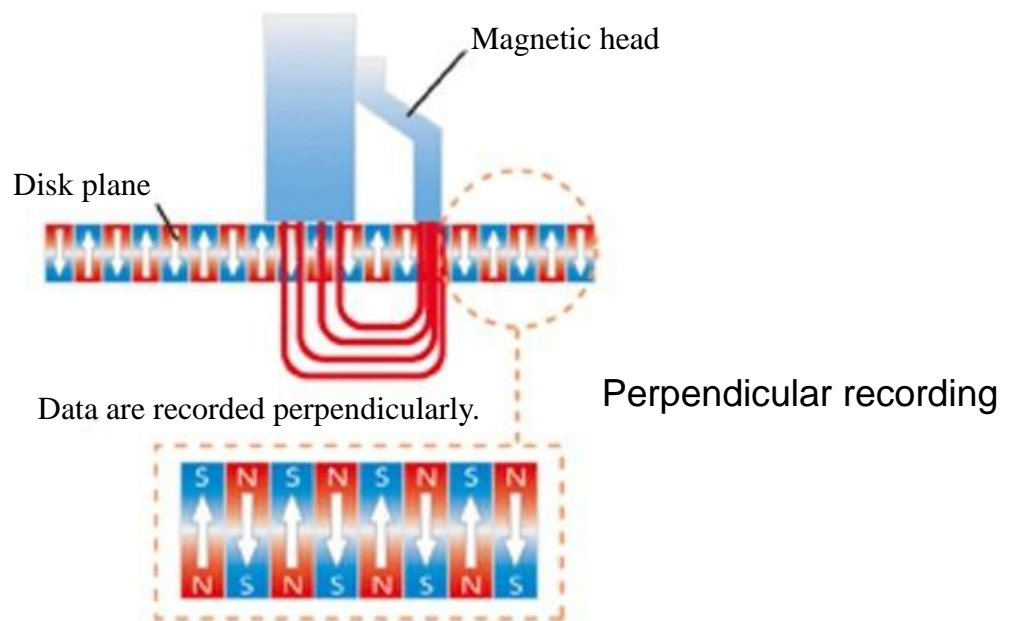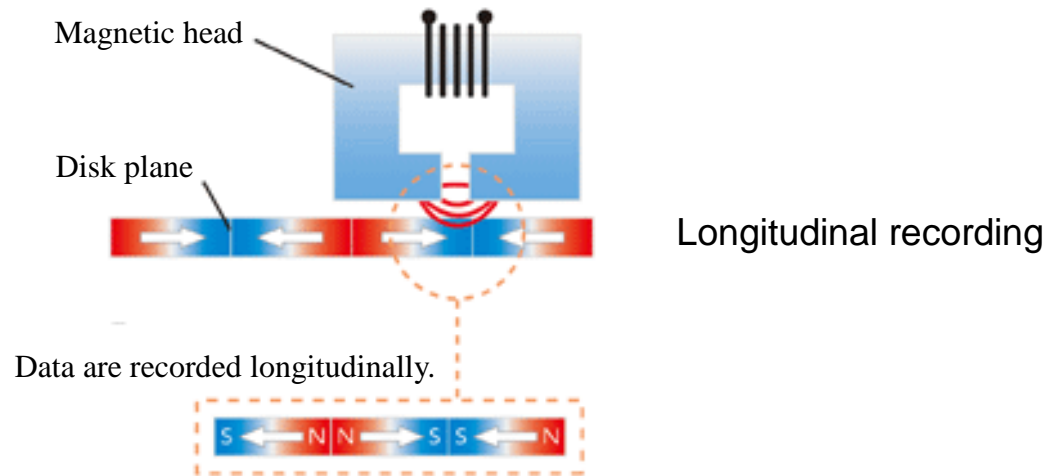Data are recorded perpendicularly.

Perpendicular recording

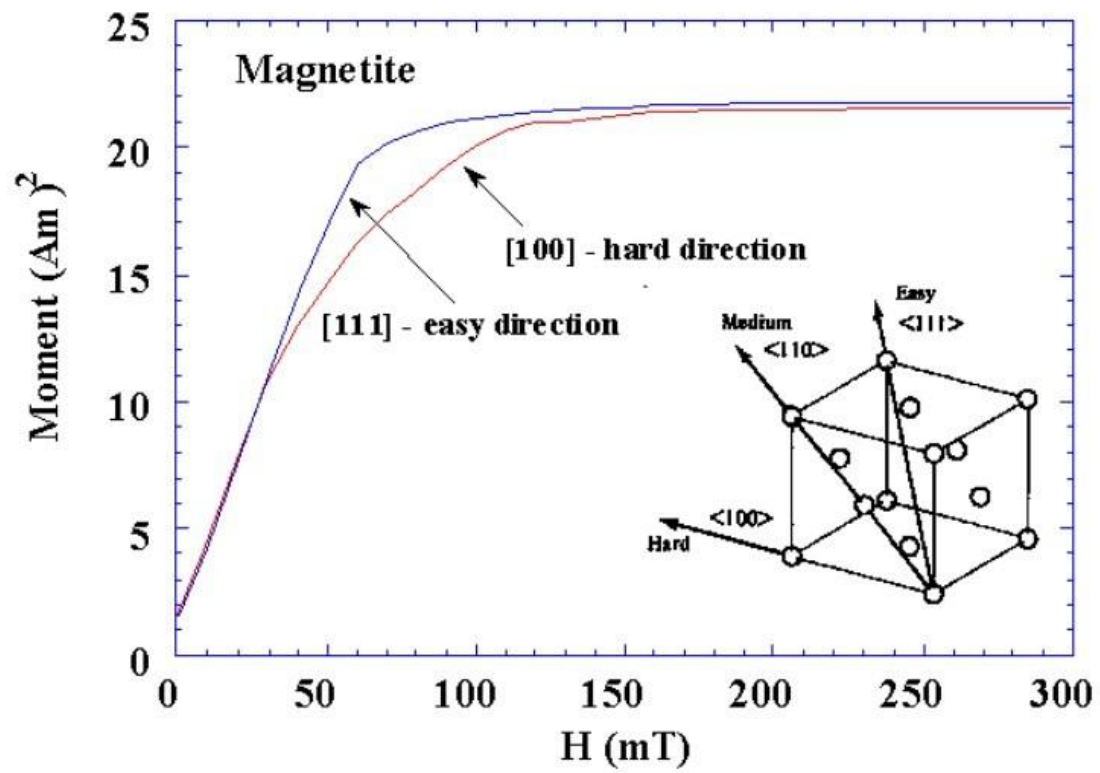Figure 1-1 Schematic diagrams of the longitudinal recording and perpendicular recording.

Figure 1-2 Magnetization curves of magnetite.

Chapter 2 Preparation and characterization of FePt/AlN layered structures

This chapter presents the experimental techniques employed to fabricate and characterize FePt/AlN layered structures in this study. DC magnetron sputtering was applied for sample preparation by using a facing target sputtering system. Structural properties of the layered structures were investigated by x-ray diffraction (XRD), x-ray reflectivity (XRR) and transmission electron microscopy (TEM). Magnetic behaviour of the samples was assessed by the vibrating sample magnetometer (VSM). Moreover, a series of typical results are also shown in this chapter.

2.1 Sample preparation

2.1.1 DC magnetron sputtering

Sputter deposition has a high degree of significance in thin film science as well as in industry. A wide range of materials can be sputter deposited, including high purity metallic films, metallic oxides, nitrides and carbides. The thickness of films so prepared can range from approximately 1 nm to several microns, and the film properties are highly reproducible. The major problems associated with the conventional sputtering technique are the low deposition rates and the poor film microstructures. A high sputtering gas pressure of ~10 Pa is typically used, otherwise the plasma formation process cannot be self-sustained. A great advance in the field of sputtering came with the introduction of the magnetron sputtering. The trajectories of electrons in the plasma can be diverted in the presence of a magnetic field, leading to a certain degree of confinement of electrons around the target surface. This effectively increases the chance of ionization of the working gas, permitting a larger deposition rate by working at a lower sputtering gas pressure. Plasma stabilization can be

realized with a working gas pressure as low as tenths of Pa to improve film crystallinity, which is impossible for conventional sputtering set-ups.[1]

In this study, the FePt/AlN layered structures were fabricated by a dual facing target DC magnetron sputtering systems. Figure 2-1 shows the schematic diagram of the apparatus. As the diagram shows, the apparatus equips with two pairs of facing targets. One pair is consisted of two Fe-Pt targets (a Fe plate with diameter of 100mm and a 50 diameter Pt plate inserted in the middle of Fe plate compose one target, and the atomic ratio of Fe to Pt for deposited films can be adjusted by adding extra small Pt plate on the Fe plate), and two Al targets form another pair. Before deposition, the sputtering chamber is pumped to a high vacuum below 5×10^{-5} Pa, by a vacuum system consisted of a rotary pump and a turbomolecular pump, to obtain high quality film. Argon and nitrogen gases are imported into the sputtering chamber as working gases by two independent gas lines, and the Ar/N_2 flow ratio can be easily controlled by the flowmeters. Thus AlN layers of wurtzite structure can be deposited by reactive sputtering at Al target side and FePt layers of FCC structure are deposited at the other side. During sputtering, the sample holder is rotated to each target side to from the FePt/AlN layered structure on the quartz glass substrate. The rotation of the sample holder is performed by a programmable motor, so the deposition time can be precisely controlled through a computer.

2.1.2 Vacuum annealing

The as-deposited FePt/AlN films are annealed in a tube furnace equipped with a vacuum system which is consisted of rotary pump and a turbomolecular pump. High vacuum (10^{-5} Pa) is achieved to avoid oxidation during annealing process. Annealing temperature is real-time monitored by thermocouple and controlled by an automatic temperature control system.

2.2 Structure characterization

For layered structures, the interface analysis is of great important. The cross-sectional transmission electron microscopy (TEM) and X-ray reflectivity (XRR) are quite suitable to investigate the interface. In this section, brief descriptions of TEM, XRR, and also, conventional x-ray diffraction (XRD) will be introduced. Some typical characterization results of FePt/AlN layered structure will also be given.

2.2.1 Transmission electron microscopy

2.2.1.1 Fundamentals of TEM

Transmission electron microscopy (TEM) is a microscopy technique that uses a beam of electrons to transmit through an ultra-thin specimen and obtain the microstructure information from the penetrate electrons. The electrons are emitted by a source and are focused and magnified by a system of magnetic lenses. The electron beam is confined by the two or three condenser lenses which also control the brightness of the beam, passes the condenser aperture and hits the sample surface. The electrons that are elastically scattered consist the transmitted beams, which pass through the objective lens. The objective lens forms the image display, and the following apertures, the objective and selected area aperture, are used to choose of the elastically scattered electrons that will form the image of the microscope. Finally, the beam goes to the magnifying system that is consisted of three lenses, the first and second intermediate lenses which control the magnification of the image and the projector lens. The formed image is shown on an imaging device, such as a fluorescent screen, on a layer of photographic film, or to be detected by a sensor such as a CCD camer.[2]

A conventional TEM generally has two working modes, the image mode and the diffraction mode. Figure 2-2 shows the ray paths of two different modes.

The objective lens forms a diffraction pattern in the back focal plane with electrons scattered by the sample and combines them to generate an image in the image plane. Thus, diffraction pattern and image are simultaneously present in the TEM. Which of them appears in the object plane of the intermediate lens and then are magnified by the projective lens decides the working mode. Switching the location of the object pane of the intermediate lens can be easily achieved by changing the strength of the intermediate lens.[3,4]

2.2.1.2 Observation for FePt/AlN layered strucure

In this study, the TEM observations were performed by a JEOL 3010 transmission electron microscope operating at a voltage of 300kV. The films for TEM observations were deposited on Si (100) wafers with a natural silicon oxide surface layer, which could provide a similar growth-condition with quartz glass substrate. On the other hand, there is a possibility that the layered structure is destroyed after annealing. To confirm the formation of the layered structure, film of AlN (20nm)/[FePt (2nm)/AlN (20nm)]$_5$ annealing at 500°C for 3 hours was prepared and observed.

Figure 2-3 shows the TEM image of the annealed film. It can be clearly observed that the periodic structure of FePt/AlN film is well formed even after annealing. The interfaces between FePt and AlN layers are flat and distinct and the degree of interface diffusion is seemed to be very low. The darkness of the FePt layers is due to the high mass-density of FePt, while the dark areas in the AlN layers are mainly from the diffraction contrast. The amount of dark areas in first AlN layer deposited directly on the substrate is much less than that in later deposited AlN layers. This indicates the crystallinity of AlN layers is improved by depositing on FePt layers, although the AlN grains are very small. Moreover, by comparing with the proportional scale shown in figure, it is seen that the thicknesses of FePt and AlN layers are equivalent to the

design values.

The electron diffraction pattern of the layered structure is shown in Figure 2-4. A FCC FePt (111) diffraction spot which overlaps a wurizite structure AlN (002) spot can be observed. This indicates the FePt layer is (111) textured and the AlN layer is (002) textured, paralleling to film surface.

2.2.2 X-ray diffraction

2.2.2.1 Fundamentals of XRD

X-ray diffraction is a powerful tool for investigating the crystal structure and the morphology of thin films and bulk materials. The method is based on the Bragg condition, i.e. constructive interference of waves scattered at the atomic planes $2d\sin\theta = n\lambda$, where d is the distance between the two adjacent atomic planes, λ is the wavelength of the x-ray and n is an integer. As the characteristic lattice distance is in the range of several Å, X-rays are used as their wavelengths correspond to such a small scale.

$\theta/2\theta$ scan is the most commonly used scan mode for XRD. Figure 2-5 illustrates the specular reflection geometry, which satisfies the condition that the incidence angle θ on the surface of the sample equals the reflection angle at the other side of the film normal. The incident angle is always half the diffraction angle in this scan mode which is therefore called as $\theta/2\theta$ mode. The detector D rotates at twice speed of the sample and the reflected intensity at the angle of 2θ is measured. This arrangement is sensitive only to the atomic planes parallel to the surface of the sample. At large angles ($\theta > 10°$) the resolved distances are in the range of the interatomic spacing, allowing the study of the crystallographic structure of the solids.[5]

For measurements of atomic planes do not parallel to the surface of the sample, $2\theta\text{-}\omega$ scan is commonly used.

2.2.2.2 Results of FePt single layer and FePt/AlN layered structure

Conventional XRD measurements ($\theta/2\theta$ scan) in this study are performed by a Bruker D8 Advance diffractometer with Cu $K\alpha$ irradiation operating at 40kV and 300mA. To investigate the influences of the formation of layered structure, layered structures of AlN (20nm)/[FePt (2nm)/AlN (20nm)]$_5$ and FePt single layer films with a thickness equivalent to the total FePt thickness in the layered structure (10nm) were prepared and measured.

Figure 2-6 shows the XRD profiles of the as-deposited layered structure and single layer film. It can be seen in Figure 2-6 (a) that the FePt single layer film shows poor crystallinity, no obvious diffraction peak can be found. For result of layered structure as shown in Figure 2-6 (b), the FePt layer and AlN layer show preferred orientations of FCC [111] and HCP [001] parallel to the growth direction, which is consistent with TEM observation. What is important is that, comparing to the single layer film, the FePt crystallinity is improved. This means the crystallinity of FePt layer can also be improved by forming the layered structure (or depositing on AlN layers).

Figure 2-7 shows the XRD profiles of the layered structure and single layer film annealed at 500°C for 3 hours. In Figure 2-7 (a), a weak FePt (111) peak are found for single layer film, indicating the crystallinity is improved upon annealing. The intensities of FePt (111) and AlN (002) peaks of the layered structure as shown in Figure 2-7 (b) are also observably increased, confirming the annealing effect on crystallinity. Moreover, for annealed layered structure, satellite peaks appears around the FePt (111) peak due to the modulation of the periodic structure, which implies the interface quality of the FePt/AlN layered structure is enhanced by annealing.

2.2.3 X-ray reflectivity

2.2.3.1 Fundamentals of X-ray reflectivity

The X-ray reflectivity (XRR) measurement is a technique which is used to analyze X-ray reflection intensity curves from grazing incident X-ray beam to determine thin-film parameters including thickness, density, and surface or interface roughness. Simply speaking, if the surface or interface is not perfectly sharp and smooth then the reflected intensity will deviate from that predicted by the law of Fresnel reflectivity. Then the deviations can be analyzed to obtain the surface or interface roughness. The density and film thickness (or period length of layered structure) can also be calculated from the critical angle for total reflection.[6]

The X-rays undergo total reflection when incident on a surface of a material at a very low grazing angle, which is known as the critical angle for total reflection, θ_c. Figure 2-8 shows the X-ray optics for the cases of the incident angles smaller, equal to, and greater than the θ_c. There is an initial drop of the reflection intensity at the critical angle. For layered structure, the period length can be obtained by the equation $2D\sqrt{\sin^2\theta_{im} - \sin^2\theta_c}=m\lambda$, where D is the period length of layered structure and m is an arbitrary integer.[7]

2.2.3.2 Measurement of FePt/AlN layered structure

The x-ray reflectivity measurements in this study are performed by a Bruker D8 Advance diffractometer with Cu $K\alpha$ irradiation operating at 40kV and 300mA.

Figure 2-9 shows the XRR profile of the layered structure of AlN (20nm)/[FePt (2nm)/AlN (20nm)]$_5$ annealing at 500°C for 3 hours. In this figure, bragg peak which is caused by the modulation of the periodic structure can be clearing observed until 10°, indicating good periodicity and interface quality for the layered structure. This result is in good agreement with the TEM observation and XRD measurement. From the bragg peak position and the critical angle for total reflection, the period length is

calculated to be 224.85 Å, which is almost equivalent to the design periodic length 220 Å of the AlN (20nm)/[FePt (2nm)/AlN (20nm)]$_5$ layered structure.

2.3 Magnetic measurement

2.3.1 Determination of the magnetic anisotropy

Hysteresis loop is a closed curve showing the variation of the magnetization of a ferromagnetic material with the external magnetic field producing it, when the magnetization is changed through a complete cycle. A great deal of information can be learned about the magnetic properties of a material by studying its hysteresis loop, such as saturation magnetization (M_s), remanence (M_r), coercivity (H_c) and anisotropy field (H_k). The determination of the magnetic anisotropy (and effective magnetic anisotropy energy) of thin film material is usually performed by measuring the hysteresis loops along the in-plane direction and direction perpendicular to the film surface.[8]

Figure 2-10 shows the typical hysteresis loops of thin film material with perpendicular magnetic anisotropy. It is clear that it is easy to obtain the magnetic saturation along perpendicular direction (which means the easy magnetization direction is along film normal), whereas an external magnetic field that is equivalent to the anisotropy field (H_k) is needed to reach saturation when magnetizing the film along in-plane direction. For such a case, we can say the film show perpendicular magnetic anisotropy, and the effective magnetic anisotropy energy K_{eff} (K_u for materials with uniaxial magnetic anisotropy) is positive and equivalent to the area between the perpendicular and in-plane hysteresis loops. For the opposite situation, i.e., easy axis of magnetization is along in-plane direction and hard axis is along film normal, we say the film show in-plane magnetic anisotropy, and the effective magnetic anisotropy energy K_{eff} is negative and also equivalent to the area between

the two hysteresis loops.

2.3.2 Fundamentals of vibrating sample magnetometer

The hysteresis loop can be obtained by the vibrating sample magnetometer (VSM), which measured the magnetic response of the sample with regards to an external applied field. Developed by Foner about half a century ago,[9, 10] the VSM is a commonly employed technique in the characterization of all kinds of magnetic samples, ranging from thin films to bulk materials, with a sensitivity generally down to the range of μemu. The technique is non-destructive, and no sample preparation is needed in general.

The principle of the measurement is simple. Sample to be examined is placed in the middle of an applied magnetic field, together with a pair of stationary pick-up coils. By vibrating the sample in a uniform field, the sample is set into relative motion with the pick-up coils and signals (in the form of induced e.m.f., according to the Faraday's Law) are generated in the pick-up coils due to the presence of the oscillating magnetic flux from the sample. By calibrating the VSM with a known strength of magnetization, absolute values of magnetic moments in the samples along the field direction can be obtained.

2.3.3 Results of FePt single layer and FePt/AlN layered structure

The hysteresis loops of the FePt/AlN layered structures in this work are measured by a RIKIN BHV-50V vibrating sample magnetometer at room temperature. The measurements are performed along two directions, parallel and perpendicular to the film plane.

Figure 2-11shows the magnetic hysteresis loops of the as-deposited FePt 10nm single layer film and AlN (20nm)/[FePt (2nm)/AlN (20nm)]$_5$ layered structure. In figure 2-11 (a), it is clear that the as-deposited FePt single layer film shows strong in-plane magnetic anisotropy. Although the FePt/AlN layered structure also shows

in-plane anisotropy as shown in figure 2-11 (b), the anisotropy field (H_k) is small comparing to the single layer film, indicating the in-plane anisotropy is weakened by forming the layered structure. This result is opposite to that of CoPt/AlN layered structure, in which the in-plane magnetic anisotropy is enhanced by forming layered structure.[11] Another phenomenon needed to be mentioned is that, the saturation magnetization of the layered structure is lower than that of single layer film. Since the sputtering of the layered structure is carried out with an argon and nitrogen gas mixture, a sort of iron-nitride may formed during the sputtering process, and then influence the magnetic property of the layered structure.

Figure 2-12 shows the hysteresis loops of FePt 10nm single layer film and AlN (20nm)/[FePt (2nm)/AlN (20nm)]$_5$ layered structure annealed at 500°C for 3 hours. In figure 2-12 (a), the annealed FePt single layer film shows enhanced in-plane anisotropy. However, for result of the layered structure as shown in figure 2-12 (b), the easy direction of the magnetization changes from in-plane to perpendicular direction upon annealing, which means PMA is achieved in FePt/AlN layered structure. Moreover, the saturation magnetization of the annealed layered structure is equivalent to that of single layer film. Because the iron-nitride would decompose during annealing, so the influence from nitride can be removed through annealing process.

2.4 Summary

In summary, FePt/AlN layered structures with designed layer thickness were fabricated. Both as-deposited and annealed layered structure show preferred orientations of FePt [111] and AlN [001] parallel to the growth direction. The crystallinity and interface quality are found to be improved upon annealing. For magnetic property, the formation of layered structure can favour the magnetization in

perpendicular direction and the thermal annealing shows very different effects on the single layer film and layered structure. In next chapter, the effect of annealing and FePt layer thickness on magnetic properties of FePt/AlN layered structures will be discussed in detail.

Reference

1. M. Ohring, The materials science of thin films, 101-109, Academic Press (1992).

2. B. Voutou and E. C. Stefanaki, Electron Microscopy: The Basics, Physics of Advanced Materials Winter School (2008).

3. David B. Williams, C. Barry Carter, Transmission Electron Microscopy (2nd Edition), Springer (2009).

4. B. Fultz, James M. Howe, Transmission Electron Microscopy and Diffractometry (3rd Edition), Springer (2008).

5. C. Kittel, Introduction to Solid State Physics (7th Edition), Chichester (1996).

6. V. Holy, J. Kubena, I. Ohlidal, K. Lischka and W. Plotz, Phys. Rev. B 47,15896-15903 (1993).

7. U. Pietsch, V. Holy and T. Baumbach, High-Resolution X-ray Scattering (2nd Edition), Springer (2004).

8. M. T. Johnson, P. J. H. Bloemen, F. J. A. den Broeder, J. J. de Vries, Rep. Prog. Phys. 59, 1409 (1996).

9. S. Foner, IEEE Trans. Magn. 17, 3358-3363 (1981).

10. S. Foner, J. Appl. Phys. 79, 4740-4745 (1996).

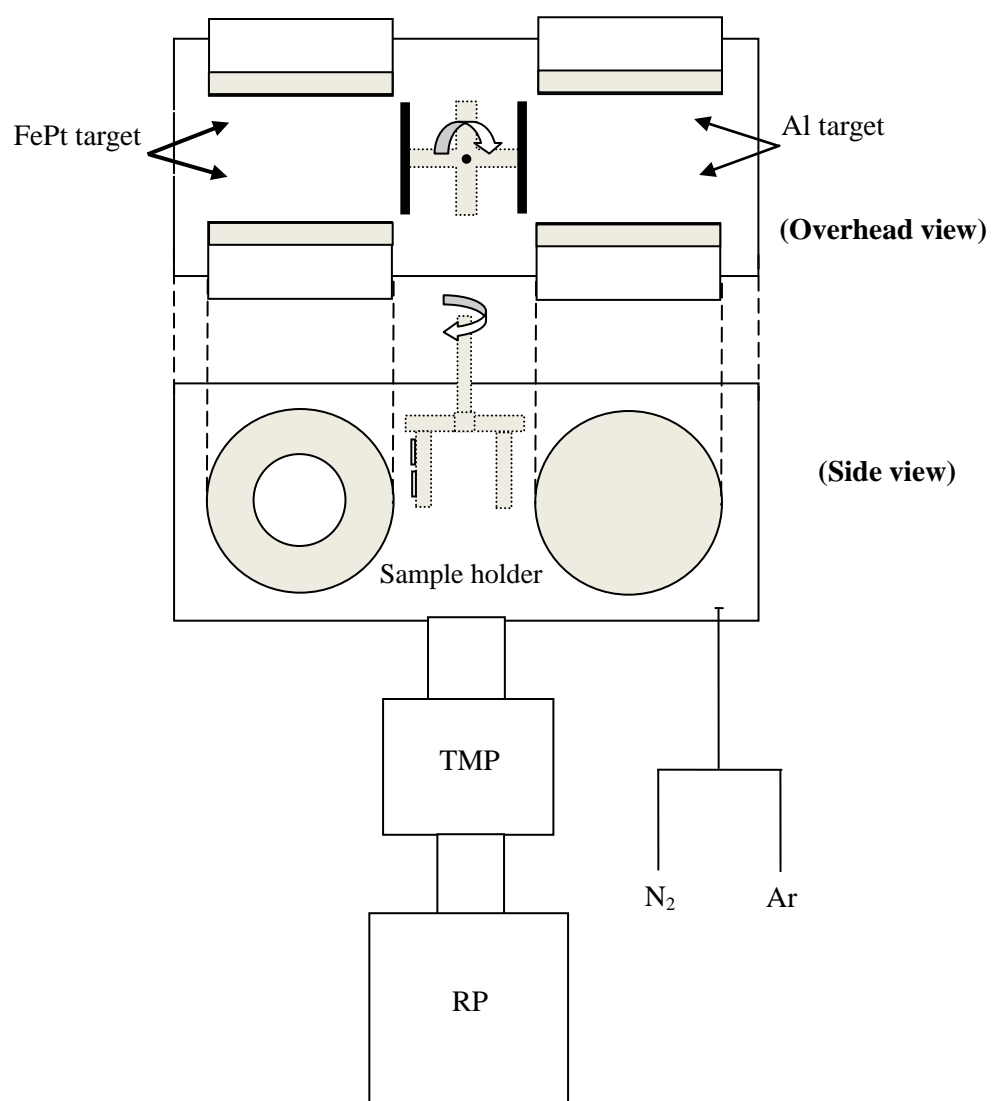11. Y. Hodumi, J. Shi, Y. Nakamura, Appl. Phys. Lett. 90, 212506 (2007).

FePt target

Al target

(Overhead view)

Sample holder

(Side view)

TMP

RP

N$_2$ Ar

Figure 2-1 Schematic diagram of the dual facing target DC magnetron sputtering apparatus.

Specimen

Objective lens

Back focal plane
objective aperture

1. intermediate image
SAED aperture

Intermediate
lens

2. intermediate
image
Projective
lens

Viewing
screen
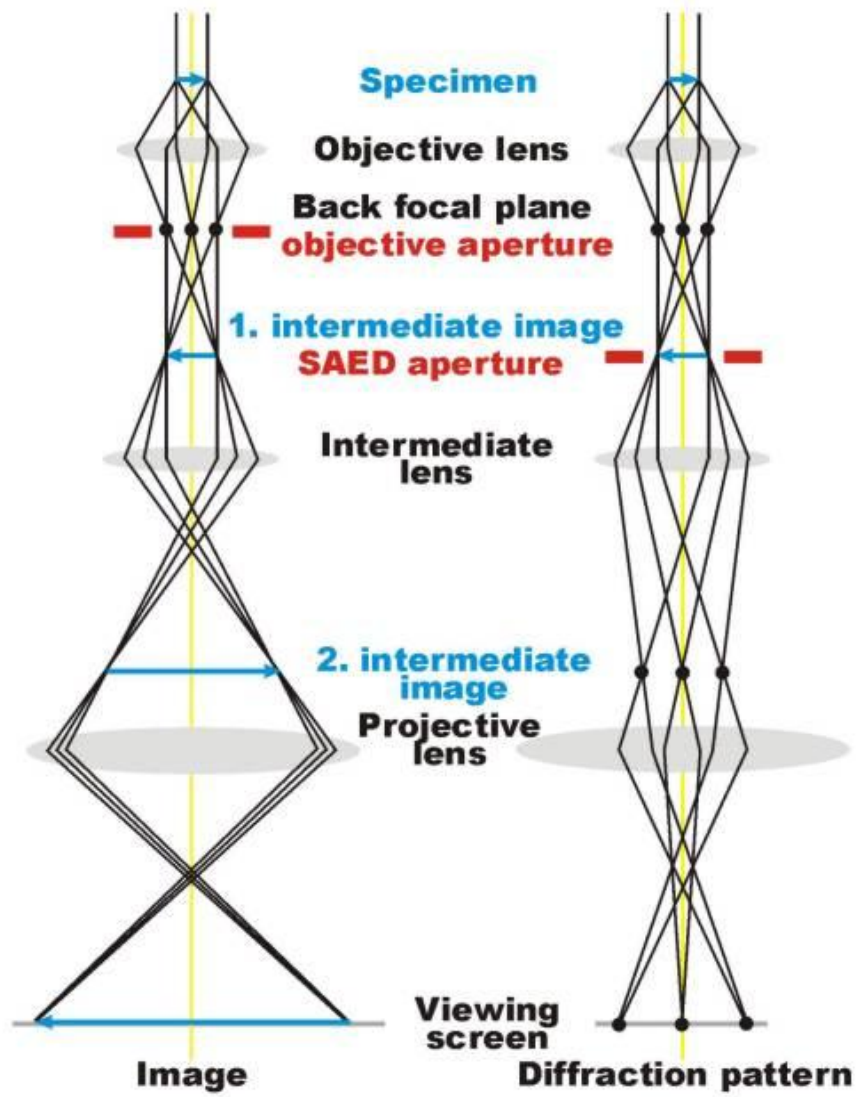
Image   Diffraction pattern

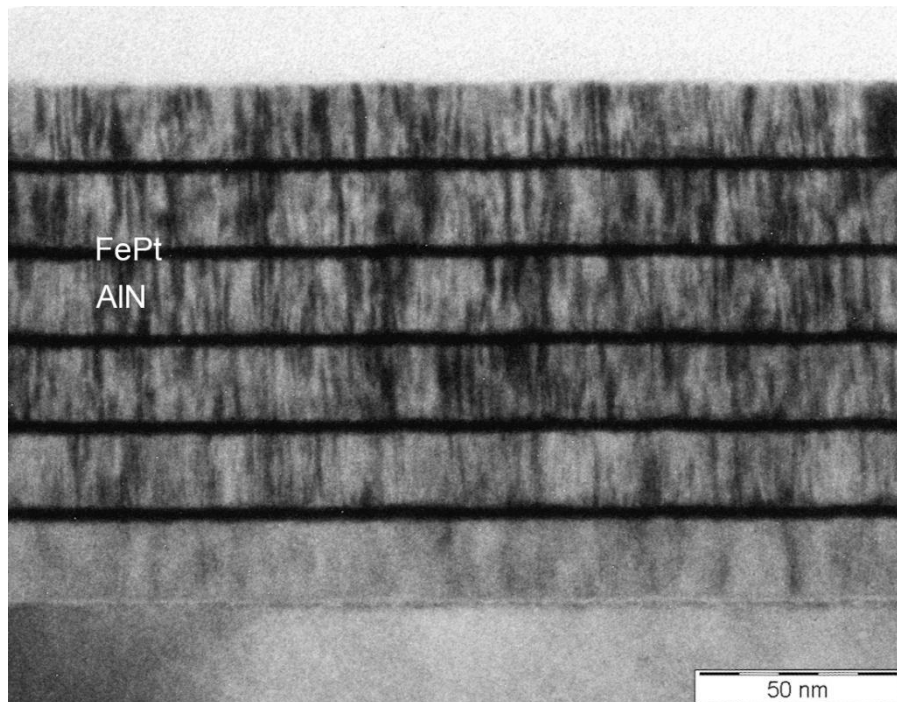Figure 2-2 Ray paths of image mode and the diffraction mode.

Figure 2-3 Cross-sectional TEM image of FePt/AlN layered structure.
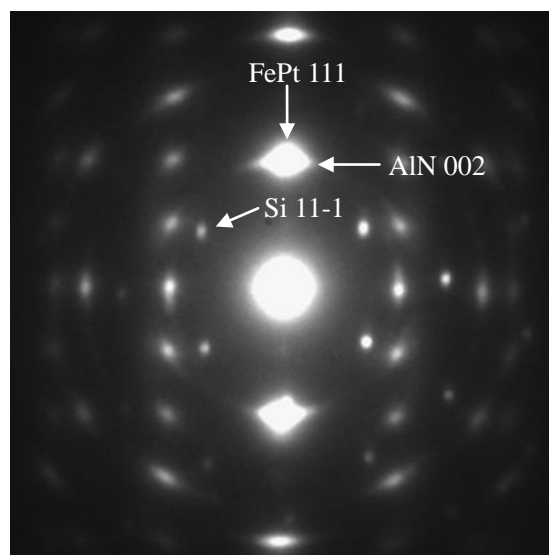

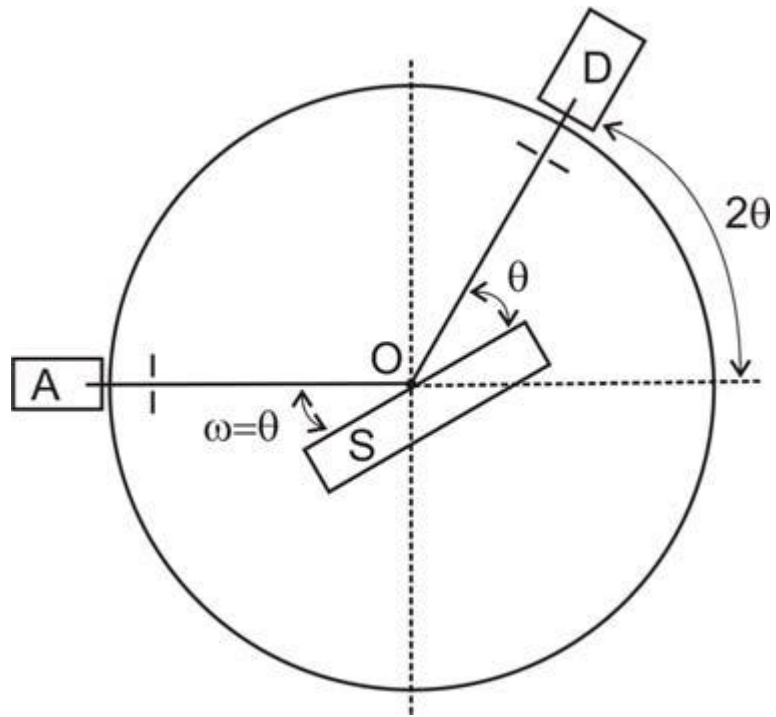Figure 2-4 Electron diffraction pattern of FePt/AlN layered structure.

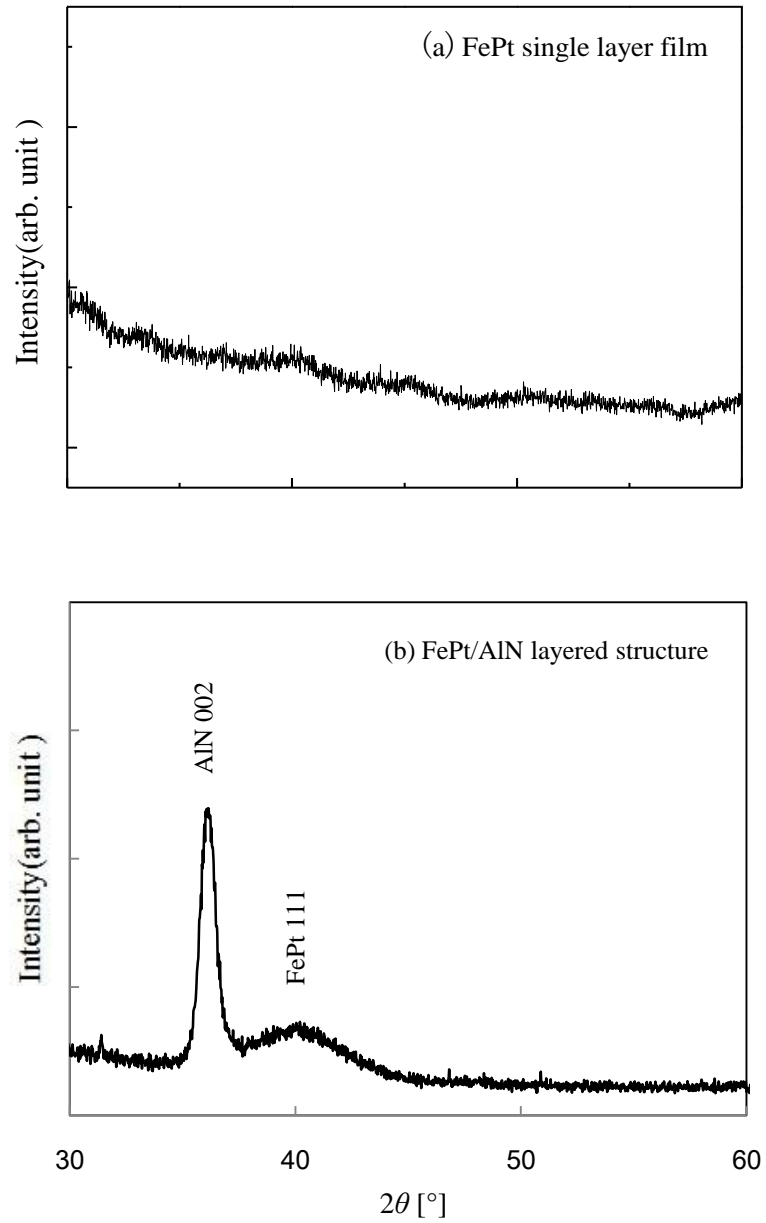Figure 2-5 Schematic of the $\theta/2\theta$ scan geometry.

Figure 2-6 XRD profiles of the as-deposited (a) FePt 10nm single layer film and (b) AlN (20nm)/[FePt (2nm)/AlN (20nm)]$_5$ layered structure.
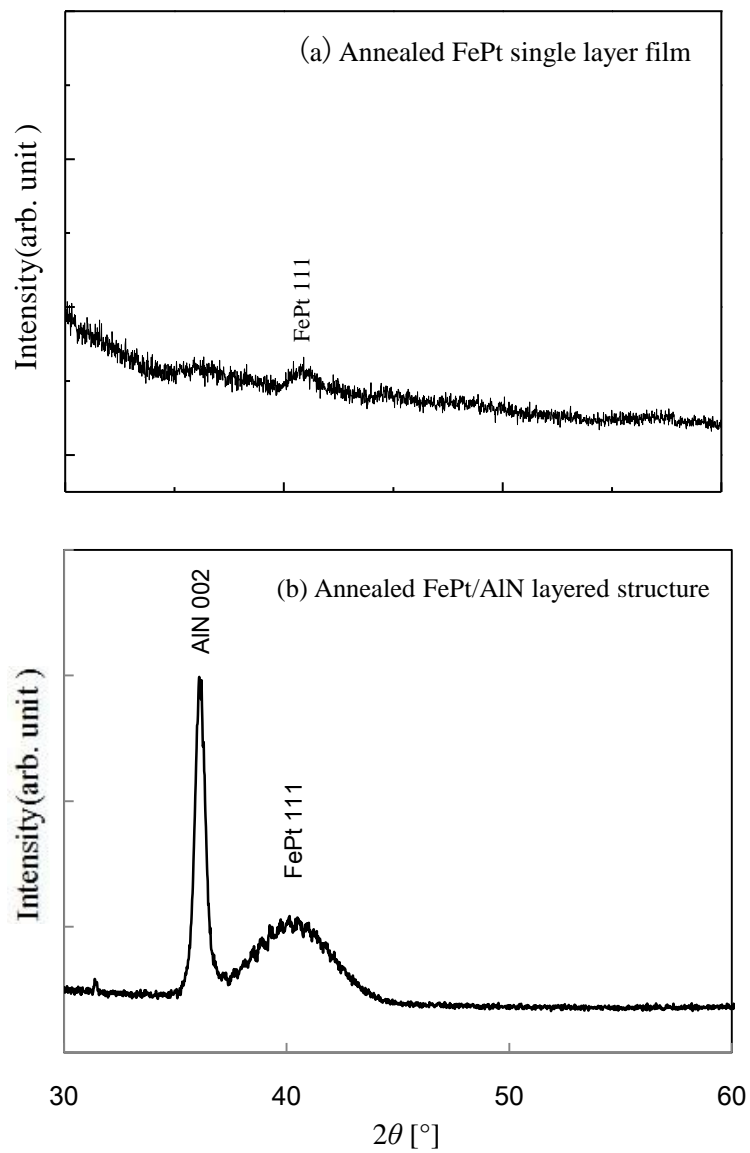
Figure 2-7 XRD profiles of the annealed (a) FePt 10nm single layer film and (b) AlN (20nm)/[FePt (2nm)/AlN (20nm)]$_5$ layered structure.

A) Incident angle < Total reflection critical angle
All incident X-rays are reflected.

B) Incident angle = Total reflection critical angle
Incident X-rays propagate along the sample surface.

C) Incident angle > Total reflection critical angle
Incident X-rays penetrate into the material by refraction

Figure 2-8 X-ray optics for the cases of the incident angles smaller, equal to, and greater than the critical θ_c.
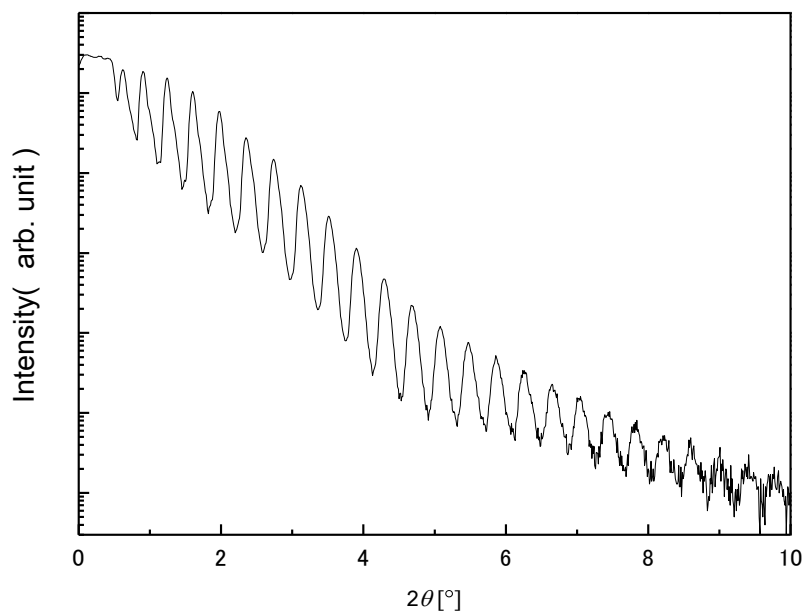
Figure 2-9 XRR profile of the annealed AlN (20nm)/[FePt (2nm)/AlN (20nm)]$_5$ layered structure.

M

M_R

M_S

$\perp$

K_{eff}

H_c

H_k

H

//

Figure 2-10 Typical hysteresis loops of thin film material with perpendicular magnetic anisotropy.

Figure 2-11 Magnetic hysteresis loops of as-deposited (a) FePt 10nm single layer film and (b) AlN (20nm)/[FePt (2nm)/AlN (20nm)]$_5$ layered structure.
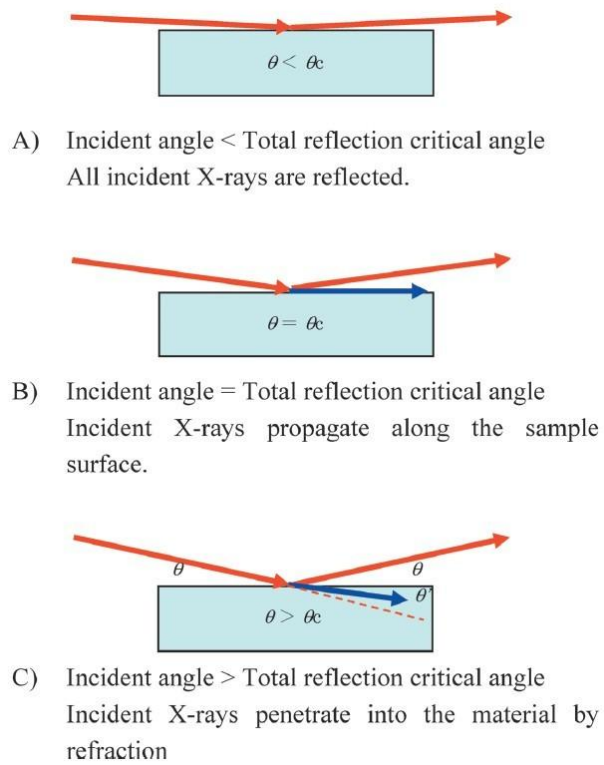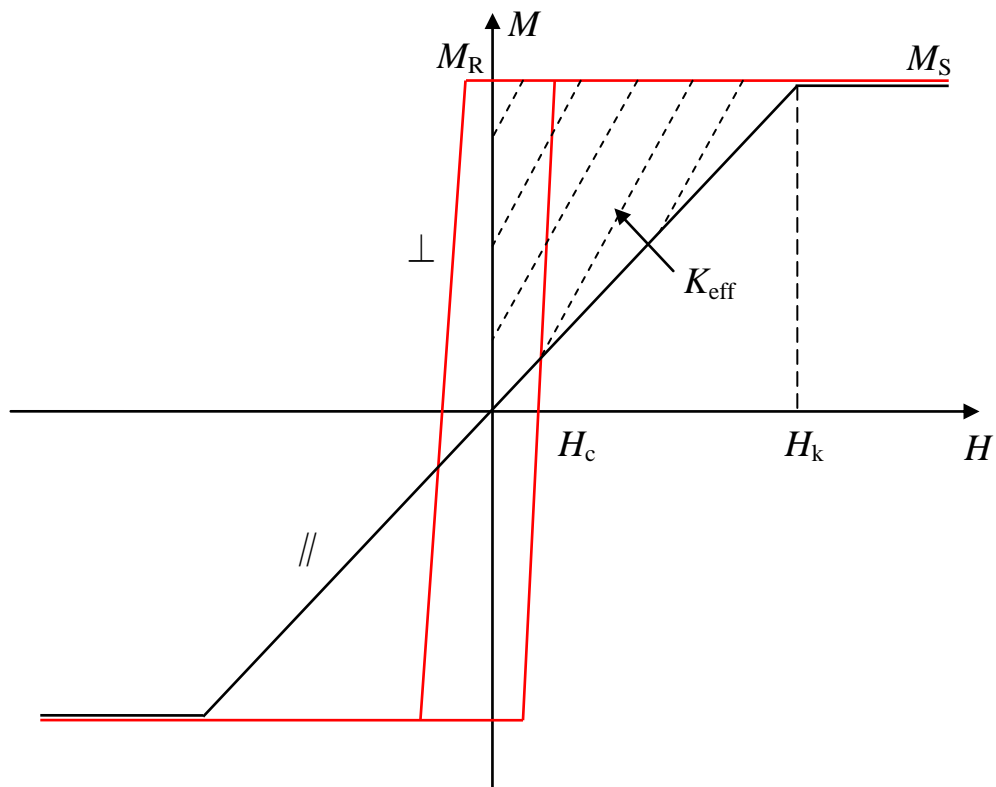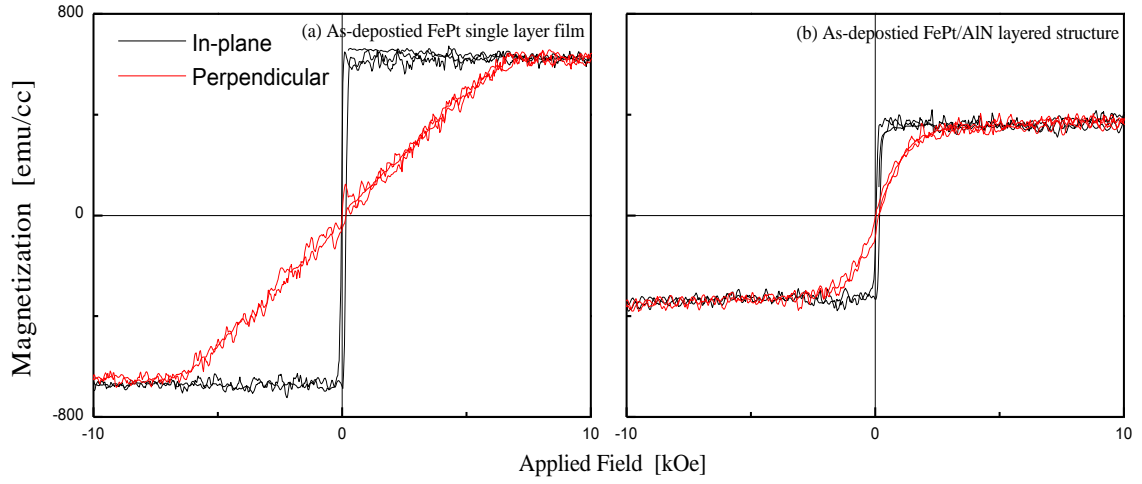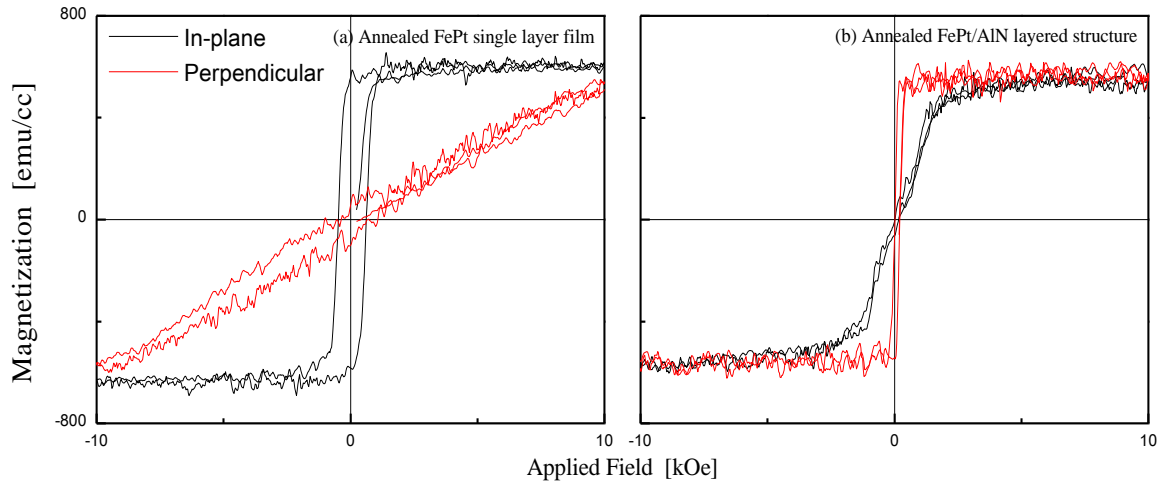

Figure 2-12 Magnetic ysteresis loops of annealed (a) FePt 10nm single layer film and (b) AlN (20nm)/[FePt (2nm)/AlN (20nm)]$_5$ layered structure.

Chapter 3 Magnetic properties of FePt/AlN layered structures

3.1 Introduction

Thin film materials with perpendicular magnetic anisotropy have been of great interest for perpendicular magnetic recording in the recent years.[1, 2] Among them, layered structure thin films offer the possibility that, because of the abundance of interfaces, the anisotropy is dominated by the existence of interface anisotropy as predicted by Néel.[3] For experiments, much work have been done on magnetic/nonmagnetic metallic layered structures, such as Co/Pt, Co/Pd, Co/Au.[4-8] In the previous work, our group firstly reported perpendicular magnetic anisotropy in metal/ceramic layered structure, CoPt/AlN layered structure. The research results of CoPt/AlN layered structure have shown the advantage of metal/ceramic layered structure for forming sharp interface and then developing strong interface magnetic anisotropy. Therefore further study on the magnetic behavior of FePt/AlN layered structure to develop potential for such kind of metal/ceramic layered structure is of great significance.

For metallic layered structures, the importance of the sharpness and flatness of interfaces for introducing perpendicular magnetic anisotropy has been proved.[9] Besides that, other factors which can influence the magnetic anisotropy also need to be noticed. Theoretical studies indicate the important role of the band structure in achieving PMA. In general, an increase in the anisotropy can be expected when the energy separation of the electronic states, one located below and the other above the Fermi level, will be reduced.[10] Such situation can occur only for a special symmetry and an appropriate position of Fermi level, which is strongly dependent on the alloy

composition and crystal texture. On the other hand, the contributions from such interface magnetic anisotropy are also influenced by the interface/volume atomic ratio as a matter of course.

In this chapter, the magnetic properties of FePt/AlN layered structure with different FePt alloy compositions have been systematically studied. The results of the influences of annealing temperature and FePt layer thickness on magnetic properties will be given as following.

3.2 Experimental parameter

Table 3-1 shows the experimental parameters used in this study. As seen in this table, FePt/AlN layered structures with different FePt alloy compositions, Fe50Pt50, Fe45Pt55 and Fe40Pt60, have been fabricated in this study. The emphasis of the study is placed on the Fe40Pt60 layered structures, which are showing strong perpendicular magnetic anisotropy. In this thesis, except for special remarks, all the FePt/AlN layered structures refer to the $Fe_{0.4}Pt_{0.6}$/AlN layered structures.

3.3 $Fe_{50}Pt_{50}$/AlN layered structures

Figure 3-1 shows the magnetic hysteresis loops of the AlN (10nm)/[$Fe_{0.5}Pt_{0.5}$ (2nm)/AlN (10nm)]$_5$ layered structures annealing at 500°C, 600°C and 700°C for 3 hours. The as-deposited film shows in-plane magnetic anisotropy, which means the easy magnetization direction is along the film plane, mainly due to the shape anisotropy (or demagnetizing field) of the FePt layers. Upon annealing, such in-plane anisotropy is weakened. The films turn to isotropy, a situation of similar magnetization behavior between the in-plane direction and perpendicular direction, when annealing at 500°C and 600°C. However, the in-plane anisotropy appears again in film annealed at 700°C, and the coercivity slightly increased. No perpendicular

magnetic anisotropy has been observed in this set of layered structures.

Figure 3-2 shows the XRD profiles of the AlN (10nm)/[Fe$_{0.5}$Pt$_{0.5}$ (2nm)/AlN (10nm)]$_5$ layered structures annealing at 500°C, 600°C and 700°C. All the films show preferred orientations with AlN [001] and FePt [111] parallel to the growth direction. As temperature increases, the intensities of the both AlN 002 and FePt 111 peak increases correspondingly, indicating the improvement of the crystal quality and the preferred orientation. For annealed layered structures, satellite peaks appears around the FePt (111) peak. That is to say, the periodic structure of the FePt/AlN films has not been broken during annealing in this work, even at 700°C. On the contrary, the periodicity was improved.

Figure 3-3 shows the magnetic hysteresis loops of the AlN (10nm)/[Fe$_{0.5}$Pt$_{0.5}$ (2.5nm)/AlN (10nm)]$_5$ layered structures annealing at 500°C, 600°C and 700°C. As seen in this figure, the in-plane magnetic anisotropy of the as-deposited layered structures is stronger than that of as-deposited FePt 2nm layered structure. At an annealing temperature of 500°C, this in-plane anisotropy grows weak, and then turns to isotropy at 600°C. When annealing at 700°C, the layered structure show in-plane anisotropy again.

Figure 3-4 shows the magnetic hysteresis loops of the AlN (10nm)/[Fe$_{0.5}$Pt$_{0.5}$ (3nm)/AlN (10nm)]$_5$ layered structures annealing at 500°C, 600°C and 700°C. It is clear that the in-plane anisotropy gets further stronger than that of layered structures with smaller FePt layer thickness. This thickness effect indicates the important role of interface/volume atomic ratio in determining the anisotropy of layered structures. Upon annealing below 700°C, the in-plane anisotropy is gradually weakening as well as described above.

Figure 3-5 shows the magnetic hysteresis loops of the AlN (10nm)/[Fe$_{0.5}$Pt$_{0.5}$ (4nm)/AlN (10nm)]$_5$ layered structures annealing at 500°C, 600°C and 700°C. The

layered structures show similar behavior of magnetic anisotropy with films introduced above. However, a phenomenon needed to mention is that, the coercivity of the layered structure annealed at 700°C is obviously increased. It is well-know that a variety of factors can influence the coercivities of ferromagnetic films, e.g., growth conditions,[11] crystalline grain size[12] and internal stress[13]. We believe the stress transition in FePt layers, which will be discussed in chapter 4, may be one reason for this increase of coercivity. For another consideration, it may be because of the occurrence of disordering-ordering transformation. For FePt alloy, a disordering-ordering transformation may occur during annealing. In that case, the alloy will transform from a disordered FCC phase to an ordered FCT phase which can introduce great magnetocrystalline anisotropy along <001> direction and significantly improve the coercivity. Therefore, the increase of the coercivity may be also due to the beginning of the ordering transformation when annealing at high temperature.

In summary, the works on the AlN (10nm)/[$Fe_{0.5}Pt_{0.5}$ (t)/AlN (10nm)]$_5$ (t is the thickness of FePt layer) layered structures have been introduced in this section. By fixing the AlN layer thickness to 10nm, the influences of annealing temperature and FePt layer thickness on magnetic properties have been studied. It is found that the as-deposited $Fe_{0.5}Pt_{0.5}$/AlN layered structures show in-plane magnetic anisotropy, and such in-plane anisotropy is enhanced as the FePt layer thickness increases. This indicates the important role of interface/volume atomic ratio in determining the anisotropy of layered structures. Upon annealing, the in-plane anisotropy is gradually weakened till the films show isotropy, which means the annealing can favour the magnetization along perpendicular direction. However, no perpendicular magnetic anisotropy has been observed in $Fe_{0.5}Pt_{0.5}$/AlN layered structures.

3.4 $Fe_{45}Pt_{55}$/AlN layered structures

Figure 3-6 shows the magnetic hysteresis loops of the AlN (10nm)/[$Fe_{0.45}Pt_{0.55}$ (2.5nm)/AlN (10nm)]$_5$ layered structures annealing at 400°C, 500°C and 600°C for 3 hours. Although the as-deposited film show in-plane magnetic anisotropy as well as $Fe_{0.5}Pt_{0.5}$/AlN layered structure, the anisotropy of the layered structure can be altered through annealing. It can be seen that, the easiness of perpendicular magnetization increases as the annealing temperature increases. And when further increasing annealing temperature to 600°C, the magnetization easy axis changes from the in-plane direction to the perpendicular direction, which means perpendicular magnetic anisotropy is achieved though the effective magnetic anisotropy energy (the area between the perpendicular and in-plane magnetic hysteresis loops) is low. Therefore, by varying the FePt alloy composition, perpendicular magnetic anisotropy has been observed in $Fe_{0.45}Pt_{0.55}$/AlN layered structures.

3.5 $Fe_{40}Pt_{60}$/AlN layered structures

According to the results of $Fe_{0.5}Pt_{0.5}$ and $Fe_{0.45}Pt_{0.55}$ layered structures, we have found that the relatively low content of Fe in FePt layer is beneficial to obtain perpendicular magnetic anisotropy. In this section, the results of the AlN (20nm)/[$Fe_{0.4}Pt_{0.6}$ (t)/AlN (20nm)]$_5$ layered structures will be given. The AlN layer thickness is fixed at 20nm, while the FePt layer thickness is varied in a wide range (from 1nm to 10nm) to systematically study the influences of FePt layer thickness and annealing temperature on magnetic properties of the layered structure.

Figure 3-7 shows the magnetic hysteresis loops of the as-deposited AlN (20nm)/[$Fe_{0.4}Pt_{0.6}$ (t)/AlN (20nm)]$_5$ (t is the thickness of FePt layer and is varied from 1nm to 10nm) layered structures. It is found that the layered structure of t = 1nm

shows superparamagnetic behavior, implying the critical thickness for the superparamagnetic/ferromagnetic transition of FePt layer at room temperature is between 1nm and 1.5nm. This result is different from that of CoPt/AlN layered structure, which shows a critical thickness between 0.5nm and 1nm. It may be resulted from the low magnetocrystalline anisotropy of FCC FePt. The film of $t =$ 1.5nm shows magnetic isotropy, whereas the FePt single layer film shows strong in-plane magnetic anisotropy as introduced in chapter 2. Therefore, the formation of the layered structure can strongly favor the magnetization along perpendicular direction for FePt film. When the FePt layer thickness increases to 2nm and above, the layered structures show in-plane magnetic anisotropy, which is mainly due to the shape anisotropy of FePt layer. A phenomenon needed to pay attention is that, the extent of such in-plane magnetic anisotropy increases obviously as FePt layer thickness increases from 1.5nm to 5nm, indicating the magnetic anisotropy of layered structure is strongly dependent on the interface/volume atomic ratio owing to the large influence from interfacial atoms. However, the influence of interfacial atoms seem that it can be neglected comparing to that of volume atoms when the FePt layer thickness increases to 9nm, because the extents of the in-plane anisotropy of $t =$ 9nm and $t =$ 10nm layered structures are almost the same. No perpendicular magnetic anisotropy has been observed in as-deposited layered structures.

Figure 3-8 shows the magnetic hysteresis loops of the AlN (20nm)/[$Fe_{0.4}Pt_{0.6}$ (t)/AlN (20nm)]$_5$ (t is the thickness of FePt layer in the unit of nanometer) layered structures annealed at 300°C. It can be seen that, the annealed layered structure of $t =$ 1nm remains in superparamagnetic state. However, one obvious difference from the as-deposited films is that the perpendicular magnetic anisotropy has been observed in the annealed FePt/AlN layered structure of $t =$ 1.5nm. When $t =$ 2nm, the layered structure shows magnetic isotropy, and the magnetization easy axis changes to the

in-plane direction again when the FePt layer thickness further increases to 3nm and above. By comparing to the results of the as-deposited films, we found the annealing can favor the magnetization along perpendicular direction for the layered structures of t = 1.5nm, 2nm and 3nm. Nevertheless, what is interesting is that the annealing shows different effect on the magnetic behavior of the layered structures with thicker FePt layer thickness. As seen in this figure, the layered structure of t = 5nm shows the same magnetic behavior with as-deposited one, and the in-plane magnetic anisotropy of the layered structures of t = 7nm, 9nm and 10nm is enhanced by annealing. Therefore, the annealing favors the magnetization along perpendicular direction in the FePt layer thickness range of 1.5nm to 3nm, while favors the in-plane magnetization for the layered structures of t = 7nm, 9nm and 10nm. About the FePt layer thickness effect, the magnetic anisotropy of the layered structure gradually changes from perpendicular to in-plane direction as the FePt layer thickness increases. Lager FePt layer thickness results in stronger in-plane magnetic anisotropy as the same as the as-deposited layered structures.

Figure 3-9 shows the magnetic hysteresis loops of AlN (20nm)/[Fe$_{0.4}$Pt$_{0.6}$ (t)/AlN (20nm)]$_5$ (t is the thickness of FePt layer in the unit of nanometer) layered structures annealed at 500°C. The 500°C annealed layered structures show similar behavior of magnetic anisotropy with the 300°C annealed layered structures. The perpendicular magnetization of the layered structures of t = 1.5nm, 2nm and 3nm is further enhanced by annealing, as a result, the critical FePt layer thickness for the transition of perpendicular/in-plane magnetic anisotropy is about 3nm, whereas the critical thickness for the 300°C annealed layered structures is 2nm. The increase in the critical FePt layer thickness indicates that some positive contributions to the perpendicular magnetic anisotropy are enhanced by increasing the annealing temperature. Therefore, comparatively strong perpendicular magnetic anisotropy can be observed in the

layered structures of $t = 1.5$nm, 2nm. On the other hand, this strong perpendicular magnetic anisotropy falls off and turns to in-plane anisotropy as the FePt layer thickness increases, and the in-plane magnetic anisotropy of the layered structures of $t = 7$nm, 9nm and 10nm is also further enhanced by annealing comparing to the 300°C annealed layered structures. Since the layered structure of $t = 5$nm still shows the same behavior of magnetic anisotropy with the as-deposited and the 300°C annealed layered structures, it seems that $t = 5$nm is the critical FePt layer thickness for the different annealing effects on the magnetic properties of the FePt/AlN layered structure.

Figure 3-10 shows the magnetic hysteresis loops of AlN (20nm)/[Fe$_{0.4}$Pt$_{0.6}$ (t)/AlN (20nm)]$_5$ (t is the thickness of FePt layer in the unit of nanometer) layered structures annealed at 700°C. The perpendicular magnetic anisotropy has been also observed in the layered structures of $t = 1.5$nm, 2nm. Although the increase in the FePt layer thickness switches the layered structure to be in-plane magnetic anisotropic as the same as the films annealed at low temperatures, the extent of the in-plane magnetic anisotropy increases more slowly. This means the in-plane magnetic anisotropy of layered structures with thick FePt layer is suppressed when annealing at 700°C.

Another important feature in this figure is the increases of coercivity. It is seen that the coercivities of the layered structures of $t = 1.5$nm, 2nm and 3nm slightly increases comparing to the layered structures annealed at low temperatures. We believe the stress transition in FePt layers, which will be discussed in chapter 4, may be one reason for this increase. For the layered structures of $t = 5$nm, 7nm, 9nm and 10nm, the coercivities increase obviously and the in-plane and out-of-plane (perpendicular direction) coercivities are almost identical, which may be due to the occurrence of disordered-ordered transformation of FePt alloy. Commonly, the

as-prepared FePt layer or nanoparticles are in chemically disordered A1 phase with very low magnetocrystalline anisotropy. The A1 phase has face centered cubic (FCC) structure and the two atoms occupy the FCC sites randomly. Upon annealing, it can transform into chemically ordered $L1_0$ phase, which has face centered tetragonal (FCT) structure and the two atom species from alternating atomic layers. Due to strong spin-orbit coupling of the Pt 5d electrons such $L1_0$ phase has very large magnetocrystalline anisotropy,[14] and the easy axis is along [001] direction.[15] Since the FePt layers in the layered structures are (111) textured, about 55° away from the [001] direction, the influences from ordered transformation will result in a trend to magnetic isotropy in FePt/AlN layered structure and increase the coercivities of both in-plane and perpendicular directions. Moreover, the ordered transformation is a size dependent effect,[16] and the characteristic size for the two-dimensional FePt layer is the thickness. Thus the ordered transformation could occur in the layered structures with thick FePt layer.

3.6 Summary

In this chapter, the results of FePt/AlN layered structure with different FePt alloy compositions have been introduced. The influences of annealing temperature and FePt layer thickness on magnetic properties of the layered structures have been systematically studied. It is found that:

1. Perpendicular magnetic anisotropy has been observed in annealed $Fe_{0.45}Pt_{0.55}$ and $Fe_{0.4}Pt_{0.6}$ layered structures.

2. The as-deposited $Fe_{0.4}Pt_{0.6}$ (t)/AlN layered structures of $t = 1.5nm$ shows magnetic isotropy, indicating the formation of the layered structure and the relatively low content of Fe in FePt layer is beneficial to the magnetization along perpendicular direction.

3. As the FePt layer thickness increases, the layered structures tend to show in-plane magnetic anisotropy. And such in-plane anisotropy further increases with the increasing of the FePt layer thickness.

4. Upon annealing, the magnetizations along perpendicular direction of the layered structures with small FePt layer thickness ($t = 1.5$nm, 2nm and 3nm) are gradually enhanced as the annealing temperature increases. The perpendicular magnetic anisotropy can be observed in annealed layered structures with FePt layer thickness below 3nm. However, for the layered structures with large FePt layer thickness ($t = 7$nm, 9nm and 10nm), the in-plane magnetizations are enhanced by the annealing process.

It is interesting that the layered structure can undergo a gradual transition from in-plane anisotropy to perpendicular magnetic anisotropy with increasing annealing temperature, and the annealing shows different effects on magnetic property in the different FePt layer thickness ranges. The origin of the perpendicular magnetic anisotropy found in annealed layered structure and the mechanisms of the FePt layer thickness and annealing effects on magnetic property will be detailed discussed in the next chapter.

Reference

1. J. P. J. Groenland, C. J. M. Egkel, J. H. J. Flultman, and R. M. de Ridder, Sens. Actuators, A 30, 89 (1992).

2. D. J. Monsma, J. C. Lodder, Th. J. A. Popma, and B. Dieny, Phys. Rev. Lett. 74, 5260 (1995).

3. L. Néel, J. Phys. Radium 15, 225 (1954).

4. P. F. Carcia, A. D. Meinhaldt, A. Suna, Appl. Phys. Lett. 47, 178 (1985).

5. P. F. Carcia, J. Appl. Phys. 63, 5066 (1988).

6. M. Sakurai, T. Takahata, I. Moritani, J. Magn. Soc. Japan. 15, 411 (1991).

7. G. Gubbiotti, G. Carlotti, F. Albertini, F. Casoli, E. Botempi, L. E. Depero, H. Koo, R. D. Gomez, Thin Solid Films 428, 102 (2003).

8. C. Chappert, P. Bruno, J. Appl. Phys. 64, 5736 (1988).

9. F. J. A. den Broeder, D. Kuiper, A. P. van de Mosselaer, W. Hoving, Phys. Rev. Lett. 60, 2769 (1988).

10. P. Bruno, Phys. Rev. B 39, 865 (1989).

11. G. Kim, Y. Sakuraba, M. Oogane, Y. Ando, and T. Miyazaki, Appl. Phys. Lett. 92, 172502 (2008).

12. R. H. Yu, S. Basu, Y. Zhang, A. Parvizi-Majidi, and John Q. Xiao, J. Appl. Phys. 85, 6655 (1999).

13. K. W. Wierman, C. L. Platt, J. K. Howard, and F. E. Spada, J. Appl. Phys. 93,7160 (2003).

14. H. Zeng, M. L. Yan, N. Powers, and D. J. Sellmyer, Appl. Phys. Lett. 80, 2350 (2002).

15. D. Alloyeau, C. Ricolleau, C. Mottet, T. Oikawa, C. Langlois, Y. Le Bouar, N. Braidy, and A. Loiseau, Nature Materials 8, 940 (2009).

16. O. Kitakami, Y. Shimada, K. Oikawa, H. Daimon, and K. Fukamichi, Appl. Phys. Lett. 78, 1104 (2001).

Table 3-1 Sputtering parameters

|	
Base pressure	Below 5×10^{-5} Pa
Sputtering gas	Ar: 3.5sccm N_2: 1.5sccm
Sputtering pressure	0.2 Pa
Deposition rate	FePt: 0.1nm/s AlN: 0.089nm/s
Substrate temperature	Room temperature
Sputter power	FePt: 80W Al: 80W
Substrate	Quartz glass
Film configuration	Sub/AlN(t_{AlN})/[FePt(t_{FePt})/AlN (t_{AlN})]$_5$ t_{FePt} = 1, 1.5, 2, 3, 5, 7, 9, 10nm t_{AlN} =5, 10, 20, 40nm
FePt alloy composition	Fe50Pt50, Fe45Pt55, Fe40Pt60
Annealing condition	500°C, 600°C, 700°C 3 hours
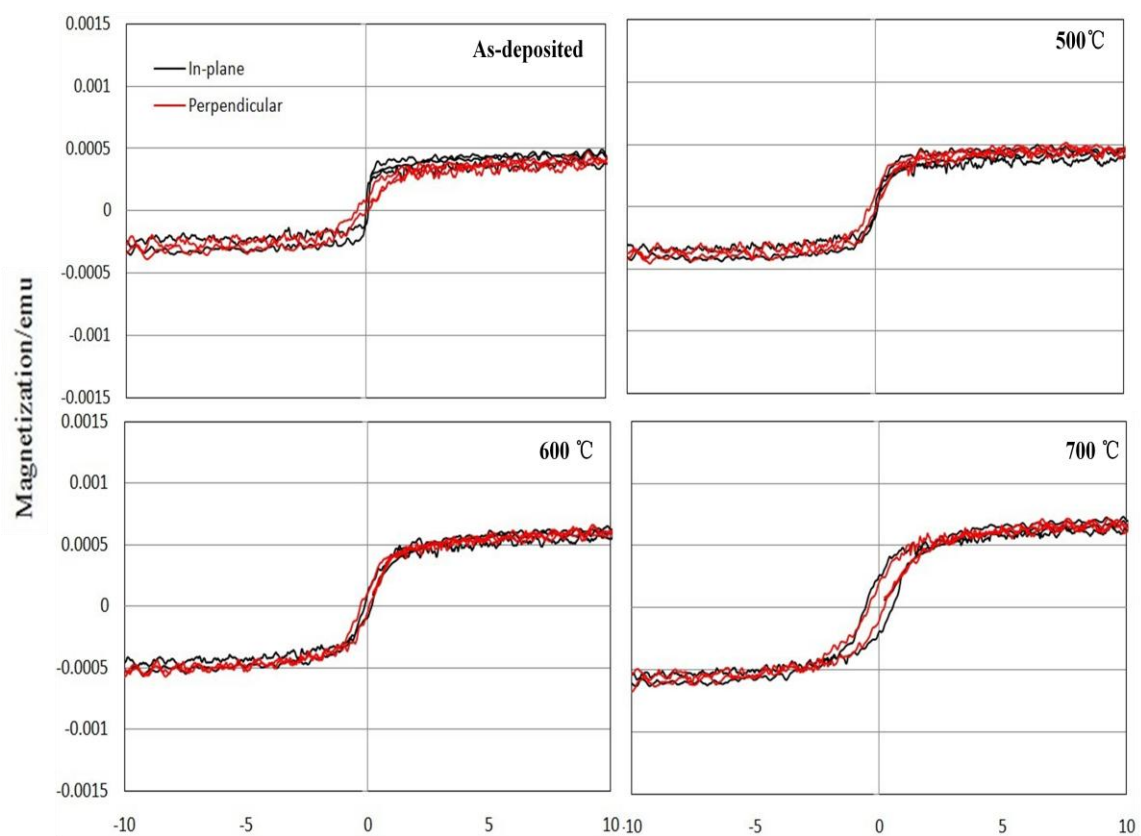
Figure 3-1 Magnetic hysteresis loops of the AlN (10nm)/[Fe$_{0.5}$Pt$_{0.5}$ (2nm)/AlN (10nm)]$_5$ layered structures annealing at 500°C, 600°C and 700°C for 3 hours.
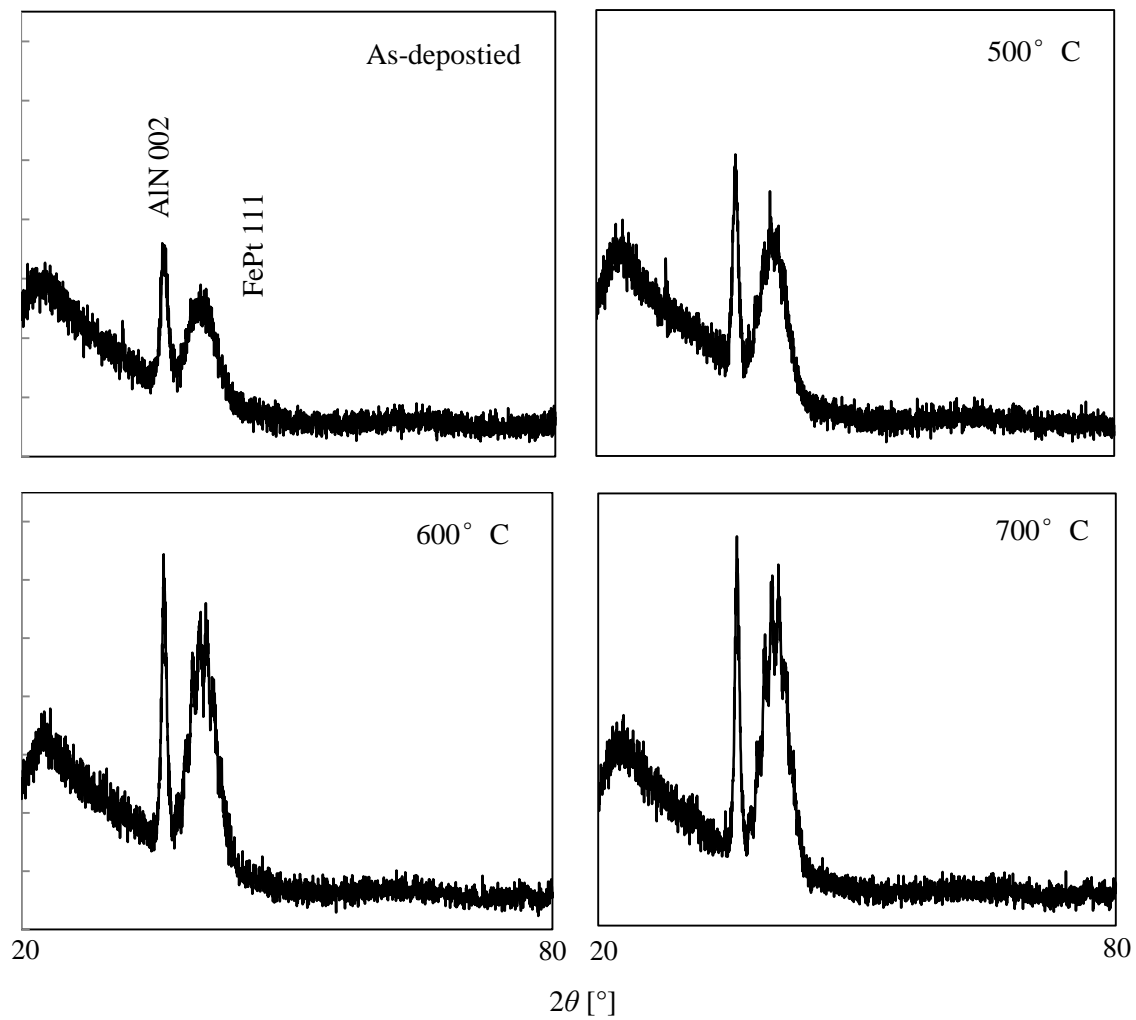
Figure 3-2 XRD profiles of the AlN (10nm)/[Fe$_{0.5}$Pt$_{0.5}$ (2nm)/AlN (10nm)]$_5$ layered structures annealing at 500°C, 600°C and 700°C.
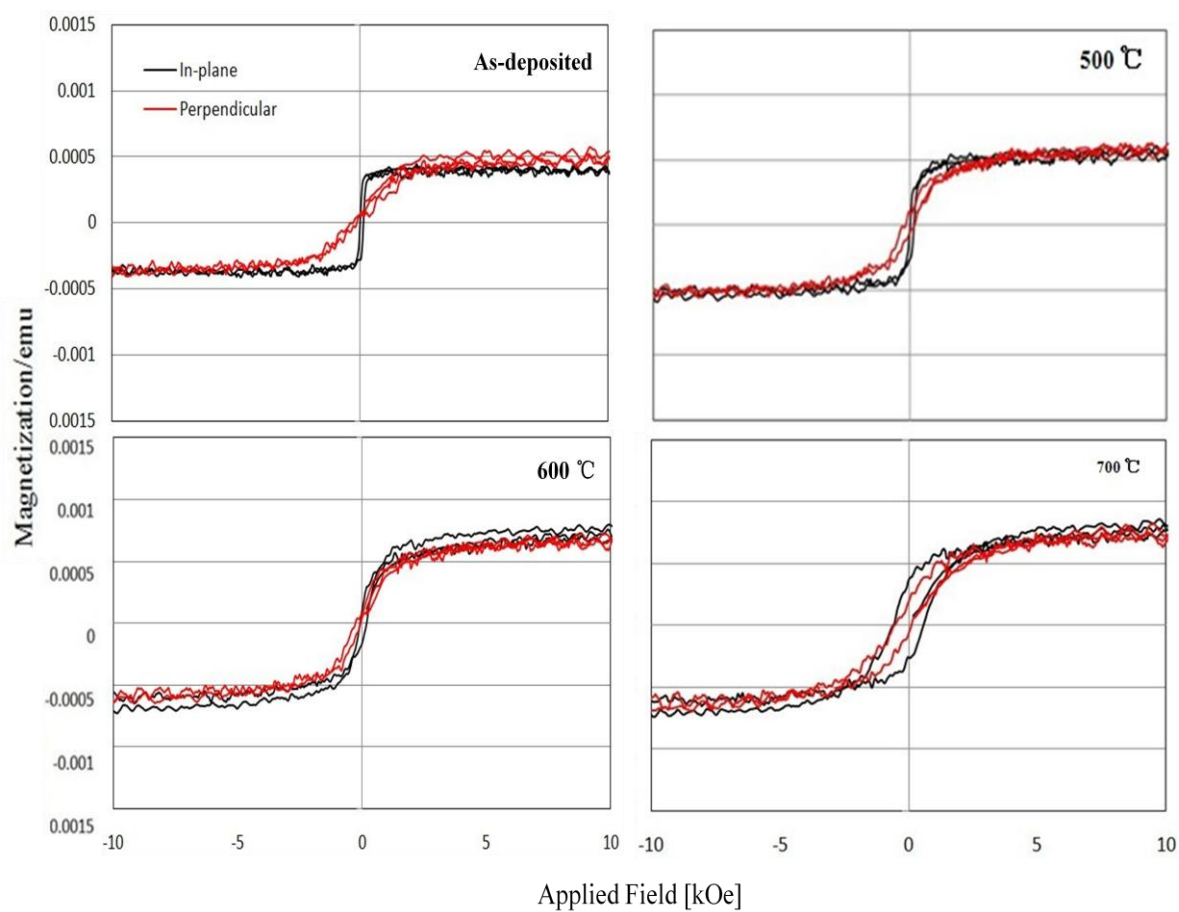
Figure 3-3 Magnetic hysteresis loops of the AlN (10nm)/[Fe$_{0.5}$Pt$_{0.5}$ (2.5nm)/AlN (10nm)]$_5$ layered structures annealing at 500°C, 600°C and 700°C.
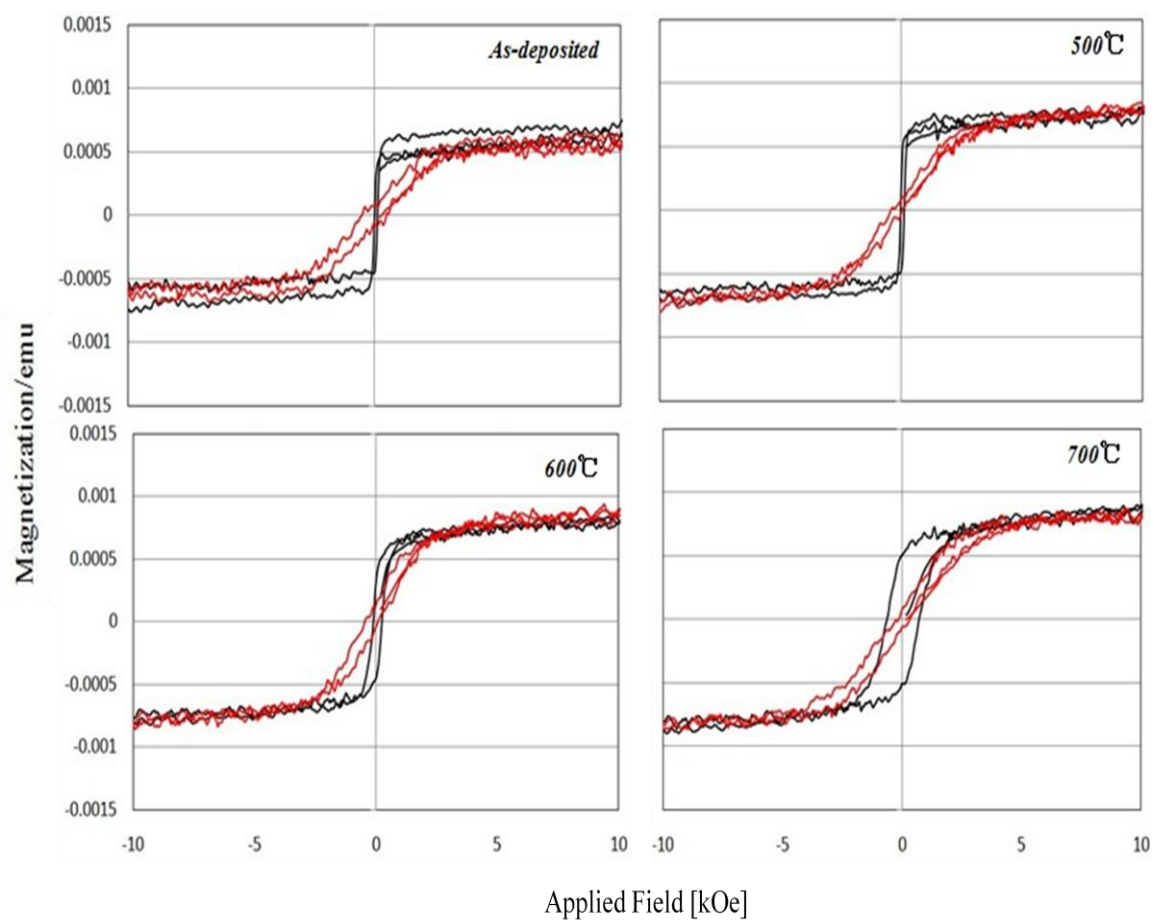
Figure 3-4 Magnetic hysteresis loops of the AlN (10nm)/[Fe$_{0.5}$Pt$_{0.5}$ (3nm)/AlN (10nm)]$_5$ layered structures annealing at 500°C, 600°C and 700°C.
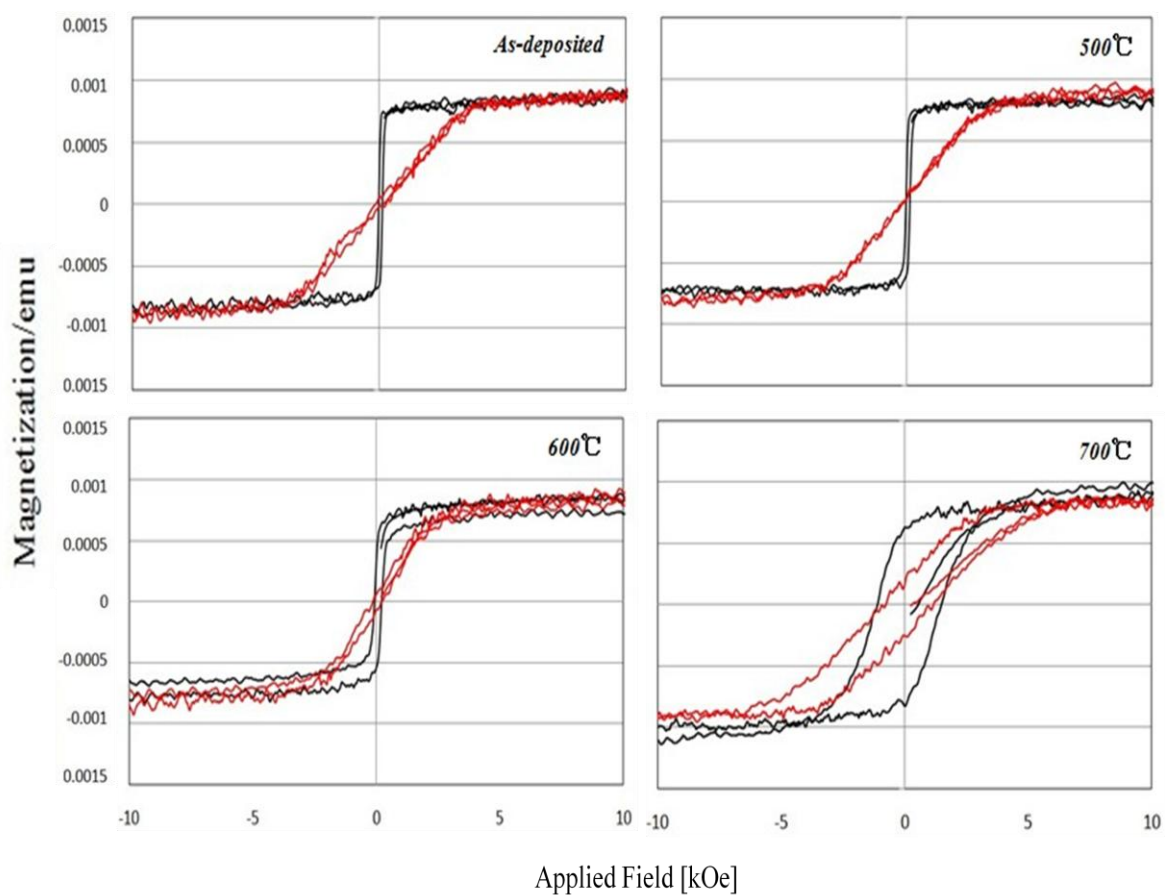
Figure 3-5 Magnetic hysteresis loops of the AlN (10nm)/[Fe$_{0.5}$Pt$_{0.5}$ (4nm)/AlN (10nm)]$_5$ layered structures annealing at 500°C, 600°C and 700°C.
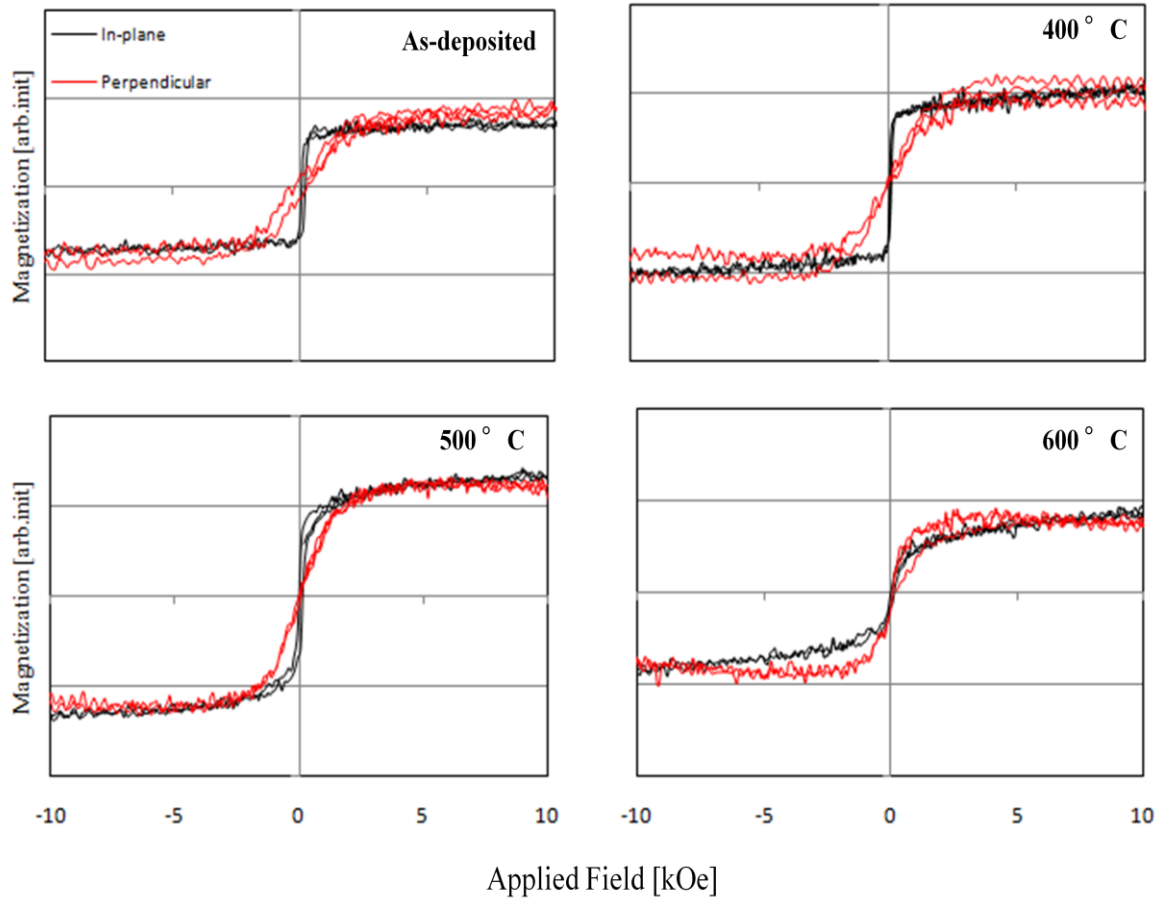
Figure 3-6 Magnetic hysteresis loops of the AlN (10nm)/[$Fe_{0.45}Pt_{0.55}$ (2.5nm)/AlN (10nm)]$_5$ layered structures annealing at 400°C, 500°C and 600°C for 3 hours.

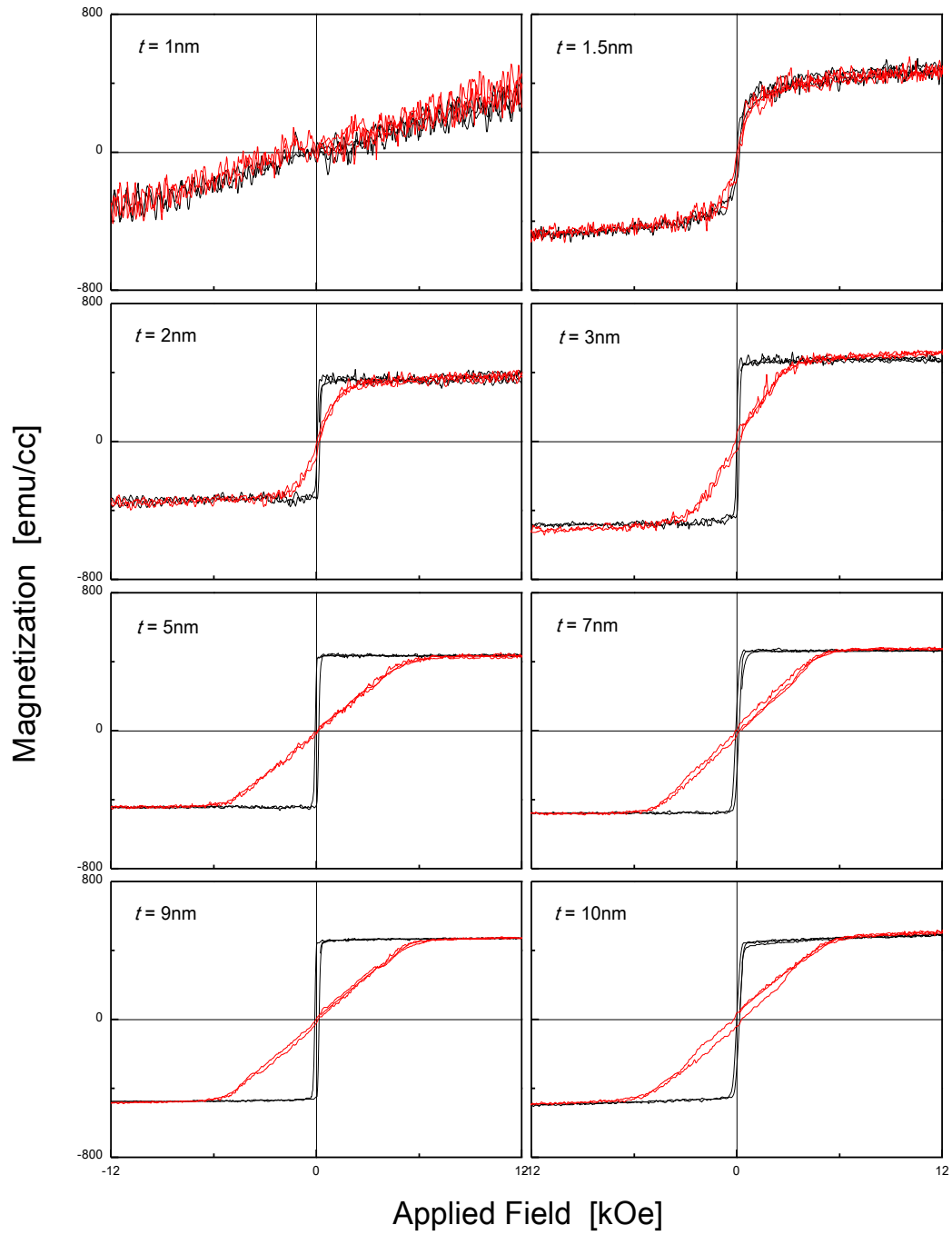Figure 3-7 Magnetic hysteresis loops of the as-deposited AlN (20nm)/[Fe$_{0.4}$Pt$_{0.6}$ (t)/AlN (20nm)]$_5$ layered structures.

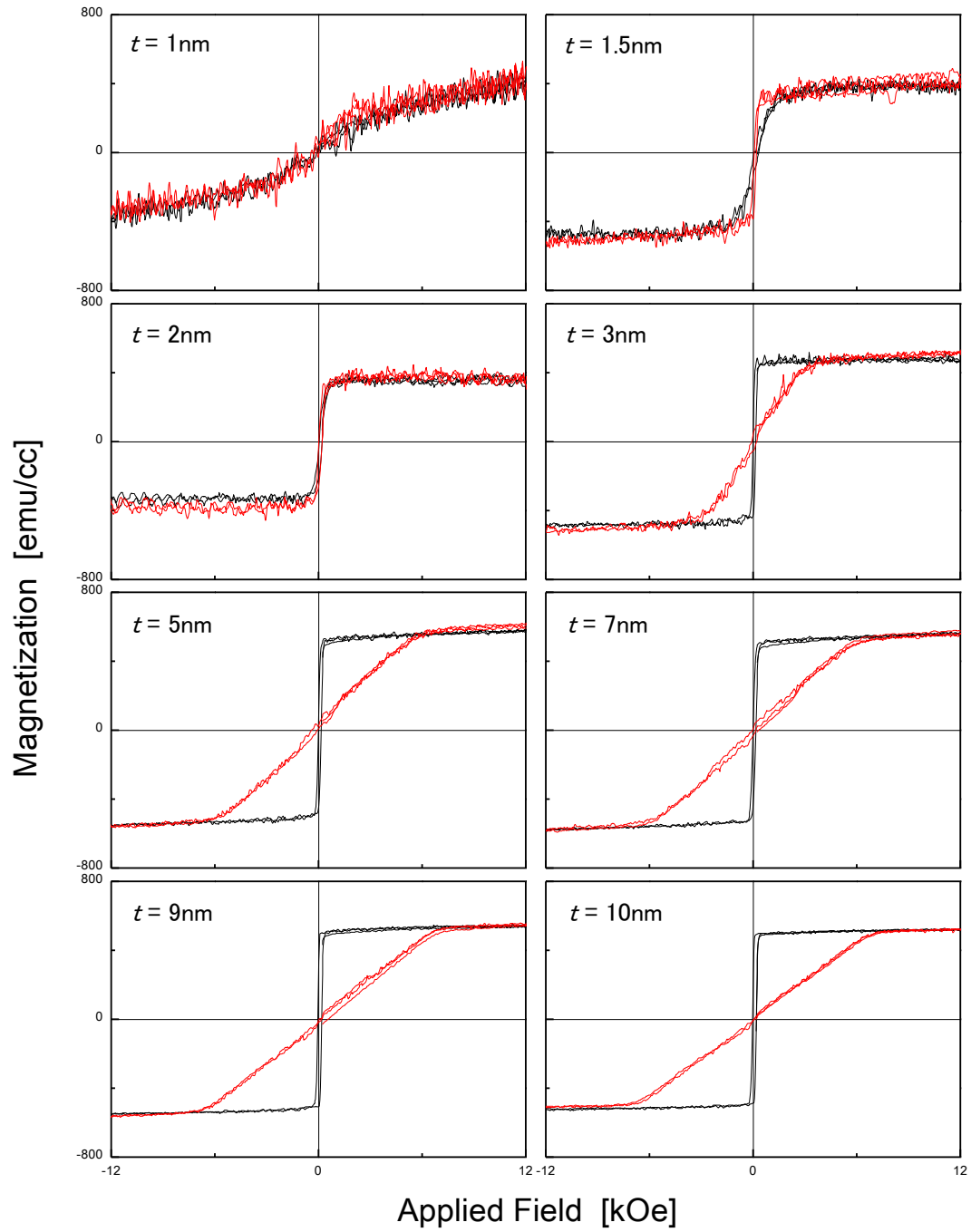Figure 3-8 Magnetic hysteresis loops of the AlN (20nm)/[Fe$_{0.4}$Pt$_{0.6}$ (t)/AlN (20nm)]$_5$ layered structures annealed at 300°C.
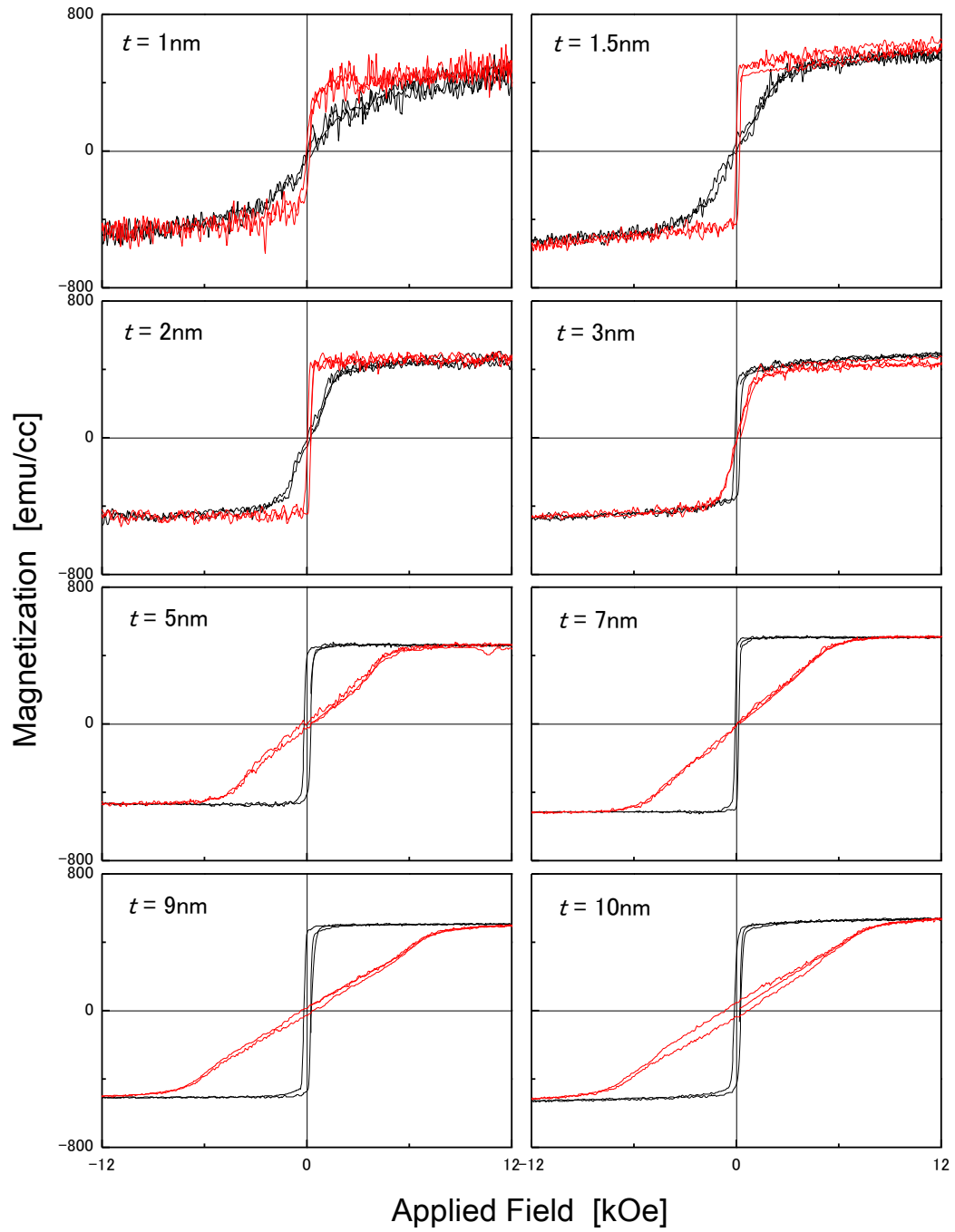
Figure 3-9 Magnetic hysteresis loops of AlN (20nm)/[Fe$_{0.4}$Pt$_{0.6}$ (t)/AlN (20nm)]$_5$ layered structures annealed at 500°C.
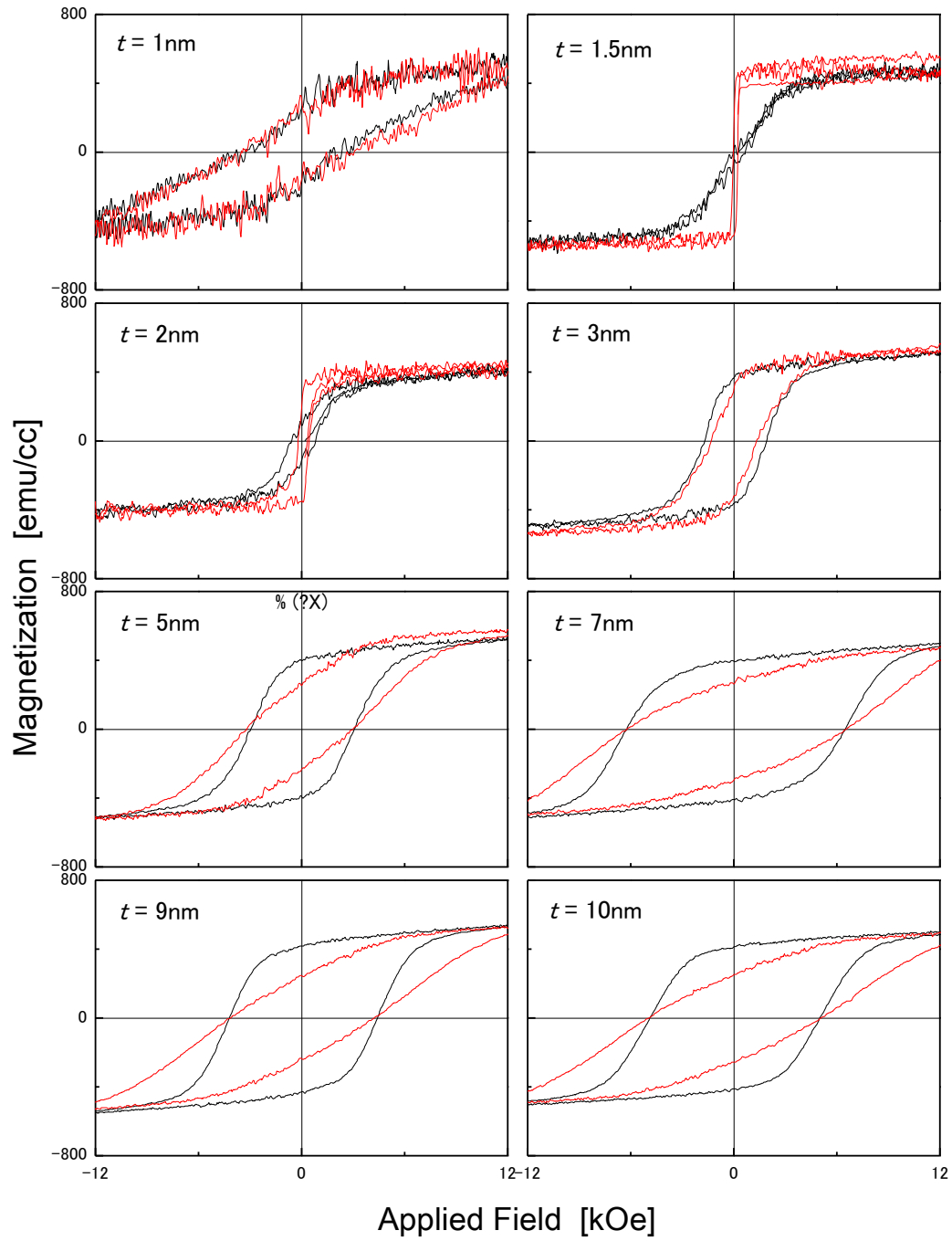
Figure 3-10 Magnetic hysteresis loops of AlN (20nm)/[Fe$_{0.4}$Pt$_{0.6}$ (t)/AlN (20nm)]$_5$ layered structures annealed at 700°C.

Chapter 4 Mechanism of magnetic anisotropy transition in FePt/AlN layered structures

4.1 Introduction

Layered structures (multilayer films) with perpendicular magnetic anisotropy (PMA) have drawn much research interest for their potential applications in high density magnetic recording.[1, 2] Figure 4-1 shows the schematic of the layered structure. Because of the abundance of interfaces, layered structures offer the possibility that the anisotropy can be dominated by the contributions of interfacial atoms. Carcia *et al* firstly reported PMA for layered structure (LS) in Co/Pd system.[3,4] They found Pd/Co layered structures have PMA when the Co layer is below 8Å and a inverse Co thickness dependence of anisotropy energy and anisotropy field, then attributed the PMA to the interface anisotropy which is originated from the lowered symmetry at the interface, as theoretically predicted by Néel for thin film materials.[5] Later, PMA has also been found in other metal/metal LS, such as Co/Pt,[4] Co/Au, Co/Ru.[6] Such interface anisotropy can be enhanced by improving the interface quality. den Broeder *et al*[7] reported that for Co/Au LS, the films show PMA until the Co thickness is 14Å after annealing at 250-300°C, and explained this effect by a strongly enhanced interface anisotropy, which is due to sharpening of the interfaces. G. Gubbiotti *et al* have also studied the effect of annealing on magnetic properties of Co/Au LS at 250°C, and confirmed the enhancement of PMA for LS with Co thickness 9 and 12 Å.[8]

Magneto-elastic effect is another important source of PMA for layered structures. Chappert *et al*[9] suggested that large strains can develop within layers because of the lattice mismatch at the interface, and such strain can significantly contribute to the

anisotropy of layered structures via magnetostriction effect. Lee *et al*[10] also considered that, for Co/Au and Co/Cu LS, magneto-elastic effect is the main source of PMA, and then explained the thickness dependence of anisotropy solely by the misfit strain variations in Co layer, which is caused by the coherent–incoherent transition as described by van der Merwe.[11] In our previous work we have firstly reported PMA in magnetic alloy/nitride-CoPt/AlN layered structures.[12] Good consistence between anisotropy transition and in-plane stress change strongly implies the contribution from magneto-elastic anisotropy.

In the previous chapter, we have found the perpendicular magnetic anisotropy in FePt/AlN layered structures. The perpendicular magnetic anisotropy appears after annealing, and the annealing shows different effects on magnetic property in the different FePt layer thickness ranges. In this chapter, the origin of the perpendicular magnetic anisotropy in annealed layered structure and the mechanisms of the FePt layer thickness and annealing effects on magnetic property will be investigated from the aspects of residual stress and interface quality.

4.2 Origin of perpendicular magnetic anisotropy in FePt/AlN layered structure

In chapter 3, we found the layered structure can undergo a gradual transition from in-plane anisotropy to perpendicular magnetic anisotropy with increasing annealing temperature. This interesting behavior is distinct from the well-studied metallic layered structures. In this section, the mechanism of such annealing temperature dependence of magnetic anisotropy will be studied using the AlN (20nm)/[FePt (2nm)/AlN (20nm)]$_5$ layered structure, which clearly shows the anisotropy transition when annealing at different temperatures.

4.2.1 Magnetic properties of AlN (20nm)/[FePt (2nm)/AlN (20nm)]$_5$ layered

structure

A series of hysteresis loops (M/H) taken from Sub/AlN20nm/(FePt2nm/AlN10nm)$_5$ layered structures annealed at different temperatures are shown in figure 4-2. The transition from in-plane anisotropy to PMA with increasing annealing temperature can be observed. The as-deposited film (figure 4-2a) shows in-plane anisotropy with magnetic anisotropy energy of -0.51×10^6 erg/cc. And then there is a crossover at an annealing temperature of 300 °C, the magnetization behaviors in the in-plane and perpendicular directions becomes almost the same (figure 4-2b). When annealed at 400 °C, the film shows clearly an easy axis of magnetization perpendicular to the film plane with a high remanent magnetization to saturation magnetization ratio in perpendicular direction (figure 4-2c). Then the magnetization in the in-plane direction becomes harder as annealing temperature further increases. When annealed at 600 °C, the film shows a relatively strong PMA with magnetic anisotropy energy of 1.06×10^6 erg/cc (figure 4-2e). However, it drops to 0.95×10^6 erg/cc for the film annealed at 700°C (figure 4-2f).

4.2.2 Microstructure

From the conventional x-ray diffraction results, as shown in figure 4-3, both as-deposited and annealed LS show preferred orientations of FePt [111] and AlN [001] parallel to the growth direction. After annealing, the intensities of the both FePt 111 and AlN 002 peak increases correspondingly, indicating the improvement of the crystalline quality and the preferred orientation. When annealing at temperatures above 500°C, highly symmetrical satellite peaks as a symbol of a periodic structure have been found around the FePt 111 peak, which stands for the interface quality of the FePt/AlN LS are enhanced by annealing in this work. Another phenomenon needed to mention is that the peak position of FePt 111 shifts to higher angles with the increasing of annealing temperature, meaning the reduction of FePt (111) interplanar

distance. The structure of the films was also characterized by electron diffraction using TEM. The electron diffraction pattern was taken from the LS annealed at 500°C, which was deposited on Si (100) wafer with a natural silicon oxide surface layer. From the inset figure in figure 4-3, a FePt (111) diffraction spot overlapping AlN (002) spot can be observed. This confirms the texture orientation of LS obtained by XRD. It also should be noted for FePt alloy, a disordered-ordered transformation may occur during annealing. In that case, the alloy will transform from a disordered FCC phase to an ordered FCT (L10) phase which possesses strong uniaxial magnetocrystalline anisotropy parallel with c-axis direction and can significantly increase the coercivity.[13-15] In the present work, no diffraction spot for the FePt (002) is found and all the films show relative small coercivity, so it is reasonable to consider that no order transformation occurred.

4.2.3 Stress analysis

The reduction in interplanar distance of FePt (111) orientated parallel with film surface strongly implies an in-plane stress transition tending to tensile inside the FePt layers. In order to understand the origin of PMA in this work, the stress change with annealing temperature was studied.

4.2.3.1 Fundamental of stress measurement by X-ray diffraction method

The X-ray diffraction method is expected to be one of the most useful techniques to measure the residual stress in polycrystalline thin films. The traditional XRD method for residual stress measurement is known as the $\sin^2\psi$ method, which is based on the measurement of the shift of a diffraction peak position recorded for different ψ angles.[16, 17] In this approach, a specific diffraction plane is selected and the interplanar spacing is measured from a coupled θ–2θ scan (standard Bragg–Brentano (B-B) geometry) of the specimen at different specimen tilt angle ψ—the angle between the diffracting plane normal and the specimen surface normal. Thereafter the

residual strain can be derived from the slope of a linear plot between the fractional change of the plane spacing (i.e. strain) and $\sin^2\psi$. In most cases a biaxial stress model is then used for thin film materials to convert the strain measured to the stress.

As shown in figure 4-4, the biaxial surface stress field is defined by the principal residual and/or applied stresses, σ_1 and σ_2, with no stress normal to the surface. The stress to be determined is the stress, σ_Φ, lying in the plane of the surface at an angle, Φ, to the maximum principal stress, σ_1. The direction of measurement is determined by the plane of diffraction. The stress in any direction (for any angle, Φ) can be determined by rotating the specimen in the x-ray beam. If the stress is measured in at least three different directions, the principal stresses and their orientation can be calculated. Consider the strain vector, $\varepsilon_{\Phi\psi}$, lying in the plane defined by the surface normal and the stress, σ_Φ, to be determined. $\varepsilon_{\Phi\psi}$ is at an angle ψ, to the surface normal, and can be expressed in terms of the stress of interest and the sum of the principal stresses as $\varepsilon_{\Phi\psi}=((1 + v)/E)\sigma_\Phi \sin^2\psi - (v/E)(\sigma_1 + \sigma_2)$. If we express the strain in terms of the crystal lattice spacing as $\varepsilon_{\Phi\psi}=(d_{\Phi\psi}-d_0)/d_0$, where d_0 is the stress-free lattice spacing, the strain becomes the lattice spacing measured in the direction Φ, ψ.[18]

However, the problem encountered in using this method is that the change of interplanar spacing is not solely due to the strain in all the cases. In generally, the interplanar spacing can be affected by the strain, symmetry change and crystal lattice distortion caused by other reasons. Therefore, the interplanar spacing change in the equation above stands for the total lattice distortion, not the strain. It will bring errors when evaluating the stress by this total crystal lattice distortion.

To solve this problem, a method which evaluates the stress via primitive cell was proposed by our group. Figure 4-5 shows the schematic of FCC unit cell, in which red lines compose the primitive cell of FCC lattice. If there is no lattice distortion in the crystal, we can get $a_p =a_{FCC, bulk}/\sqrt{2}$, $\alpha = 60°$, where a_p, $a_{FCC, bulk}$ are the lattice

constants of the primitive cell and FCC unti cell (bulk value) respectively, α is the lattice angle of primitive cell. Therefore, the lattice distortion can be exactly described by the change of the lattice parameter of primitive cell. For example, the schematic of the FePt (111) textured structure is shown in figure 4-6. If there is no lattice distortion, the lattice parameters of primitive cell are equivalent to bulk values. When a_p is larger than the bulk value and α remains unchanged, this stands for a simple expansion. If the α is larger than 60°, this means the crystal texture is undergoing a tensile stress.

For (111) textured film, α can be obtained by measuring the interplanar distances of (111) and (11-1) planes at $\psi = 0°$ and 70.5°, respectively. The interplanar distance of primitive cell can be expressed as

$$\frac{1}{d_{h_p k_p l_p}^2} = \frac{(h_p^2 + k_p^2 + l_p^2)\sin^2\alpha_p + 2(h_p k_p + k_p l_p + h_p l_p)(\cos^2\alpha_p - \cos\alpha_p)}{a_p^2(1 - 3\cos^2\alpha_p + 2\cos^3\alpha_p)}.$$

It can be further written as

$$\left(\frac{d_{1\bar{1}\bar{1}}}{d_{111}}\right)^2 = \left(\frac{d_{0_p 0_p 1_p}}{d_{1_p 1_p 1_p}}\right)^2 = \frac{3\sin^2\alpha_p + 6(\cos^2\alpha_p - \cos\alpha_p)}{\sin^2\alpha_p} = 3\left(\frac{1 - \cos\alpha_p}{1 + \cos\alpha_p}\right).$$

Therefore, α can be expressed by the interplanar distances of FCC (111) and (11-1) planes as

$$\alpha_p = \cos^{-1}\left(\frac{3 - \left(\frac{d_{1\bar{1}\bar{1}}}{d_{111}}\right)^2}{3 + \left(\frac{d_{1\bar{1}\bar{1}}}{d_{111}}\right)^2}\right) = \cos^{-1}\left(\frac{3d_{111}^2 - d_{1\bar{1}\bar{1}}^2}{3d_{111}^2 + d_{1\bar{1}\bar{1}}^2}\right).$$

For the plane stress under an equi-biaxial state, it can be derived by the deviation of α from 60°,

$$\Delta\alpha_p = \frac{2\sqrt{3}}{9}\frac{S_2^{111}\sigma_{\parallel}}{1 + (2S_1^{111} + (1/9)S_2^{111})\sigma_{\parallel}}.$$

4.2.3.2 Stress evaluation for AlN (20nm)/[FePt (2nm)/AlN (20nm)]5 layered structure

The residual stresses in thin film is in most cases under the plane stress state, and considering the FePt layers have fiber texture with the axis of <111> perpendicular to the film surface, it is reasonable to assume a state of equi-biaxial stress, i.e. $\sigma_1=\sigma_2=\sigma_\parallel$, $\sigma_3=0$, where $\sigma_\parallel$ is the stress of any direction in the film plane. Therefore, the in-plane stresses can be derived by measuring the interplanar distance of FePt {111} planes at $\psi=0°$ and 70.53°.

Figure 4-7 shows the 2θ-ω XRD profiles of layered structures with different tilting angle of scattering vector, $\omega=0°$ (figure 4-7(a)) and $\omega=70.53°$ (figure 4-7(b)), with respect to the film normal. Peak fittings were performed and the interplanar distances were specified by software highexpert. Then the in-plane stresses can be derived with $S_{11}=8.24\times10^{-3}$ GPa^{-1}, $S_{12}=-3.41\times10^{-3}$ GPa^{-1} and $S_{44}=10.5\times10^{-3}$ GPa^{-1}, which are calculated from the stiffness tensor of bulk FCC FePt crystals ($C_{11}=291.2$ GPa, $C_{12}=205.3$ GPa and $C_{44}=95.1$ GPa).[19]

The lattice angle of primitive cell are plotted with annealing temperature and shown in figure 4-8. And the in-plane stresses are also plotted with annealing temperature and shown in figure 4-9. Large compressive stresses are found in the as-deposited film. Upon annealing, such stresses are gradually released as temperature increases. When annealed at 700 °C, the stresses turn to tensile. Generally speaking, stresses in thin films have three main origins: intrinsic stresses (usually compressive) brought about by the nature of the sputtering process; thermal stresses due to the differences in thermal expansion coefficients of two constituents and stress caused by lattice mismatch between two dissimilar layers.[20,21] We believe the stress transition in the FePt layer can be attributed to the relaxation of in-plane compressive stress through annealing and the interfacial constraints coming from AlN layer. It is known

that FePt alloy has a thermal expansion coefficient in bulk value more than twice as large as AlN,[22] so the contraction of FePt layers along the in-plane directions will be restricted by AlN layer in the cooling process after annealing, then a tensile stress can be introduced.

The existence of stress can affect the magnetic anisotropy in the form of magnetoelastic energy. The magneto-elastic energy per unit volume inside a film is given by $E_{me}=-(3/2)\lambda\sigma\cos^2\theta$,[23] where λ is the magnetostriction constant along the magnetization direction, σ is the stress and θ is the angle between the magnetization and stress directions. It is known that the FePt alloy has a positive magnetostriction constant,[24, 25] so in-plane compressive stresses ($\sigma<0$) can result in a positive magnetoelastic anisotropy which favours the magnetization in perpendicular direction according to the equation above. However, the PMA of the annealed layered structures cannot be explained solely by the magnetoelastic effect, because the as-deposited films undergo larger compressive stress, nevertheless, they show in-plane magnetic anisotropy.

4.2.4 Interface quality analysis

As mentioned above, the interface quality plays an important role in determining the interface anisotropy. Draaisma *et al*[26] also reported higher interface anisotropy for vapor-deposited Co/Pd LS which was attributed to their sharper interfaces. However, for *M*/*M* films, interfacial diffusion is often occurred accompanying by the weakening of the satellite reflections and a decrease of the anisotropy.[27] According to the XRD results (figure 4-3) shown above, it is found that the interfacial diffusion are effectively avoided by using nitride AlN layers and the interface quality is improved by annealing process. To confirm this effect of annealing on the interface quality, XRR measurement and TEM observation were performed. Figure 4-10 shows the XRR profiles of the films annealed at different temperatures. A number of

superlattice peaks can be identified for all the films, indicating good periodicity of the layered structures. What is important is that, the decay rate of amplitude of the oscillation at higher angles decreases with increasing annealing temperature. This suggests that the sharpness and flatness of interfaces are gradually improved by annealing. The TEM image as shown in figure 4-11 is taken from the film annealed at 500°C. The image reveals flat and distinct interfaces between FePt and AlN layers, which confirm such improvement. The annealing effect on interface flattening can be explained by the removal of defects and the coalescence of grains. On the other hand, den Broeder *et al* suggested a backward diffusion between two insoluble layers, which meant the mixed regions could turn back to the pure layers by thermal treatment. They found the Co/Au interfaces become sharper due to this "negative" diffusion by annealing at 250°C or 300°C, but when annealed at 400°C the periodic structure was found to be destroyed.[7] In this work, it is proved that the interface quality can be improved through annealing until relative higher temperature, while the periodic structure is maintained.

4.2.5 Discussions on the origin of perpendicular magnetic anisotropy in FePt/AlN layered structure

It is known that the interface anisotropy arises from the asymmetric environment of interface atoms as compared with bulk atoms, so it is very sensitive to the precise distribution of magnetic and nonmagnetic atoms at the interface. With a rough interface, some in-plane neighbors are lacking, leading to a reduction of this asymmetry as compared to atoms located at the middle of flat areas. The relation between interface anisotropy and interface quality can be express as $\Delta K_N/K_N = -2\sigma/\xi$,[9] where σ is roughness and ξ *is* the correlation length. Therefore, the reduction of interface anisotropy can be restrained by the interface flattening, that is to say, the improvement of interface quality will result in a strongly enhanced interface

anisotropy, and then promote the magnetization in perpendicular direction for the annealed FePt/AlN layered structures. For the weakening of PMA in film annealed at 700°C, it can be explained by the relative larger change in stress between 600°C and 700°C, which may override the contribution from interface anisotropy.

In summary, the interface anisotropy and the magnetoelastic anisotropy can both contribute to the magnetization in perpendicular direction, resulting in weaker in-plane anisotropy of as-deposited FePt/AlN layered structure comparing to the FePt single layer film. Upon annealing, although the contribution of magnetoelastic anisotropy is decreasing due to the stress transition, the enhancement of interface anisotropy is dominated. Therefore, the perpendicular magnetic anisotropy appears in the annealed layered structure.

For the FePt alloy composition dependence of magnetic property, one consideration is that since the number of valence electrons is related to the composition of FePt alloys, the position of Fermi level, which affects the magnetocrystalline anisotropy, are varied by changing the alloy composition. On the other hand, the magnetostriction constant that is sensitive to alloy composition can affect the magnetic anisotropy in the form of magnetoelastic energy as discussed above. The expected magnetostriction constant change may be also responsible for the different magnetic behaviors of FePt/AlN layered structures with different FePt alloy compositions.

4.3 Magnetic anisotropy energy of FePt/AlN layered structure

In the previous section, the magnetic behavior of AlN (20nm)/[FePt (2nm)/AlN (20nm)]$_5$ layered structure has been discussed. In this section, the magnetic anisotropy energy of layered structures with different FePt layer thicknesses and annealing temperatures are studied for giving an overview of magnetic anisotropy transition in FePt/AlN layered structure.

4.3.1 Calculations of magnetic anisotropy energy

The (effective) magnetic anisotropy energy (K_{eff}) is calculated by measuring the area between the in-plane and the perpendicular hysteresis loops as introduced in chapter 2. To ease understanding, it is defined that the positive (negative) K_{eff} indicates the perpendicular (in-plane) magnetic anisotropy.

Figure 4-12 shows the products of the K_{eff} and FePt layer thickness t_{FePt} for the FePt/AlN layered structures shown in figure 3-7 to figure 3-10. As seen in this figure, the as-deposited layered structures undergo a magnetic anisotropy transition from isotropy (K_{eff} is about zero) to in-plane anisotropy (K_{eff} is negative) as FePt layer thickness increases. For the annealed films, perpendicular magnetic anisotropy (K_{eff} is positive) appears in layered structures with small t_{FePt}, and transits into in-plane anisotropy when t_{FePt} is over a critical thickness. However, the annealing shows different effects on magnetic anisotropy in the different t_{FePt} range as mentioned in chapter 3, and it can be clearly observed in this figure. The magnetizations in perpendicular direction are gradually enhanced as annealing temperature increases for layered structures with t_{FePt} below 5nm, resulting in the improvement of perpendicular magnetic anisotropy and the increase of critical t_{FePt} for magnetic anisotropy transition from perpendicular to in-plane direction. The layered structures of t_{FePt}= 1.5 and 2nm annealed at 500°C show magnetic anisotropy energies of 0.90×10^6 erg/cc and 0.52×10^6 erg/cc respectively. For the layered structures with t_{FePt} above 5nm, the in-plane magnetic anisotropy is enhanced upon annealing, and such enhancement is more obvious in the films with larger t_{FePt}. It is seemed that 5nm is the critical thickness for the different annealing effects, because the 5nm layered structure shows almost the same magnetic anisotropy energy when annealing at different temperatures.

4.3.2 Volume contribution and interface contribution of magnetic anisotropy

energy

The effective magnetic anisotropy energy K_{eff} (erg/cm^3) could be phenomenologically separated in a volume contribution K_V (erg/cm^3) and an extra interface contribution K_S (erg/cm^2) and approximately expressed as $K_{eff} = K_V + 2K_S/t$, where t is the thickness of a magnetic layer. This relation represents a weighted average of the magnetic anisotropy energy of the interface atoms and the inner atoms of a magnetic layer of thickness t. Also the layer is assumed to be bounded by two identical interfaces accounting for the prefactor 2. This equation can be also written as $K_{eff} \cdot t = K_V \cdot t + 2K_S$. Therefore, by estimating the value of $K_{eff} \cdot t$ at $t_{FePt} = 0$, the K_S can be directly determined from figure 4-12. For layered structures as-deposited, annealed at 300°C and 500°C, the $2K_S$ are 0.21 erg/cm^2, 0.40 erg/cm^2 and 0.69 erg/cm^2 respectively. It is clear that the K_S (K_S incorporates Néel-type interface anisotropy, this will be introduced in the next section) is gradually enhanced as annealing temperature increases, which is responsible for the magnetic anisotropy transition discussed in the previous section. This result has shown the advantage of metal/ceramic layered structure in improving the K_S, because the K_S of metallic layered structures is always strongly depressed by the interdiffusion or intermixing, especially after thermal annealing.

4.4 Mechanism of magnetic anisotropy transition in FePt/AlN layered structure

In the previous sections, we have found the interface anisotropy and magnetoelastic anisotropy can affect the magnetic behavior of FePt/AlN layered structure. In this section, the mechanism of magnetic anisotropy transition as shown in section 4.3 is discussed from the aspects of residual stress and interface quality analyses.

4.4.1 Residual stress in FePt/AlN layered structure

The magnetoelastic anisotropy is caused by reverse magnetostriction effect as introduced in chapter 1. The existence of stress can affect magnetic anisotropy in the form of the magnetoelastic energy. Therefore, it is necessary to study the residual stress transition in FePt/AlN layer structure when changing the FePt layer thickness and annealing temperature.

The in-plane residual stresses in FePt layer are analyzed by measuring the interplanar distance of FePt {111} planes at $\psi=0°$ and $70.53°$, with respect to the film normal. The 2θ-ω XRD profiles of as-deposited and annealed AlN (20nm)/[FePt (t)/AlN (20nm)]$_5$ (t =3nm, 5nm, 7nm and 9nm) layered structures measured at different tilting angle of scattering vector are shown in figure 4-13 to figure 4-16. It is clear that all the layered structures show preferred orientations of FePt [111] and AlN [001] parallel to the growth direction. Upon annealing, the (111) peak positions of all the layered structures with different FePt layer thicknesses shift toward higher angle as annealing temperature increases, which implies the gradual change of residual stress inside the FePt layers. The FePt (111) peak position also shows some dependence on the FePt layer thickness, indicating the residual stress is also affected by the FePt layer thickness. In addition, the full widths at half maximum of FePt (111) peaks become smaller and smaller as the FePt layer thickness increases, owing to the increase of the FePt grain size in perpendicular direction. On the other hand, the FePt (11-1) peaks can be clearly observed in all the layered structures measured at $\psi=70.53°$, however, there is almost no position shift for the FePt (11-1) peaks as annealing temperature increases. All the peaks were fitted and the interplanar distances were specified by software HIGHEXPERT.

The in-plane stresses calculated from figure 4-13 to figure 4-16 are plotted against FePt layer thickness and shown in figure 4-17. Large compressive stresses,

brought about by the nature of the sputtering process, are found in the as-deposited layered structures with small FePt layer thickness. Such compressive stresses decreases gradually as the FePt thickness increases until 7nm. It is considered that the compressive stress is relieved through dislocations, which occurs more easily with larger thickness. Similar trends are also found in annealed layered structures, while the films show smaller and smaller compressive stresses as the annealing temperature increases, which can be explained by the stress relief due to annealing. Another important feature is that tensile stresses are developed in annealed films, and grow larger at high annealing temperature. We ascribe the appearance of this annealing temperature dependent tensile stresses to the large difference in thermal expansion coefficient between FePt and AlN. It is known that FePt has a thermal expansion coefficient in bulk value more than twice as large as AlN.

The magnetoelastic effect or magnetoelastic anisotropy energy can be described as $K_{me}=-(3/2)\lambda\sigma$, where λ is the magnetostriction constant along the magnetization direction, σ is the in-plane stress.[28] Since the FePt alloy has a positive magnetostriction constant, in-plane compressive stresses ($\sigma<0$) can result in a positive magnetoelastic energy which favours the magnetization in perpendicular direction according to the equation above. Therefore, as the annealing temperature increases, the residual stress transition from compressive to tensile in FePt layer will decrease this magnetoelastic energy which contributes to the perpendicular magnetization. When the stresses become tensile, the magnetoelastic energy turns to negative and favours the in-plane magnetization.

4.4.2 Interface quality of FePt/AlN layered structure

It is known that the interface quality plays an important role in determining the interface anisotropy. By improving the interface quality, the interface anisotropy can be strongly enhanced, and then promote the magnetization in perpendicular direction

for layered structure. In the previous section, we have found the interface quality of FePt/AlN layered structure is gradually improved upon annealing. In this section, the influence of FePt layer thickness on interface quality is studied.

The x-ray reflectivity measurements are performed by a Bruker D8 Advance diffractometer with Cu Kα irradiation operating at 40kV and 300mA. Figure 4-18 shows the XRR profile of the layered structure of AlN (20nm)/[FePt (3nm)/AlN (20nm)]$_5$ annealed at different temperatures. Bragg peaks which are caused by the modulation of the periodic structure can be clearing observed in all the films, indicating good periodicity and interface quality of the layered structures. The decay rate of amplitude of the oscillation at higher angles decreases as annealing temperature increases, indicating the interface quality is improved by annealing as well as the FePt 2nm layered structure discussed in section 4.2. Figure 4-19 shows the XRR profile of the as-deposited and annealed (300°C) AlN (20nm)/[FePt (5nm)/AlN (20nm)]$_5$ layered structures. The improvement effect of annealing on interface quality is also found. Figure 4-20 shows the XRR profile of the as-deposited AlN (20nm)/[FePt (9nm)/AlN (20nm)]$_5$ layered structure. The film maintains good interface quality. By summarizing the results shown above, it is found that the FePt layer thickness shows little influence on the interface quality, and the annealing process can improve the interface quality in whole FePt thickness range of this study. Therefore, the interface magnetic anisotropy of FePt/AlN layered structures with different FePt layer thicknesses can be considered to be the same, the magnitude of contribution from K_S depends only on the interface/volume atomic ratio according to the equation of $K_{eff} = K_V + 2K_S/t$.

4.4.3 Discussions on the mechanism of magnetic anisotropy transition in FePt/AlN layered structure

In general, shape anisotropy (or demagnetization energy), magnetocrystalline

anisotropy, magnetoelastic anisotropy $K_{me,V}$ compose the volume contribution K_V, and interface contribution K_S incorporates Néel-type interface anisotropy, magnetoelastic interface anisotropy $K_{me,S}$ originated from coherent stresses. However, since the lattice misfit between FePt and AlN layer is about 13% at interface, it is reasonable to consider that there is no coherent-incoherent strain transition occurred in FePt layers. The interface is supposed to be incoherent, consisting large quantity of dislocations. Under such assumption $K_{me,S}$ can be neglected in this work, and K_S is almost solely Néel-type. So for layered structure of t_{FePt} below 5nm, although the relief of compressive stress caused by annealing (shown in figure 4-17) will decrease the perpendicular (positive) magnetoelastic anisotropy as discussed above, the enhanced interface anisotropy becomes dominant then K_{eff} of annealed films increases. When t_{FePt} becoming thick, the contribution from K_S is relatively small according to the equation of $K_{eff} = K_V + 2K_S/t$, and tensile stresses developed during annealing will result in a negative magnetoelasitc anisotropy which overwhelms the interface anisotropy, thus decreases K_{eff} as shown in figure 4-12.

4.5 Summary

In this chapter, the origin of perpendicular magnetic anisotropy in FePt/AlN layered structure has been studied. It is found that the interface quality and residual stress in FePt layer strongly affect the magnetic anisotropy of layer structure in the form of interface anisotropy and magnetoelastic anisotropy respectively. Therefore, the mechanism of magnetic anisotropy transition in FePt/AlN layered structure has been investigated by disclosing the influences of annealing temperature and FePt layer thickness on the interfaces and stress condition. The conclusions are made as following:

1. The interface anisotropy and the magnetoelastic anisotropy can both contribute to

the magnetization in perpendicular direction, resulting in weaker in-plane anisotropy of as-deposited FePt/AlN layered structure comparing to the FePt single layer film.

2. The FePt/AlN interface quality is gradually improved with increasing annealing temperature, leading to the promotion of interface anisotropy which is responsible for the perpendicular magnetic anisotropy found in the annealed layered structure.

3. The residual stress in FePt layer undergoes a transition from compressive to tensile as annealing temperature increases. This will decrease the positive magnetoelastic energy which contributes to the perpendicular magnetization. When the stresses become tensile, the magnetoelastic energy turns to negative and favours the in-plane magnetization.

4. For layered structure of FePt layer thickness below 5nm, the enhanced interface anisotropy is dominant then the magnetic anisotropy energies of annealed films increases. When FePt layer thickness is above 5nm, the contribution from interface anisotropy is relatively small, and stress transition caused by annealing will modify the magnetoelasitc anisotropy then decreases the magnetic anisotropy energies as annealing temperature increases.

References

1. J. P. J. Groenland, C. J. M. Egkel, J. H. J. Flultman, R. M. deRidder, Sens. Actuators. A 30, 89 (1992).

2. D. J. Monsma, J. C. Lodder, Th. J. A. Popma, B. Dieny, Phys. Rev. Lett. 74, 5260 (1995).

3. P. F. Carcia, A. D. Meinhaldt, A. Suna, Appl. Phys. Lett. 47, 178 (1985).

4. P. F. Carcia, J. Appl. Phys. 63, 5066 (1988).

5. L. Néel, J. Phys. Radium 15, 225 (1954).

6. M. Sakurai, T. Takahata, I. Moritani, J. Magn. Soc. Japan. 15, 411 (1991).

7. F. J. A. den Broeder, D. Kuiper, A. P. van de Mosselaer, W. Hoving, Phys. Rev. Lett. 60, 2769 (1988).

8. G. Gubbiotti, G. Carlotti, F. Albertini, F. Casoli, E. Botempi, L. E. Depero, H. Koo, R. D. Gomez, Thin Solid Films 428, 102 (2003).

9. C. Chappert, P. Bruno, J. Appl. Phys. 64, 5736 (1988).

10. C. H. Lee, H. He, F. J. Lamelas, W. Vavra, C. Uher, R. Clarke, Phys. Rev. B 42, 1066 (1990).

11. J. H. van der Merwe, J. Appl. Phys. 34, 123 (1963).

12. Y. Hodumi, J. Shi, Y. Nakamura, Appl. Phys. Lett. 90, 212506(2007).

13. J. Bai, Z. Yang, F. Wei, M. Matsumoto, A. Morisako, J. Magn. Magn. Mater. 257, 132 (2003).

14. M. L. Yan, H. Zeng, N. Powers, D. J. Sellmyer, J. Appl. Phys. 91, 8471 (2002).

15. M. Daniil, P. A. Farber, H. Okumura, G. C. Hadjipanayis, D. Weller, J. Magn. Magn. Mater. 246, 297 (2002).

16. M. E. Hilley, Residual Stress Measurement by X-ray Diffraction, SAE J784a, Society of Automotive Engineers, Warrendale, PA (1971).

17. I.C. Noyan, J.B. Cohen, Residual Stress, Measurement by Diffraction and Interpretation, Springer-Verlag (1987).

18. P. S. Prevéy, Adv. in X-ray Analysis 20, 345-354 (1977).

19. J. S. Kim, Y. M. Koo, B. J. Lee, J. Appl. Phys. 99, 053906 (2006).

20. J. R. Jeong, S. C. Shin, Phys. Status Solidi B 241, 1706 (2004).

21. J.R. Jeong, S.C. Shin, J. Appl. Phys. 87, 6851 (2000).

22. X. Li, Z. H. Li, X. Liu, Y. B. Li, J. M. Bai, F. L. Wei, D. Wei, IEEE Trans. Magn. 46, 2024 (2010).

23. M. T. Johnson, P. J. H. Bloemen, F. J. A. den Broeder, J. J. de Vries, Rep. Prog. Phys. 59, 1409 (1996).

24. M. Pardavi-Horváth, L. I. Vinokurova, V. Yu. Ivanov, J. Magn. Magn. Mater. 41, 349 (1984).

25. M. Vásquez Mansilla, J. Gómez, E. Sallica Leva, F. Castillo Gamarra, A. Asenjo Barahona, A. Butera, J. Magn. Magn. Mater. 321, 2941 (2009).

26. H. J. G. Draaisma, F. J. A. den Broeder, W. J. M. de Jonge, J. Magn. Magn. Mater. 66, 351 (1987).

27. H. M. van Noort, F. J. A. den Broeder, H. J. G. Draaisma, J. Magn. Magn. Mater. 51, 273 (1985).

28. S. Honda, J. Ago, M. Nawate and N. Morita: IEEE Trans. Magn. **28** (1992) 2677-2679.
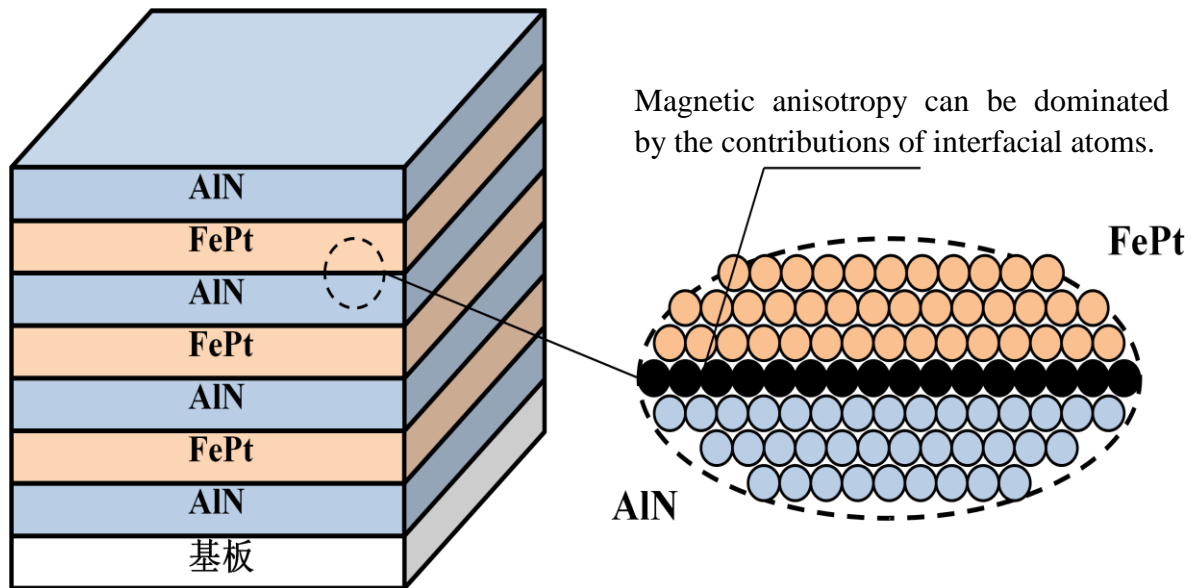
Figure 4-1 Schematic of the layered structure.
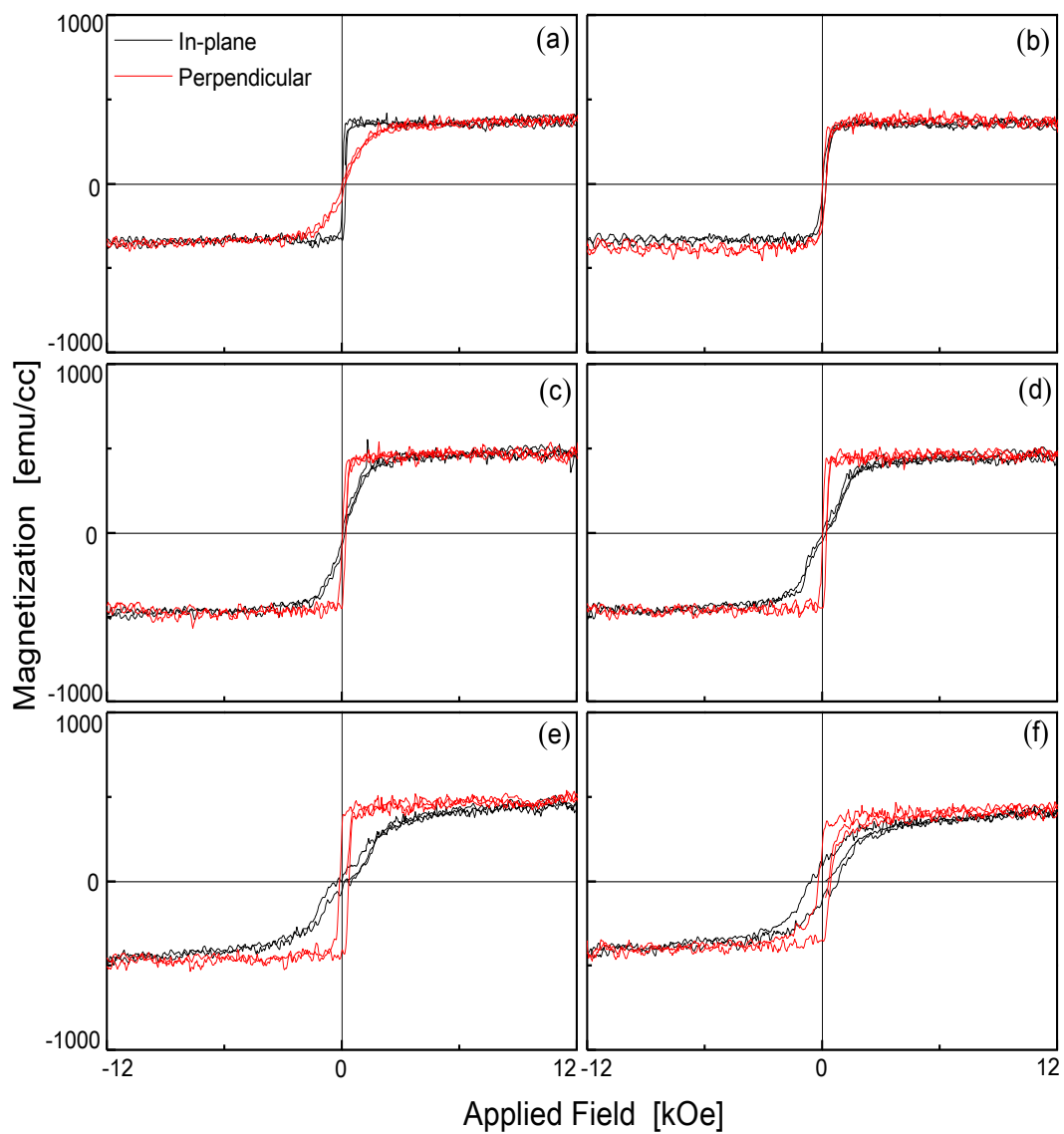
Figure 4-2 Hysteresis loops (M/H) of Sub/AlN20nm/(FePt2nm/AlN10nm)5 layered structures, (a) as-deposited, (b)-(f) vacuum annealed at 300 °C, 400 °C, 500 °C, 600 °C and 700 °C.
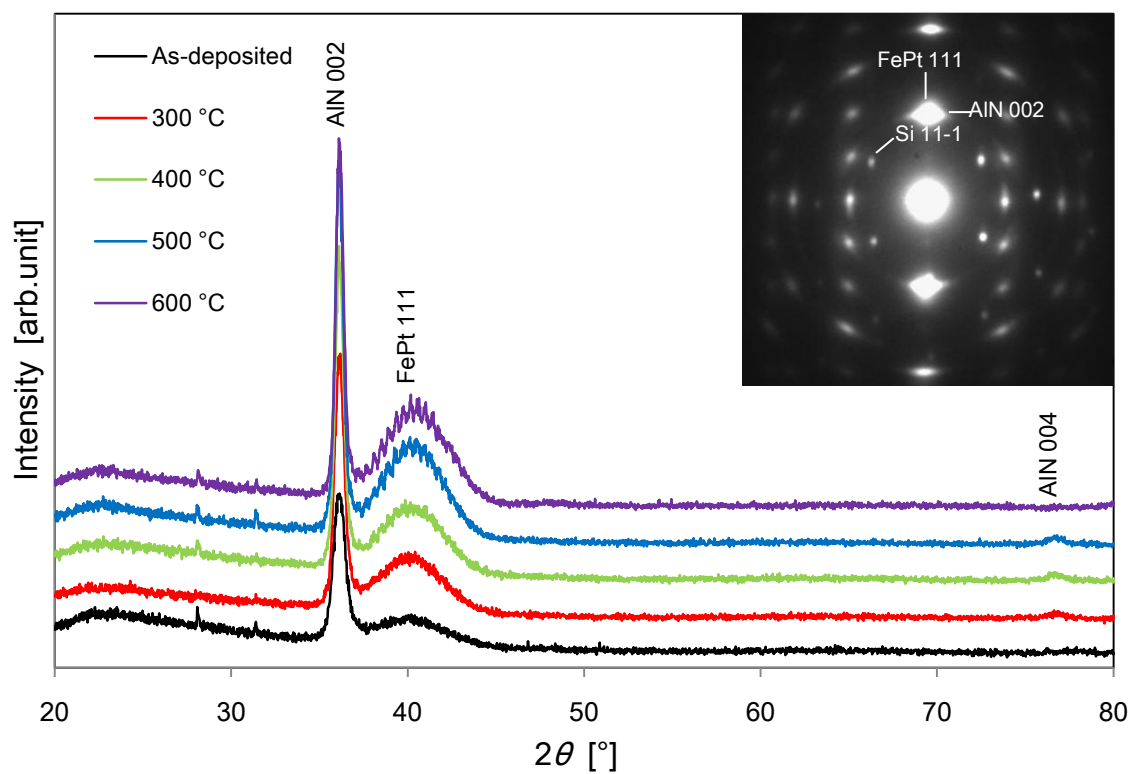
Figure 4-3 Conventional X-ray profiles of as-deposited and annealed AlN (20nm)/[FePt (2nm)/AlN (20nm)]$_5$ layered structure. The inset electron diffraction pattern is taken from a film annealed at 500 °C
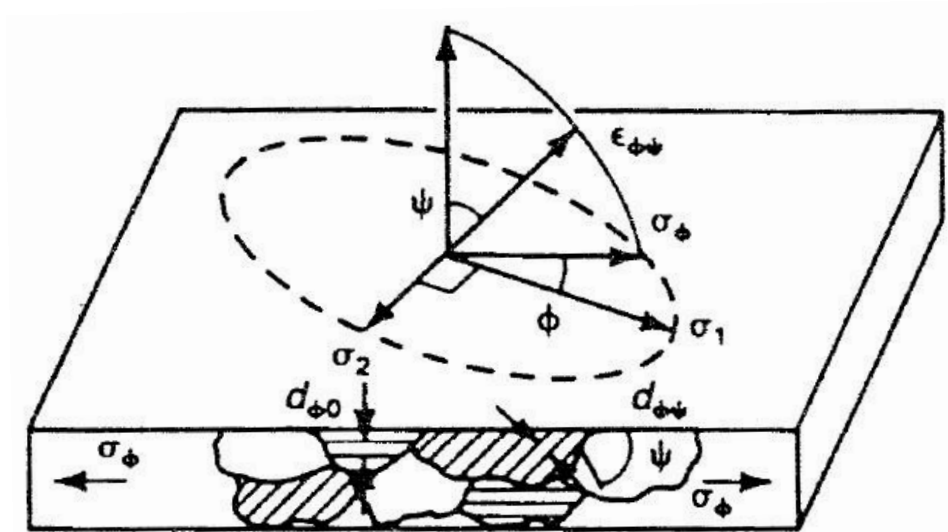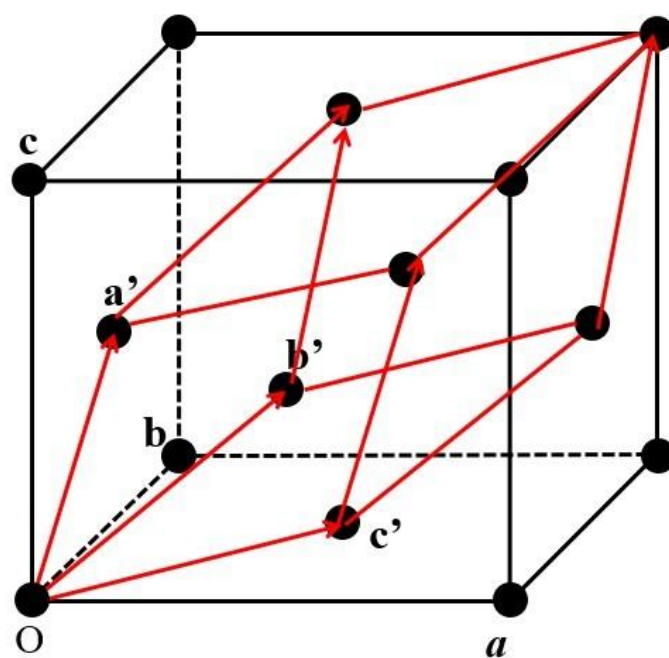
Figure 4-4 Plane Stress at a Free Surface.

Figure 4-5 Schematic of FCC unit cell. Red lines compose the primitive cell of FCC lattice.

FePt (111) texture

(111) plane

Bulk FePt

$a_p = a_{FCC, bulk}/\sqrt{2}$

$\alpha = 60°$

In-plane tensile stress

Simple expansion

$a_p \approx a_{FCC, bulk}/\sqrt{2}$

$\alpha > 60°$

$a_p > a_{FCC, bulk}/\sqrt{2}$

$\alpha = 60°$
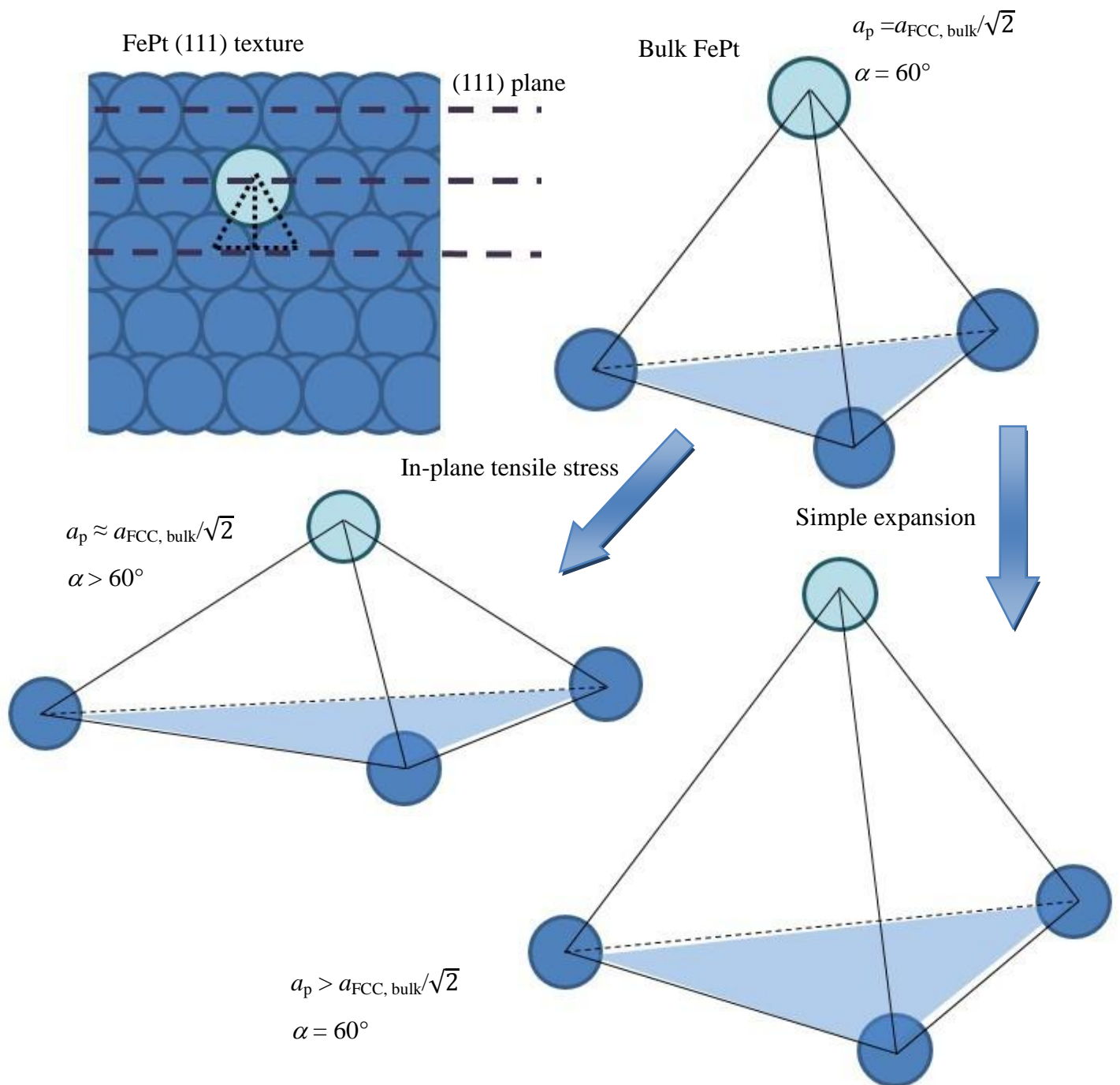
Figure 4-6 Stress determination by using primitive cell.
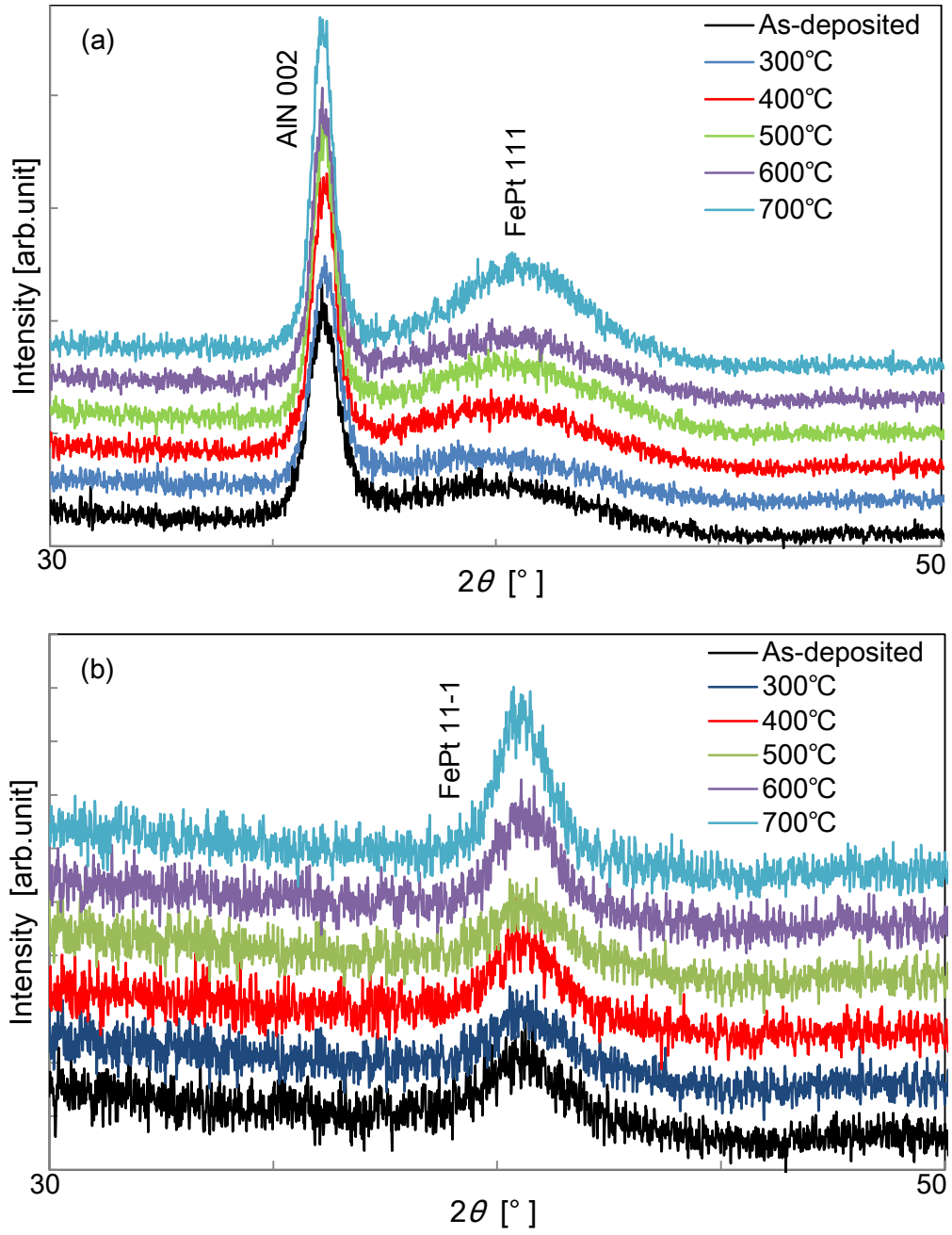
Figure 4-7 2θ-ω XRD profiles of AlN (20nm)/[FePt (2nm)/AlN (20nm)]$_5$ layered structures with different tilting angle of scattering vector, (a) ω=0° and (b) ω=70.53°.
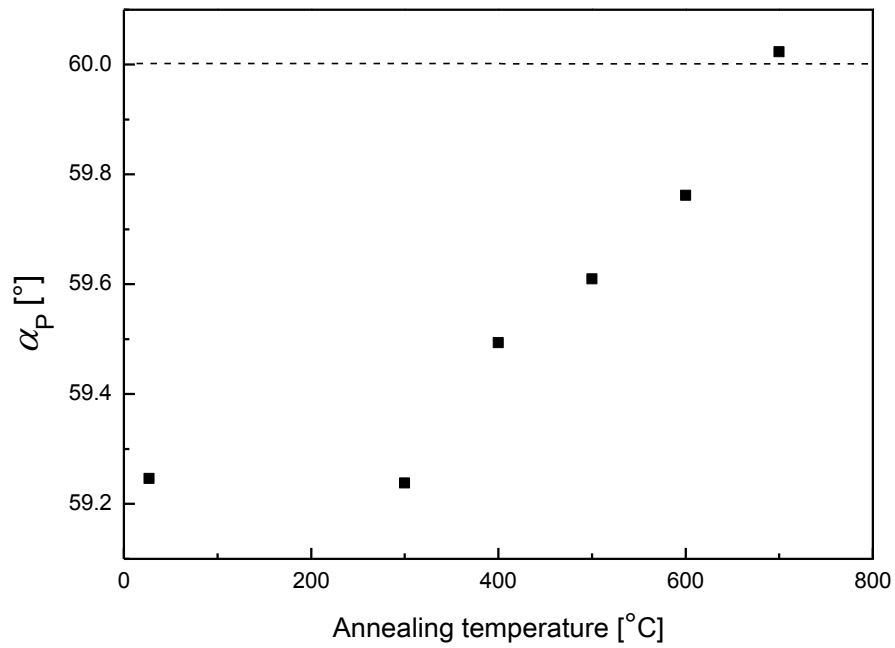
Figure 4-8 Lattice angle of primitive cell plotted with annealing temperature.
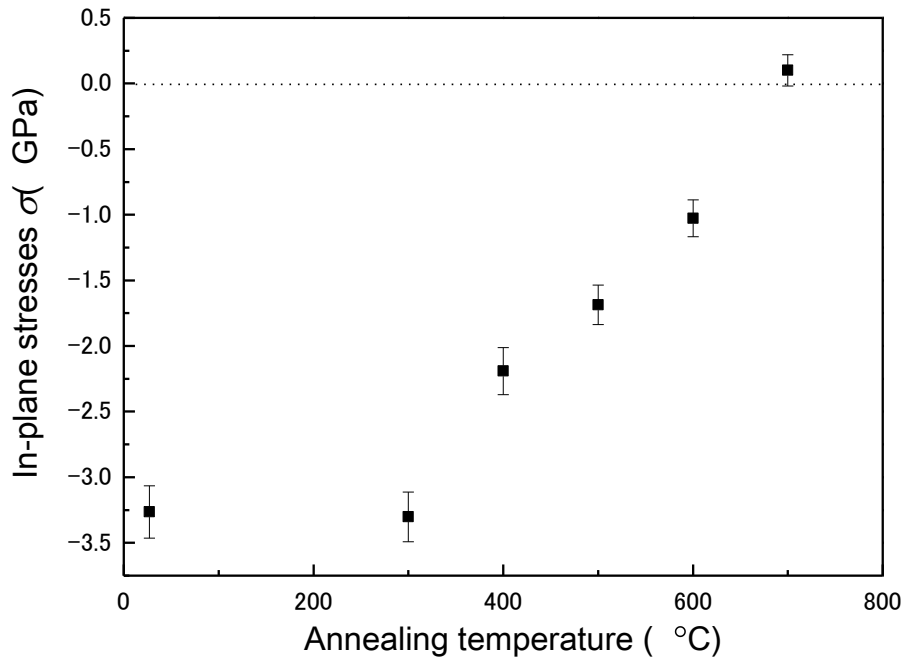
Figure 4-9 In-plane stresses in FePt layers as a function of annealing temperature.
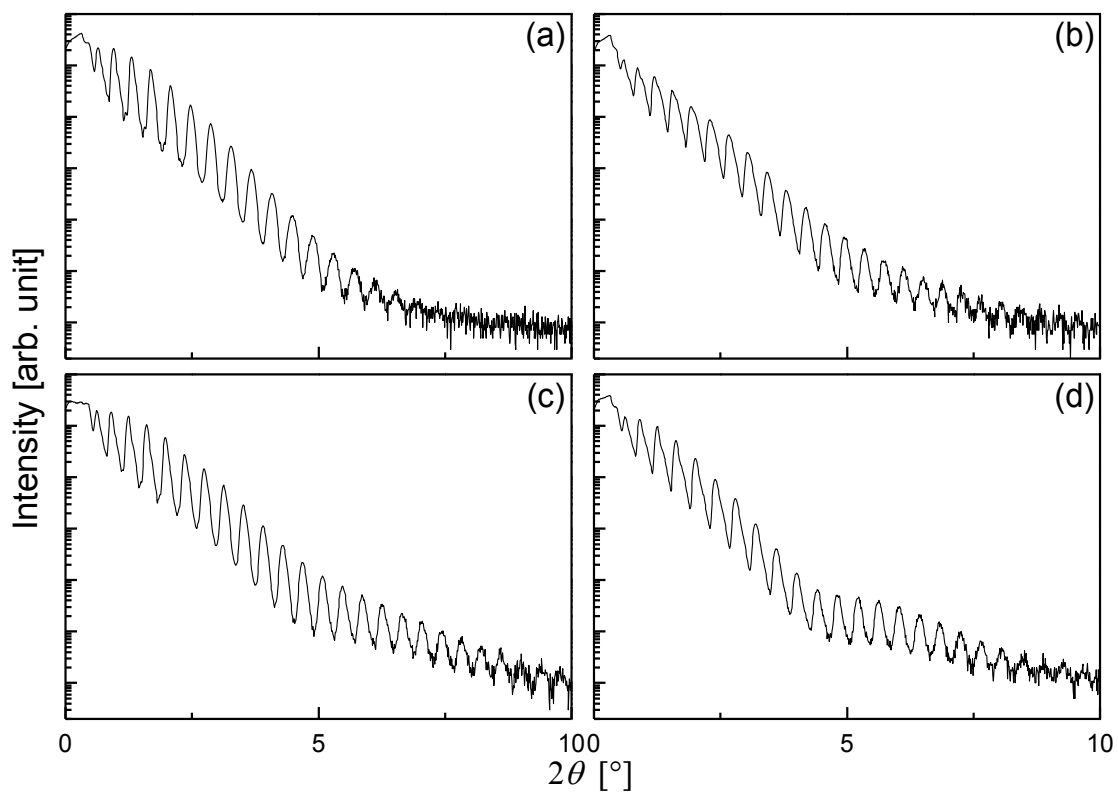
Figure 4-10 XRR profiles of AlN (20nm)/[FePt (2nm)/AlN (20nm)]$_5$ layered structures, (a) as-deposited, (b)-(d) annealed at 400 °C, 500 °C and 700 °C
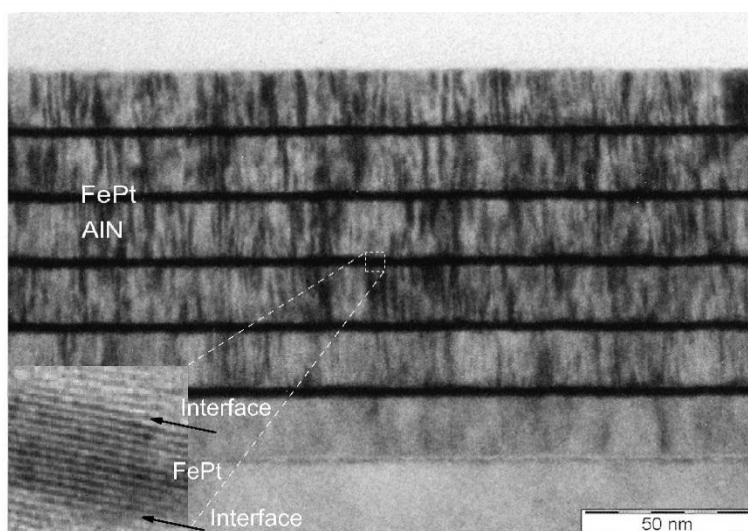
Figure 4-11 Cross-sectional TEM image of AlN (20nm)/[FePt (2nm)/AlN (20nm)]$_5$ layered structure annealed at 500°C.
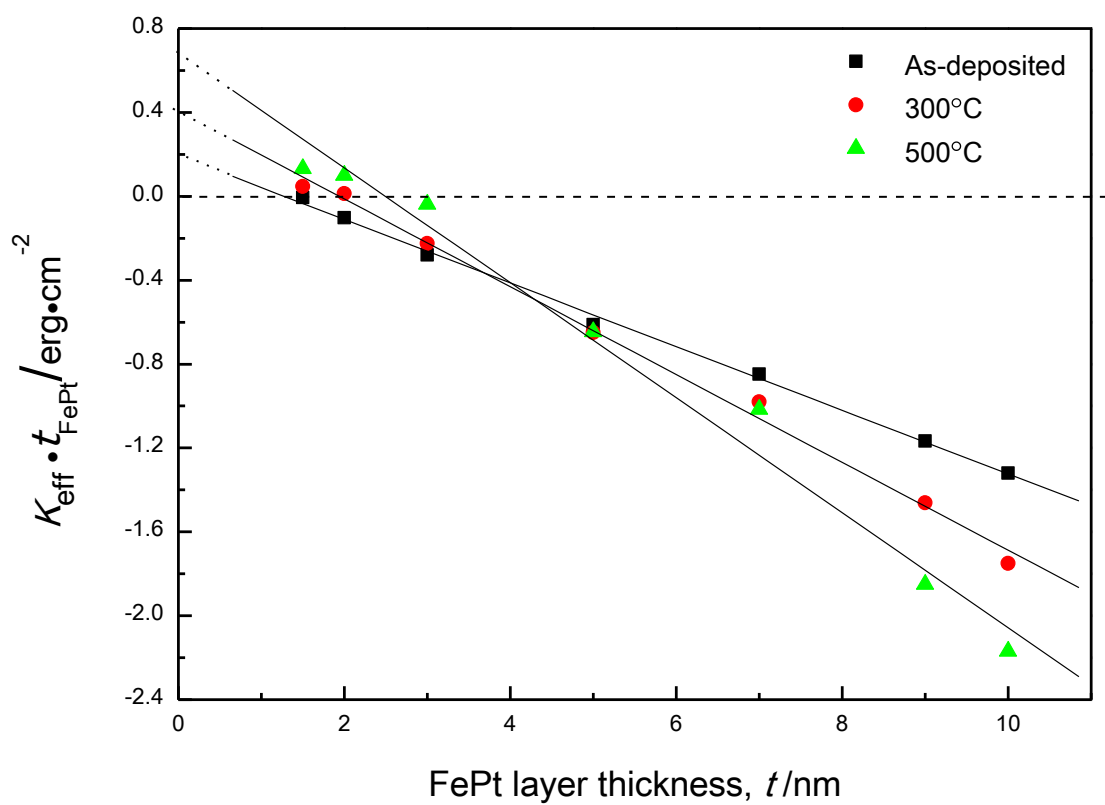
Figure 4-12 $K_{eff}\cdot t_{FePt}$ plotted against t_{FePt} for FePt/AlN layered structures annealed at different temperature.
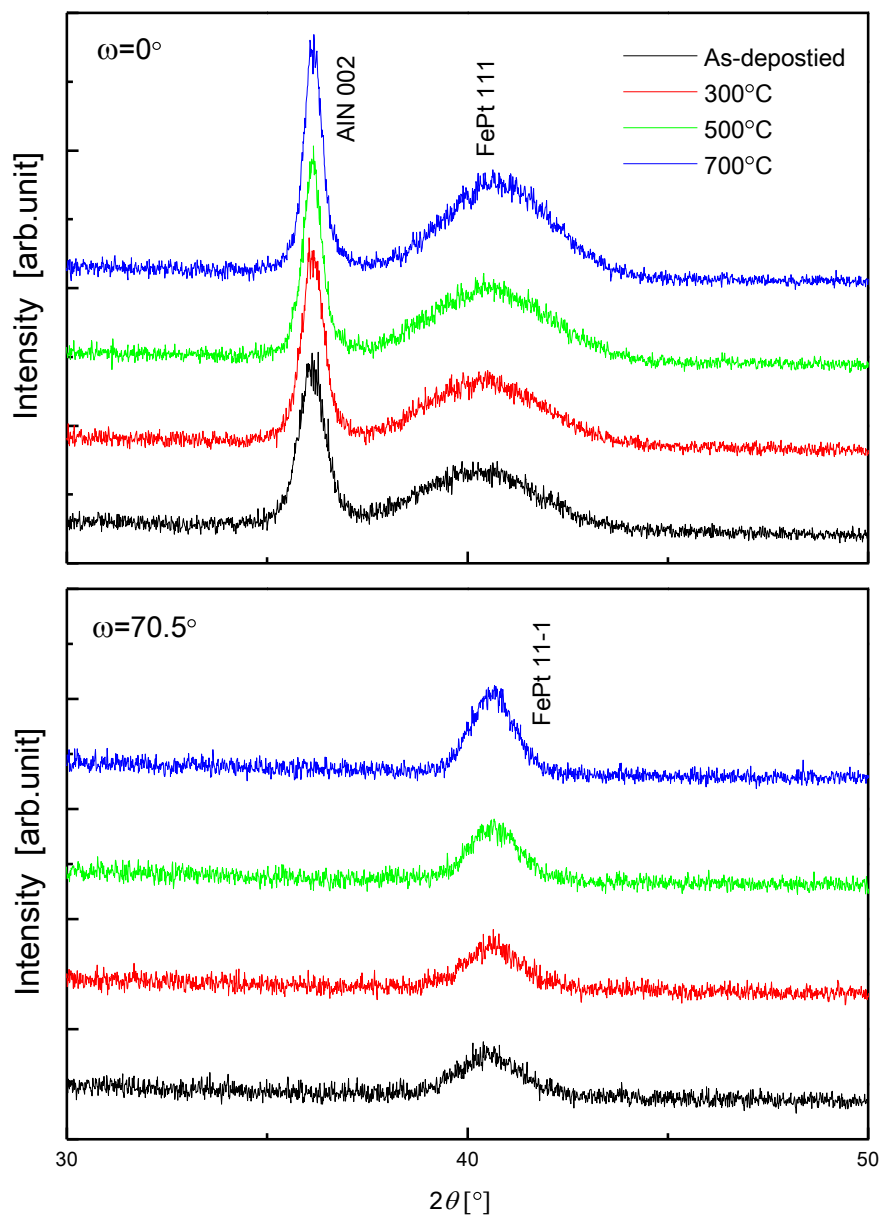
Figure 4-13 $2\theta\text{-}\omega$ XRD profiles of as-deposited and annealed AlN (20nm)/[FePt (3nm)/AlN (20nm)]$_5$ layered structures measured at different tilting angle of scattering vector.
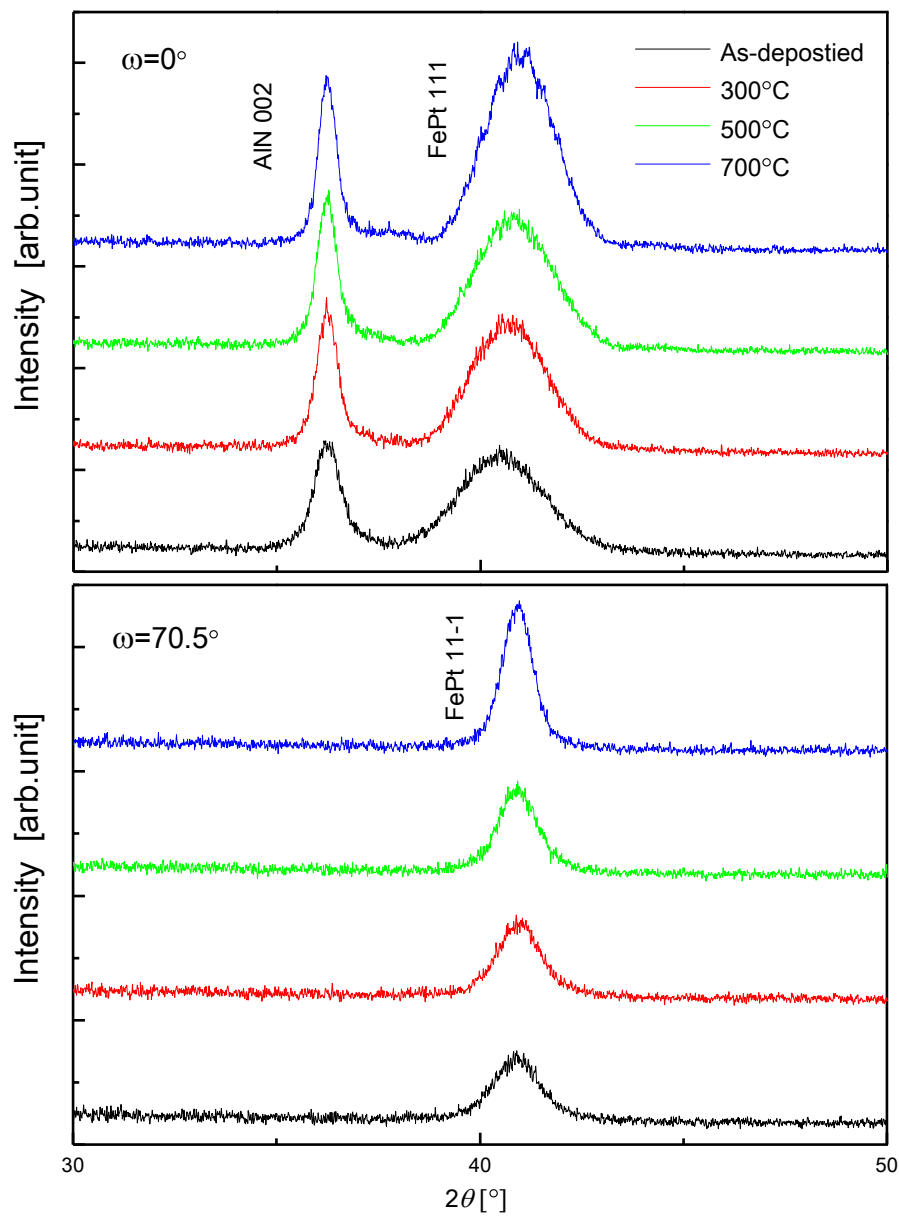
Figure 4-14 2θ-ω XRD profiles of as-deposited and annealed AlN (20nm)/[FePt (5nm)/AlN (20nm)]$_5$ layered structures measured at different tilting angle of scattering vector.
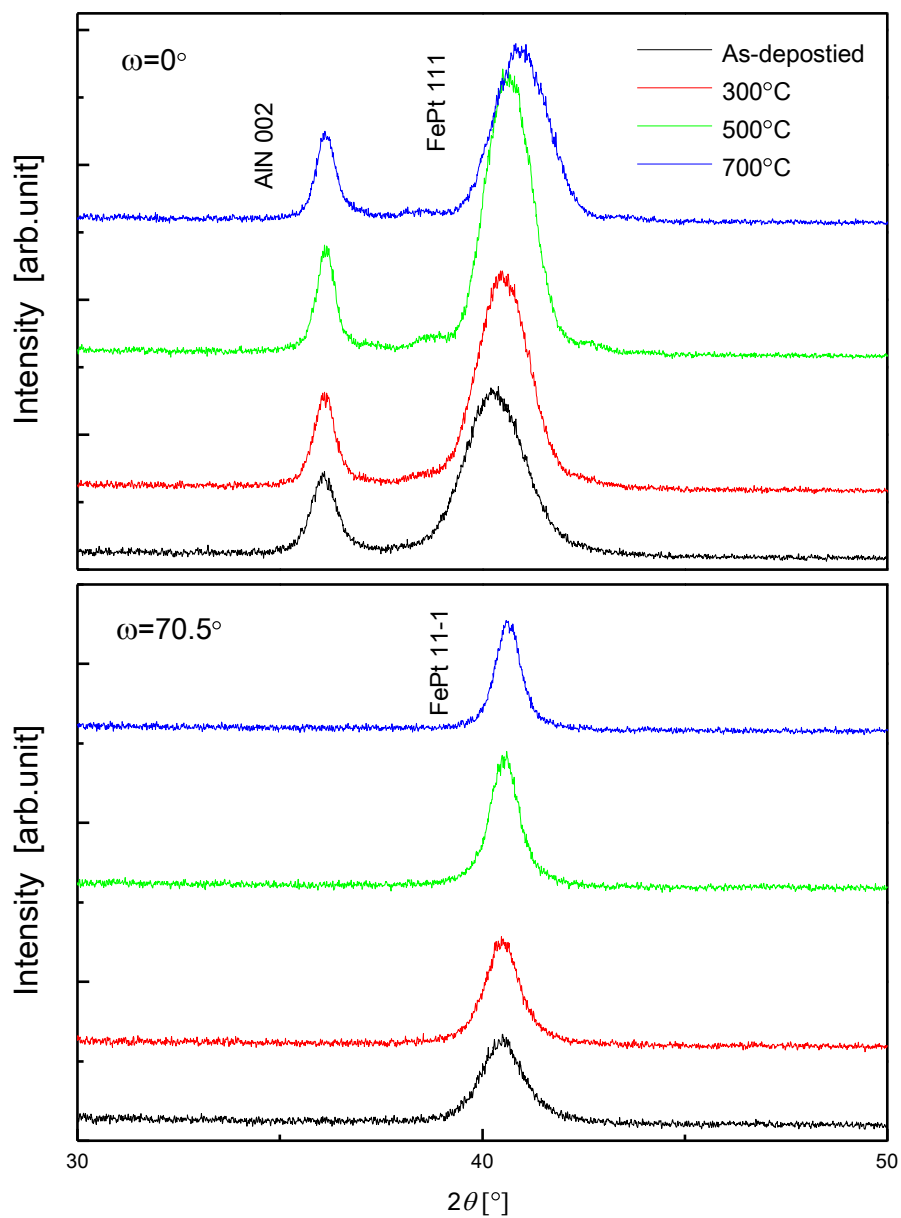
Figure 4-15 2θ-ω XRD profiles of as-deposited and annealed AlN (20nm)/[FePt (7nm)/AlN (20nm)]$_5$ layered structures measured at different tilting angle of scattering vector.

Figure 4-16 2θ-ω XRD profiles of as-deposited and annealed AlN (20nm)/[FePt (9nm)/AlN (20nm)]$_5$ layered structures measured at different tilting angle of scattering vector.
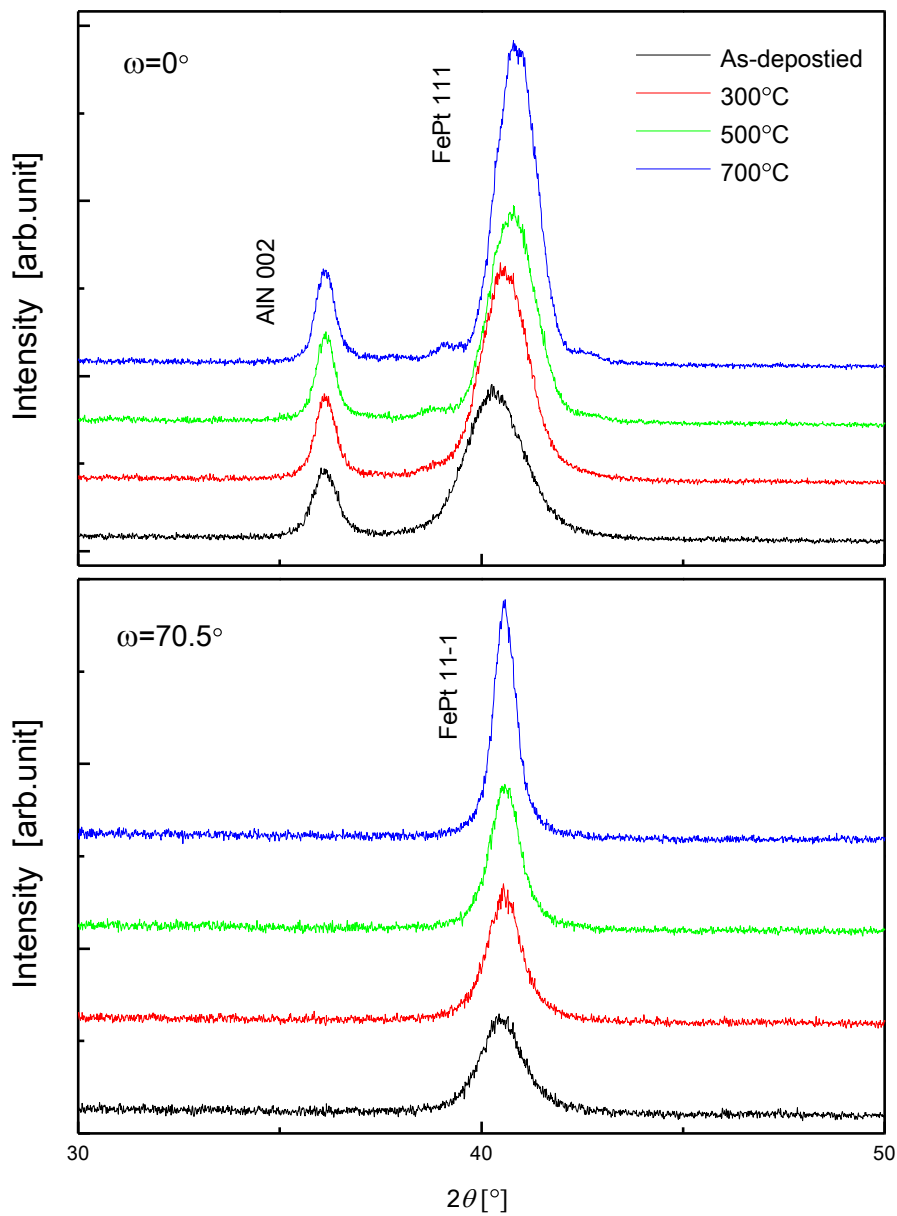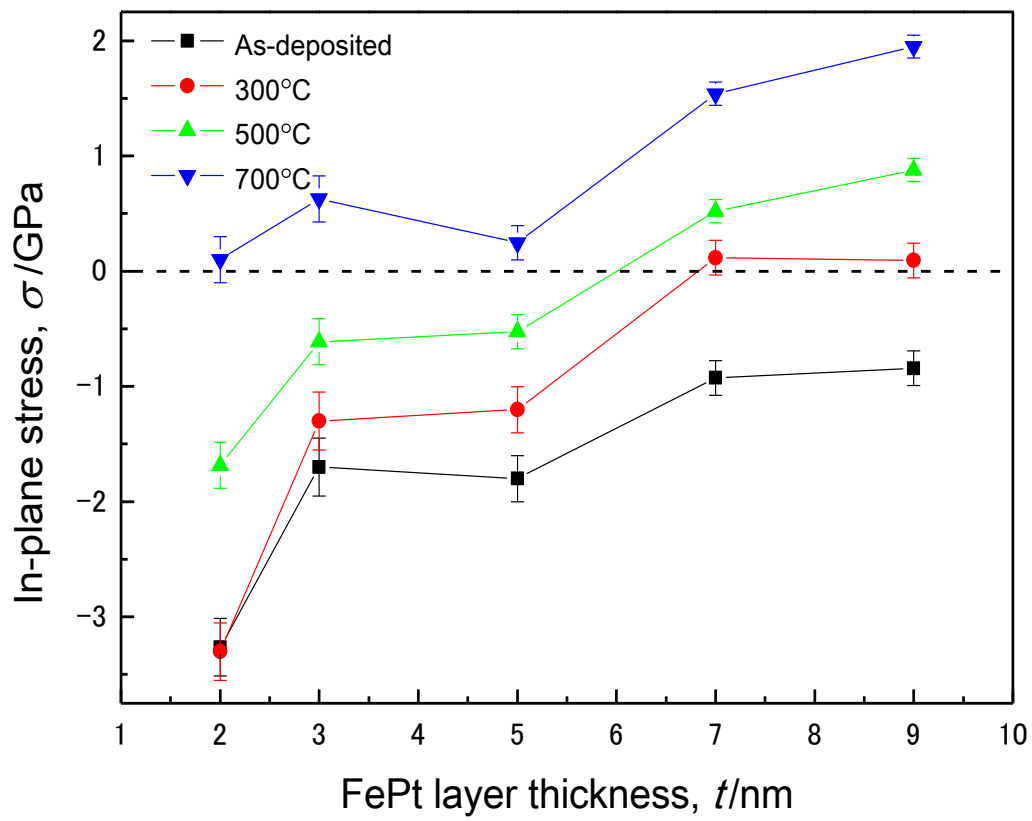
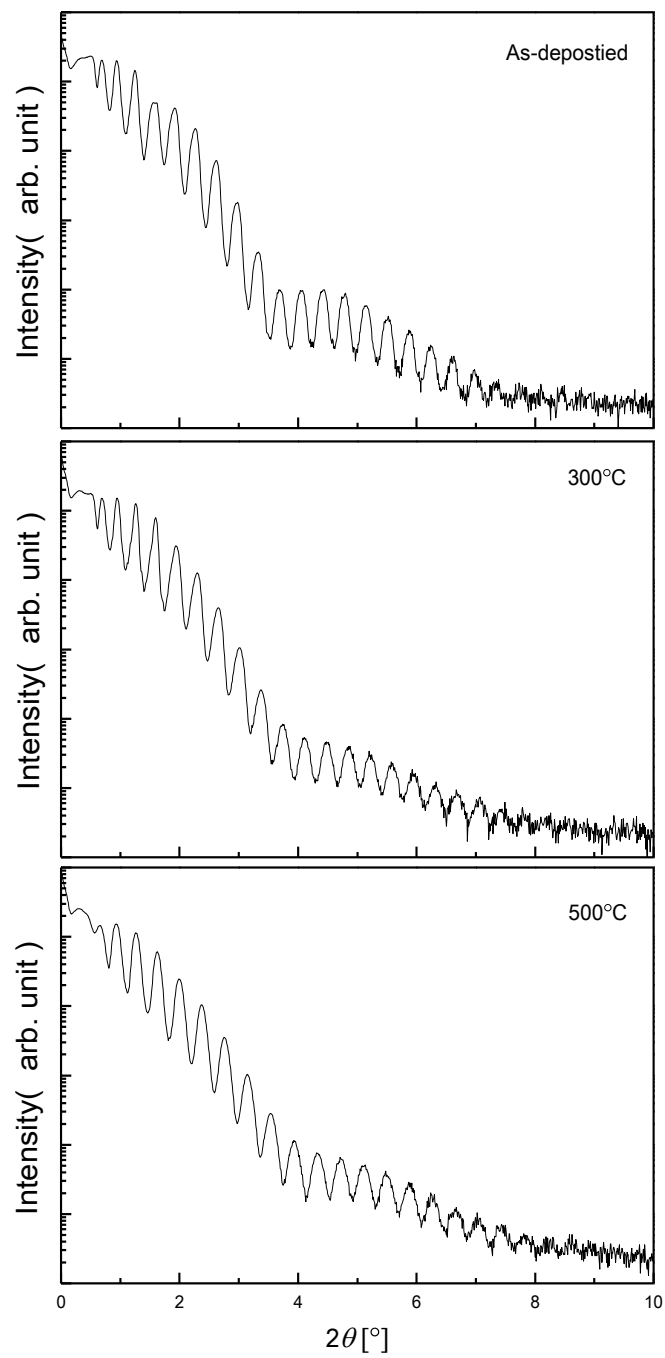Figure 4-17 In-plane stresses in FePt layers as a function of FePt layer thickness.

Figure 4-18 XRR profile of the layered structure of AlN (20nm)/[FePt (3nm)/AlN (20nm)]$_5$ annealed at different temperatures.
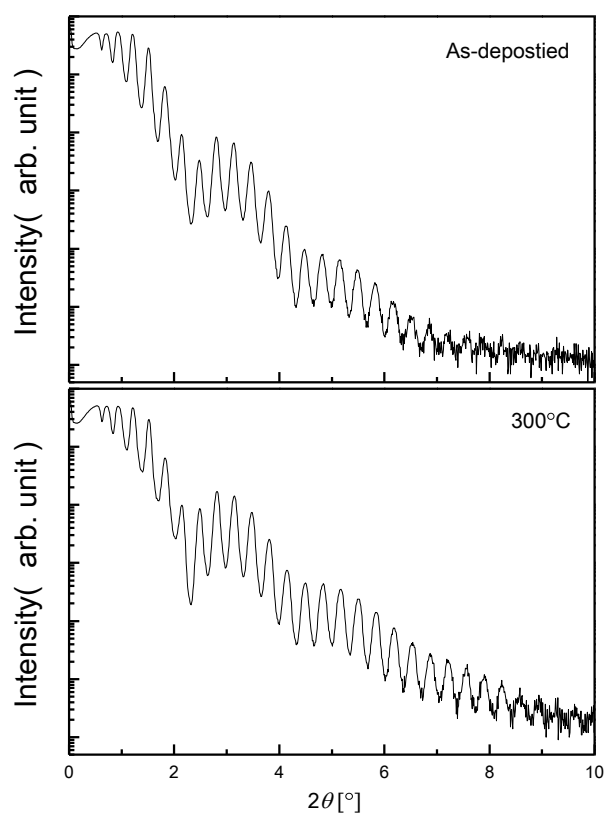
Figure 4-19 XRR profile of the as-deposited and annealed (300°C) AlN (20nm)/[FePt (5nm)/AlN (20nm)]$_5$ layered structures.
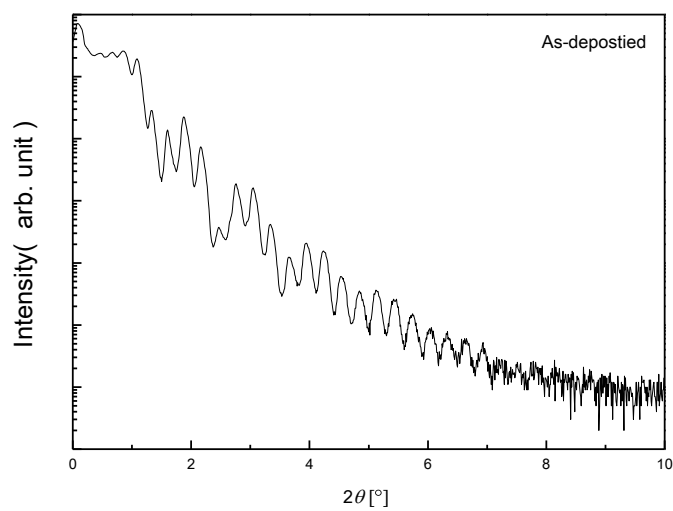

Figure 4-20 XRR profile of the as-deposited AlN (20nm)/[FePt (9nm)/AlN (20nm)]$_5$ layered structure.

Chapter 5 Influence of AlN layer thickness on the magnetic anisotropy of FePt/AlN layered structures

5.1 Introduction

By using nitride AlN layer, metal/ceramics layered structures can show better thermal stability than the metal/metal layered structures.[1] In this work, we have found that the interfacial diffusion are effectively avoided and the interface quality is improved by annealing process. In addition, the AlN layer thickness is also found to show influences on the magnetic anisotropy of FePt/AlN layered structure.

In this chapter, the influence of AlN layer thickness on the magnetic anisotropy of FePt/AlN layered structure is studed. Since we have found that the interface anisotropy strongly contributes to the perpendicular magnetic anisotropy for FePt/AlN layered structure, the emphasis of the study is placed on the effects of AlN layer thickness on the interface anisotropy.

5.2 Experimental details

FePt/AlN layered structure were sputter deposited on fused quartz substrates at ambient temperature. The base pressure prior to deposition was lower than 5×10^{-5} Pa. The sputtering gases were Ar and N_2 with a flow rate ratio of 7:3. $Fe_{0.4}Pt_{0.6}$ layers of solid solution with FCC structure were deposited at Fe-Pt target side at a rate of 0.1nm/s. AlN layers of wurtzite structure were deposited by reactive sputtering at Al target side at a rate of 0.089 nm/s. The layered structures were deposited as sub/AlN(t) nm/[FePt 2nm/AlN (t) nm]$_5$ (t = 5nm, 10nm, 20nm, 40nm). The deposited films were subsequently annealed in a vacuum condition with the pressure below 5×10^{-4} Pa at 300°C, 500°C and 700°C.

The microstructure was investigated by conventional x-ray diffraction (XRD),

X-ray reflectivity (XRR) and transmission electron microscopy (TEM). The XRD and XRR profiles were measured by a Bruker D8 Advance diffractometer with Cu K_α irradiation operating at 40kV and 300mA. The cross-sectional TEM observations were performed by a JEOL 3010 transmission electron microscope operating at a voltage of 300kV. The specimens for TEM observations were prepared by a standard procedure, i.e., mechanical thinning, followed by Ar^+ ion milling at 10.0 kV. The magnetic properties were investigated using a RIKIN BHV-50V vibrating sample magnetometer.

5.3 Magnetic properties of AlN (*t*)/[FePt (2nm)/AlN (*t*)]₅ layered structure

Figure 5-1 shows the magnetic hysteresis loops of the as-deposited AlN (*t*)/[FePt(2nm)/AlN (*t*)]₅ (*t* = 5nm, 10nm, 20nm, 40nm) layered structures. All the films show small in-plane magnetic anisotropy, and no obvious difference is found between layered structures with different AlN layer thicknesses. Figure 5-2 shows the magnetic hysteresis loops of the AlN (*t*)/[FePt(2nm)/AlN (*t*)]₅ (*t* = 5nm, 10nm, 20nm, 40nm) layered structures annealed at 300°C for 3 hours. There are crossovers at an annealing temperature of 300 °C, the magnetization behaviors in the in-plane and perpendicular directions becomes almost the same for all the films. However, it can be seen that the magnetization in perpendicular direction is slightly enhanced as the AlN layer thickness decreases. Figure 5-3 shows the magnetic hysteresis loops of the AlN (*t*)/[FePt(2nm)/AlN (*t*)]₅ (*t* = 5nm, 10nm, 20nm, 40nm) layered structures annealed at 500°C for 3 hours. As seen in this figure, all the films show perpendicular magnetic anisotropy. What is important is that the perpendicular magnetic anisotropy grows stronger significantly as the AlN layer thickness decreases. The AlN (5nm)/[FePt(2nm)/AlN (5nm)]₅ layered structure shows the strongest perpendicular magnetic anisotropy with magnetic anisotropy energy of 1.40×10^6 erg/cc, while the

magnetic anisotropy energy of AlN (40nm)/[FePt(2nm)/AlN (40nm)]$_5$ layered structure is only 0.64×10^6 erg/cc. This result is different from that of CoPt/AlN layered structure, whose optimized AlN layer thickness for high perpendicular magnetic anisotropy is 10nm.[2] Figure 5-4 shows the magnetic hysteresis loops of the AlN (t)/[FePt(2nm)/AlN (t)]$_5$ (t = 5nm, 10nm, 20nm, 40nm) layered structures annealed at 700°C for 3 hours. The 700°C annealed layered structures show similar behavior of magnetic anisotropy with the 500°C annealed layered structures. The AlN (5nm)/[FePt(2nm)/AlN (5nm)]$_5$ layered structure shows clearly perpendicular magnetic anisotropy, whereas, it changes into isotropy when the AlN layer thickness increases to 40nm.

In summary, the perpendicular magnetic anisotropy of FePt/AlN layered structure can be enhanced by decreasing the AlN layer thickness. Such AlN layer thickness effect is more obviously in the layered structures annealed at high temperature.

5.4 Interface quality analysis of AlN (t)/[FePt (2nm)/AlN (t)]$_5$ layered structure

Considering the interface anisotropy strongly depends on the interface quality, the influence of AlN layer thickness on the interface quality is studied. XRR measurements were performed to evaluate the interface quality of FePt/AlN layered structure.

Figure 5-5 shows the XRR profiles of the layered structure of AlN (t)/[FePt (2nm)/AlN (t)]$_5$ (t = 5nm, 10nm, 20nm, 40nm) annealed at 500°C. Bragg peaks which are caused by the modulation of the periodic structure can be observed in all the films, standing for the good periodicity of the layered structures. However, the layered structures with larger AlN layer thickness are found to show higher oscillation decay rate at high angles, indicating the roughness of interface increases as the AlN layer

thickness increases.[3] For quantitative comparison, simulations are performed on the AlN (5nm)/[FePt(2nm)/AlN (5nm)]$_5$ layered structure which shows strong perpendicular magnetic anisotropy and AlN (20nm)/[FePt(2nm)/AlN (20nm)]$_5$ layered structure which is studied in chapter 4. Simulations were performed by a LEPTOS software. An abrupt interface model with Debye exponent shape was used to simulate the theoretical XRR curves. Through fitting these simulative curves to the experimental curves by a Levenberg-Marquardt algorithm, the FePt/AlN interface roughness can be derived. The derived root-mean square roughnesses (R_{rms}) are 0.14nm and 0.4nm for the layered structures of AlN layer thickness 5nm and 20nm, respectively. Therefore, it is proved that the interface quality of FePt/AlN layered structure can be affected by the thickness of AlN layer.

5.5 Microstructures

Microstructures of AlN (t)/[FePt (2nm)/AlN (t)]$_5$ layered structure are also studied by conventional x-ray diffraction (XRD) and transmission electron microscopy (TEM), to disclose the mechanism of the AlN layer thickness effect.

5.5.1 X-ray diffraction results

Figure 5-6 shows the XRD profiles of the layered structure of AlN (t)/[FePt (2nm)/AlN (t)]$_5$ (t = 5nm, 10nm, 20nm, 40nm) annealed at 500°C. The layered structures with t = 5-40nm show preferred orientations with AlN [001] and FePt [111] parallel to the growth direction. As the AlN layer thickness increases, the intensity of the AlN 002 peak increases correspondingly, indicating that each AlN layer grown on the FePt layers conserves the preferred orientation. However, the most striking feature in this figure is that, the intensity of FePt 111 reflections increases significantly as the AlN layer thickness decreases, indicating the crystallinity of FePt layer strongly depends on the AlN layer thickness. In addition, for the layered structures with t =

5nm and 10nm, highly symmetrical satellite peaks are found around the main peak of FePt 111, which indicates high-quality interface and periodic structure. This result is consistent with the XRR measurement.

5.5.2 Cross-sectional TEM observation

Figure 5-7 shows the high resolution TEM images of the layered structure of AlN (t)/[FePt (2nm)/AlN (t)]$_5$ (t = 5nm and 20nm) annealed at 500°C. It can be seen in both films that the AlN grains show (002) preferred orientations. However, the AlN (5nm)/[FePt(2nm)/AlN (5nm)]$_5$ layered structure clearly shows flatter interfaces comparing to the AlN (20nm)/[FePt(2nm)/AlN (20nm)]$_5$ layered structure. In the AlN (20nm)/[FePt(2nm)/AlN (20nm)]$_5$ layered structure, we can see that the preferred orientations of the HCP AlN grains are not highly parallel to the film normal, but deviated from the film normal within a small angle. It is considered that the deviation of the preferred orientation of AlN grain from the film normal is probably the main reason for the roughness of FePt layers, because it is obviously seen that the AlN/FePt interface is rougher than the FePt/AlN interface. For the AlN (5nm)/[FePt(2nm)/AlN (5nm)]$_5$ layered structure, the AlN layer shows good crystallinity with smaller deviation, then resulting in a AlN/FePt interface with smaller roughness. Such flat AlN/FePt interface can give positive effect on the growth of (111) texture of the subsequent FePt layer. Therefore, we believe that the flattening of interface is responsible for the high intensity of FePt 111 reflections found in the layered structures with small AlN layer thickness.

5.6 Discussions on the mechanism of AlN layer thickness effect

According to the results of XRR measurement and TEM observation, we have found that the layered structures with smaller AlN layer thickness show flatter interfaces. Since the interface roughness can affect the interface magnetic anisotropy

as discussed in chapter 4, the interface anisotropy can be enhanced as the interface roughness decreases and then promote the perpendicular magnetic anisotropy for the layered structures with smaller AlN layer thickness. On the other hand, the crystallinity of FePt layer may also show influences on the interface anisotropy. Engel et al.[4] reported that for a system of epitaxially grown Co/Pd superlattices, the interface magnetic anisotropy is positive, large, and orientation independent. Thus, distinctions in anisotropy between superlattices with interfaces in the (111), (100), and (011) directions arise only from magnetostriction and the small bulk Co anisotropy. These results are surprising since the three interfaces involved have very different geometries and atomic areal densities and because previous experiments on Co/Pt and Co/Pd did not display the effect. Later, Victora et al.[5] suggested that this surprising "orientation independence" of the Co/Pd interface anisotropy found experimentally is an accidental consequence of the precise degree of strain exhibited by this system and is not generally expected. Under a specific strain condition, they obtained the same interface anisotropy in Co/Pd layered structures with interfaces in the (111) and (100) directions. However, this result did not persist in the unstrained layered structures. Thus, they suggested that strain was crucial in obtaining the orientation independence, i.e., the orientation independence only occurs if the strain is fortuitously chosen. For the FePt/AlN layered structure, it is found that the strain/stress inside FePt layer can be altered through annealing. The strain/stress condition of the annealed layered structure may result in an orientation dependent interface anisotropy, which can be enhanced as the crystallinity of FePt (111) texture improves. Therefore, the AlN layer thickness effect is more obviously in the annealed layered structures.

5.7 Summary

In this chapter, the influences of AlN layer thickness on the magnetic properties of FePt/AlN layered structure have been studied. It is found that the perpendicular magnetic anisotropy of FePt/AlN layered structure can be enhanced by decreasing the AlN layer thickness. The AlN (5nm)/[FePt(2nm)/AlN (5nm)]$_5$ layered structure annealed at 500°C shows strong perpendicular magnetic anisotropy with magnetic anisotropy energy of 1.40×10^6 erg/cc. According to the results of microstructure analysis, such enhancement of perpendicular magnetic anisotropy is attributed to the decrease of interface roughness and the improvement of FePt crystallinity, as the AlN layer thickness decreases.

References

1. Y. Hodumi, J. Shi, Y. Nakamura, Appl. Phys. Lett. 90, 212506(2007).

2. Y. Yu, Y. Hodumi, J. Shi, and Y. Nakamura, Vacuum 84, 158 (2009).

3. M. Yasaka, The Rigaku Journal 26 (2), 2010.

4. B. N. Engel, C. D. England, R. A. Van Leeuwen, M. H. Wiedmann, and C. M. Falco, Phys. Rev. Lett. 67, 1910 (1991).

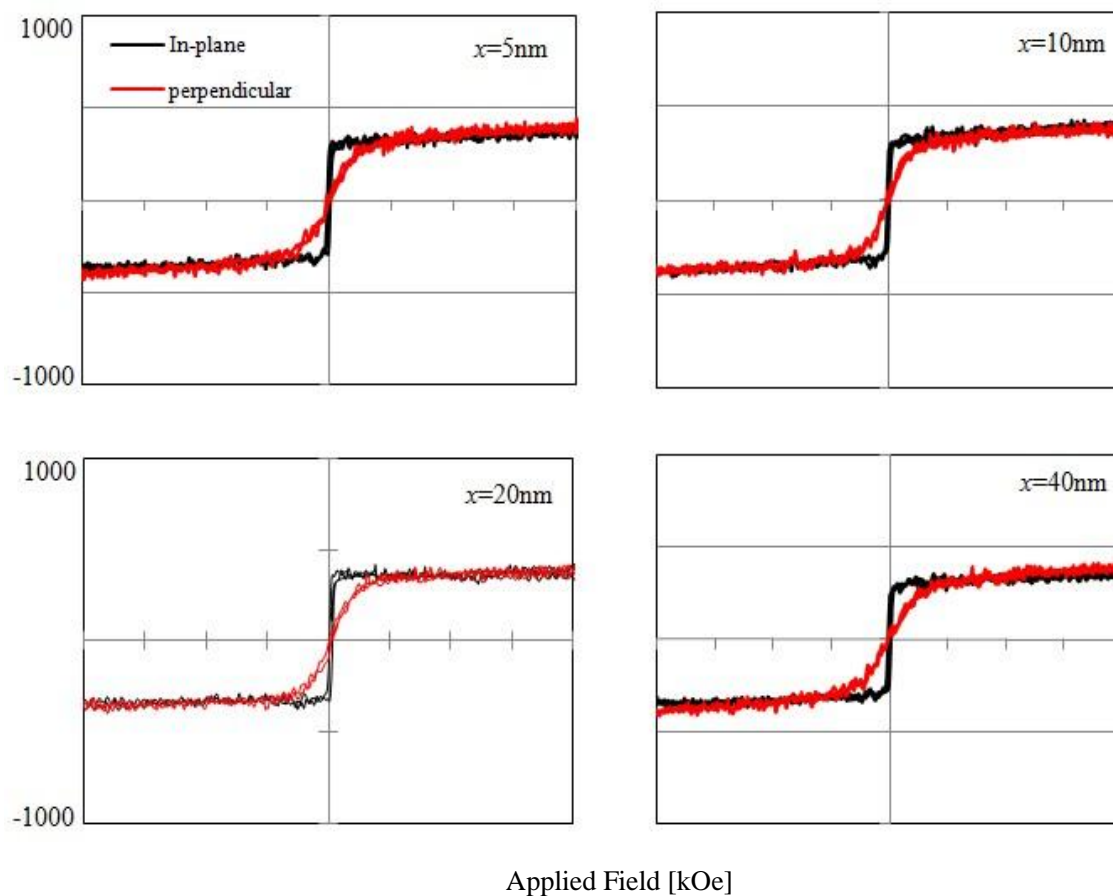5. R. H. Victora, J. M. MacLaren, Phys. Rev. B 47, 11583 (1993).

Applied Field [kOe]

Figure 5-1 Magnetic hysteresis loops of the as-deposited AlN (*t*)/[FePt(2nm)/AlN (*t*)]$_5$ (*t* = 5nm, 10nm, 20nm, 40nm) layered structures.

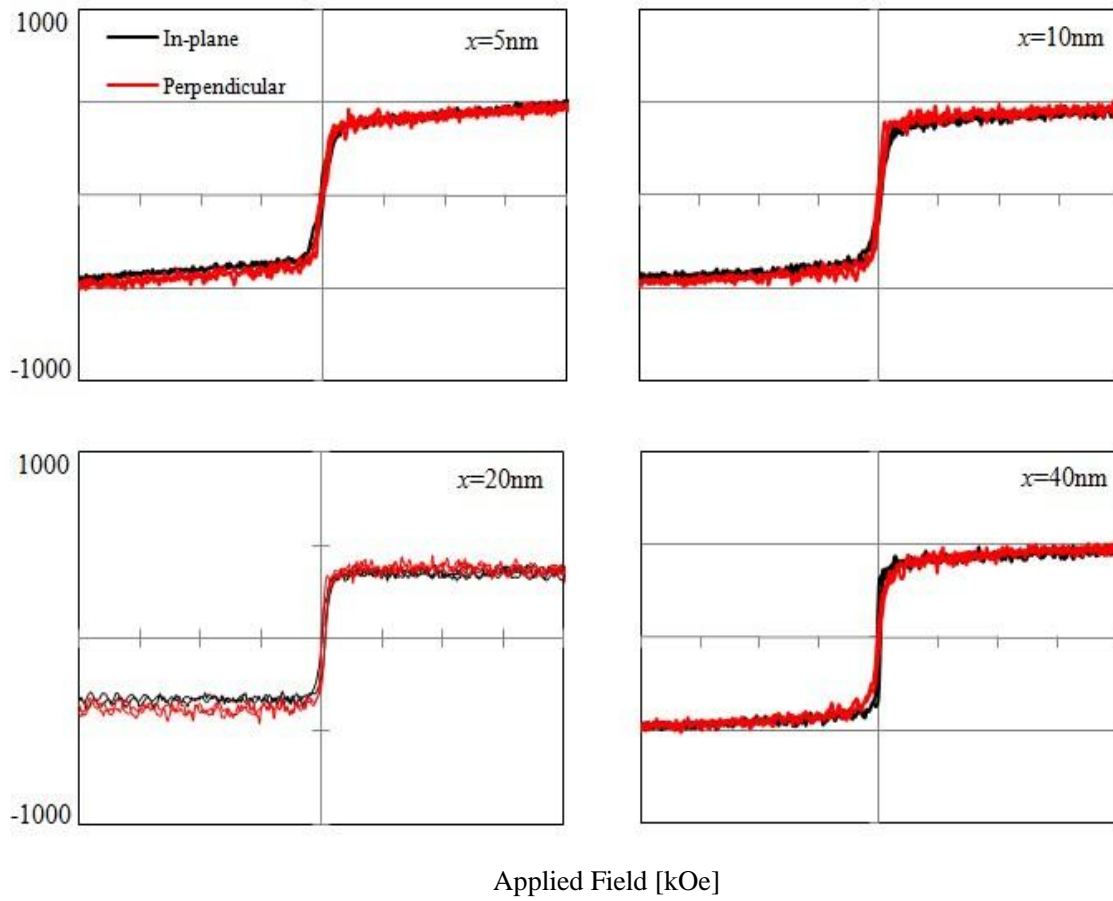Applied Field [kOe]

Figure 5-2 Magnetic hysteresis loops of the AlN (*t*)/[FePt(2nm)/AlN (*t*)]$_5$ (*t* = 5nm, 10nm, 20nm, 40nm) layered structures annealed at 300°C for 3 hours.
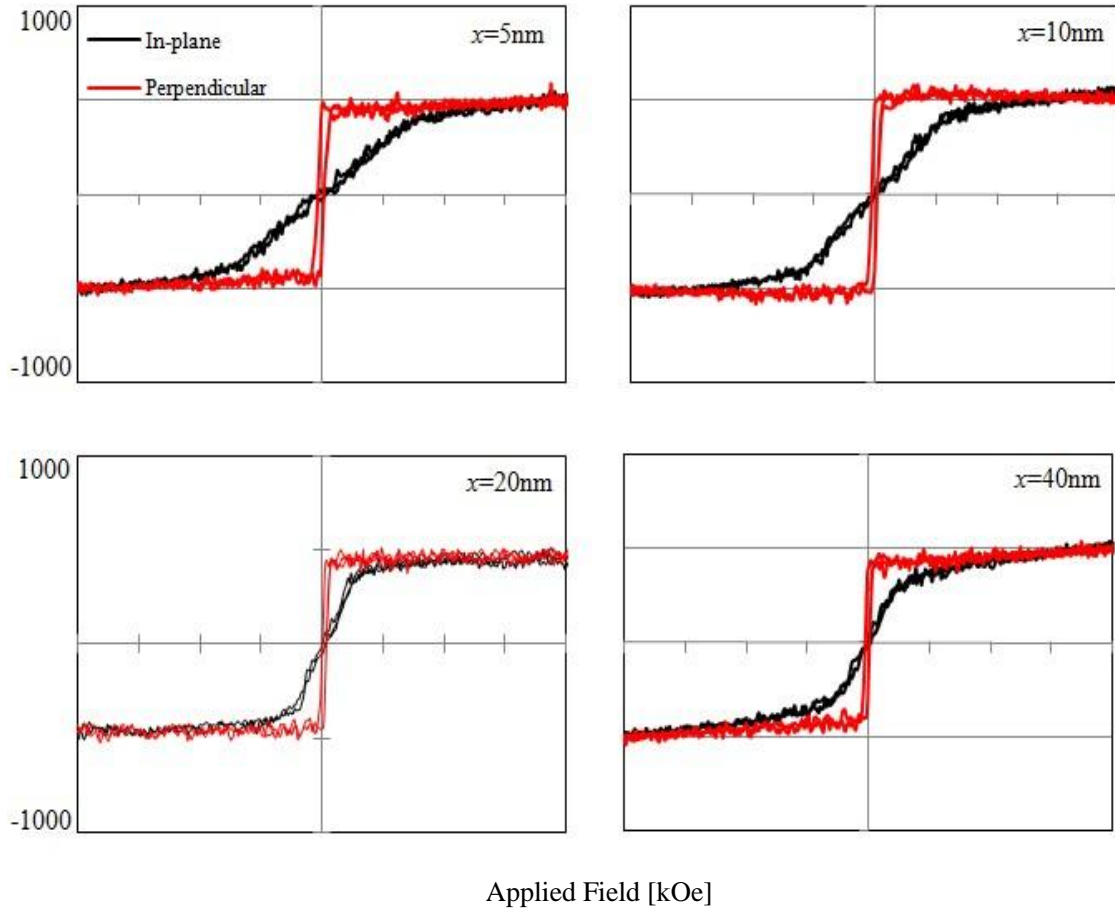
Applied Field [kOe]

Figure 5-3 Magnetic hysteresis loops of the AlN (*t*)/[FePt(2nm)/AlN (*t*)]$_5$ (*t* = 5nm, 10nm, 20nm, 40nm) layered structures annealed at 500°C for 3 hours.
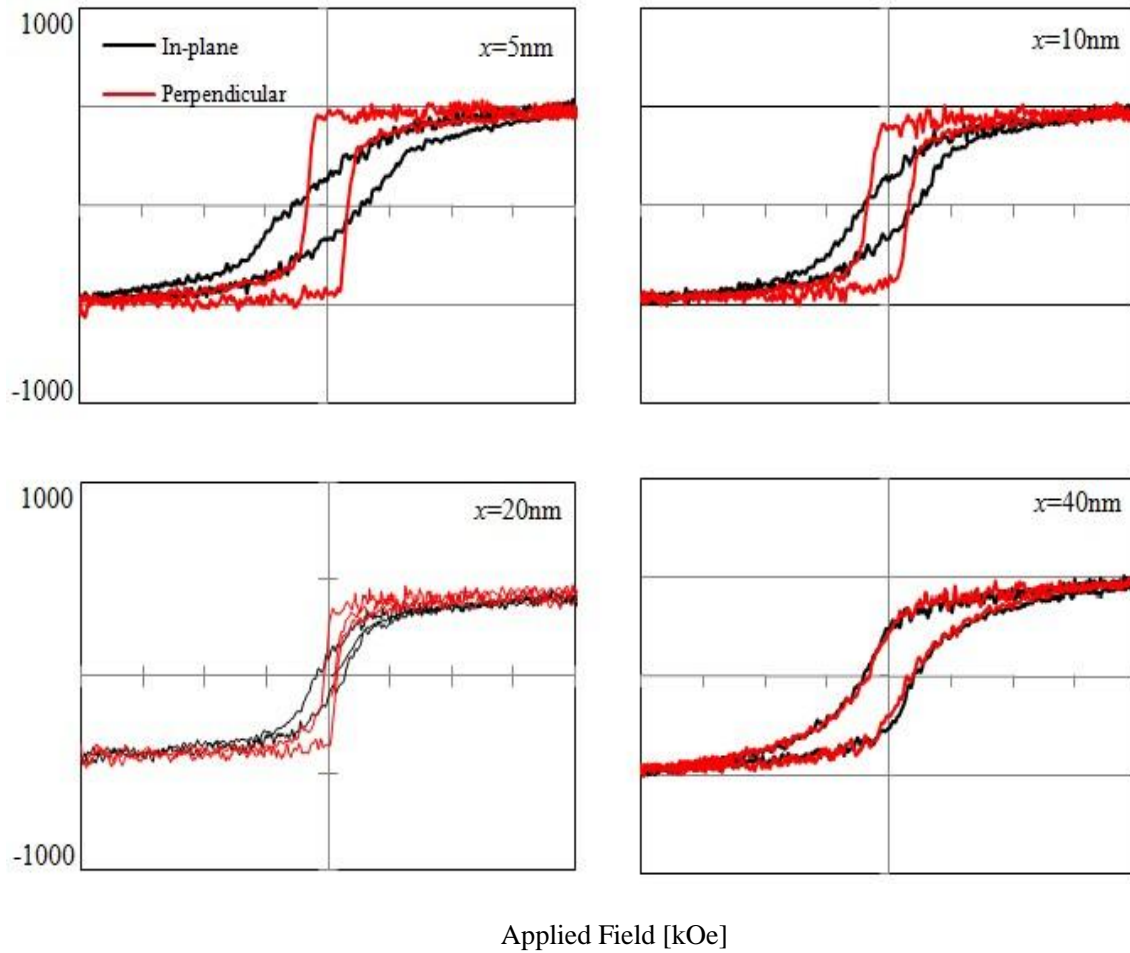
Applied Field [kOe]

Figure 5-4 Magnetic hysteresis loops of the AlN (t)/[FePt(2nm)/AlN (t)]$_5$ (t = 5nm, 10nm, 20nm, 40nm) layered structures annealed at 700°C for 3 hours.
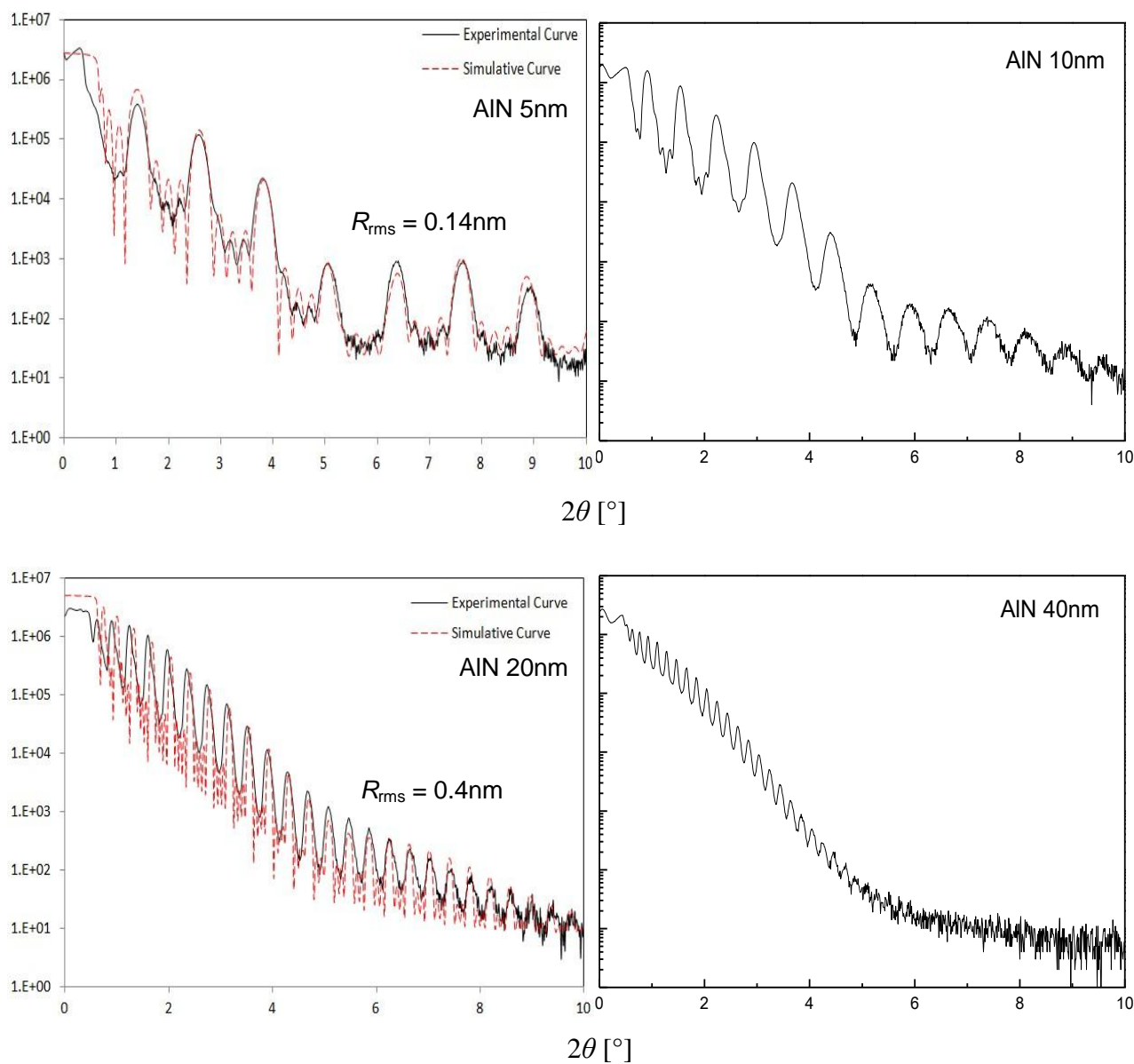
Figure 5-5 XRR profiles of the layered structure of AlN (*t*)/[FePt (2nm)/AlN (*t*)]$_5$ (*t* = 5nm, 10nm, 20nm, 40nm) annealed at 500°C.
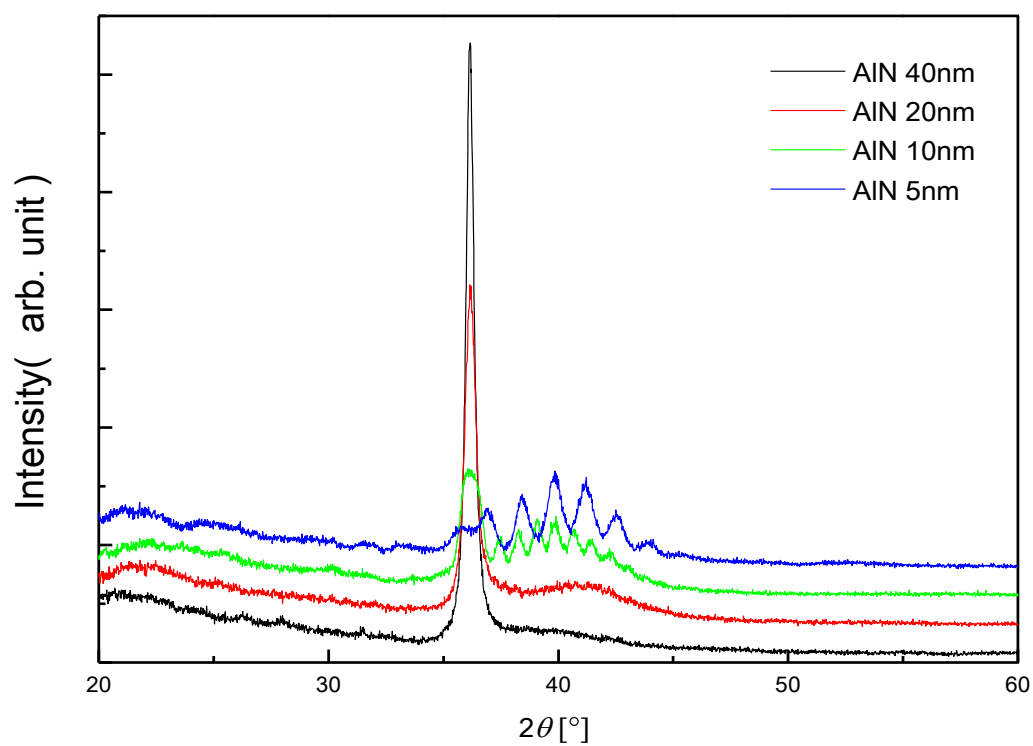
Figure 5-6 XRD profiles of the layered structure of AlN (t)/[FePt (2nm)/AlN (t)]$_5$ (t = 5nm, 10nm, 20nm, 40nm) annealed at 500°C.
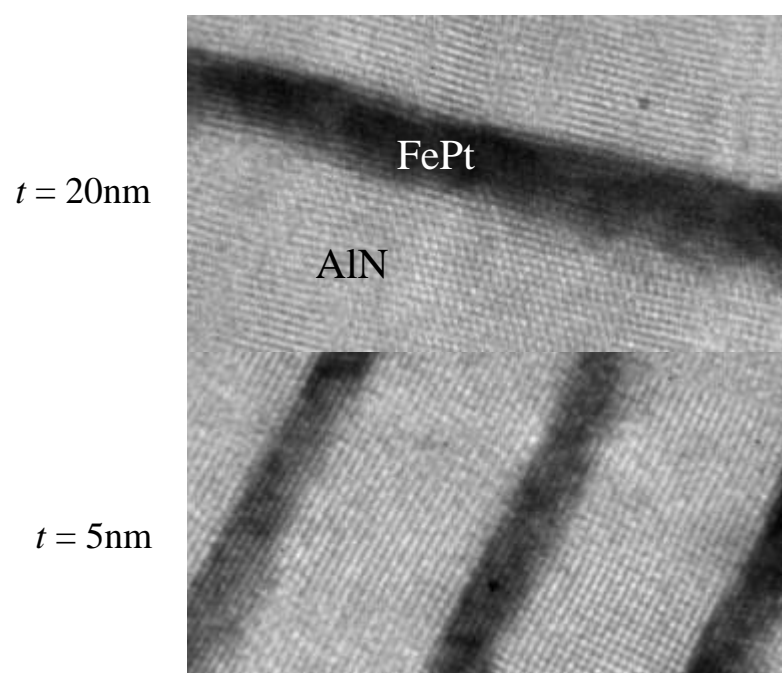
Figure 5-7 TEM images of AlN (t)/[FePt (2nm)/AlN (t)]$_5$ layered structures (t = 5nm and 20nm) annealed at 500°C.

Chapter 6 Conclusions

The magnetic anisotropy transition of FePt/AlN layered structure has been studied in this thesis. The FePt/AlN layered structures were fabricated by DC magnetron sputtering using quartz glass substrate. The magnetic properties of FePt/AlN layered structure have been systematically studied by varying annealing temperature, FePt layer thickness and AlN layer thickness. To disclose the origin of perpendicular magnetic anisotropy in annealed layered structure and the mechanism of magnetic anisotropy transition, microstructures, residual stress and interface quality of the FePt/AlN layered structure have been investigated. The experimental results are summarized, and the conclusions of this thesis are made as following.

The FePt/AlN layered structures with good periodicity and accurate layer thickness are successfully fabricated. The as-deposited layered structure shows weak in-plane magnetic anisotropy (the easy direction of magnetization is along the film plane) comparing to the FePt single layer film, indicating the formation of layered structure can favor the magnetization in perpendicular direction. As the FePt layer thickness increases, the in-plane magnetic anisotropy of layered structure is enhanced.

The magnetic anisotropy of FePt/AlN layered structure can be altered through annealing. For layered structure with small FePt layer thickness, it is found that the easy magnetization direction gradually changes from in-plane direction to perpendicular direction as annealing temperature increases. The AlN 20nm/(FePt2nm/AlN10nm)$_5$ layered structures annealed at 600°C show strong perpendicular magnetic anisotropy (the easy direction of magnetization is along the film normal) with magnetic anisotropy energy of 1.06×10^6 erg/cc. As the FePt layer thickness increases, the annealed layered structures undergo a transition of magnetic anisotropy from perpendicular to in-plane direction. However, in contrary to the

layered structure with thin FePt layer, the in-plane magnetic anisotropy of layered structures with larger FePt layer thickness is enhanced with the increase of annealing temperature. It seems that 5nm is the critical FePt layer thickness for the different annealing effects.

The interface quality analysis shows that the interface quality of FePt/AlN layered structure is improved by annealing. The flattening of interface can strongly enhance the Néel-type interface anisotropy and promote the magnetization in perpendicular direction. On the other hand, according to the stress analysis we find the residual stresses inside FePt layer turn from compressive to tensile as annealing temperature increases. With a positive magnetostriction constant, this will decrease the positive magnetoelastic energy which can contribute to the perpendicular magnetic anisotropy. In conclusion, FePt/AlN layered structures show strong interface anisotropy, which is the main origin of perpendicular magnetic anisotropy in FePt/AlN layered structures.

The effective magnetic anisotropy energies K_{eff} of the FePt/AlN layered structures with different FePt layer thicknesses and annealing temperatures have been calculated. The effective magnetic anisotropy energy K_{eff} (erg/cm^3) is phenomenologically separated in a volume contribution K_V (erg/cm^3) and an extra interface contribution K_S (erg/cm^2). Because of the large lattice misfit between FePt and AlN layer, it is reasonable to consider that K_S is solely Néel-type interface anisotropy and the magnetoelastic anisotropy is part of K_V. The K_S is gradually enhanced by annealing and shows a value of 0.4 erg/cm^2 in the layered structures annealed at 500°C, indicating the perpendicular magnetic anisotropy of the annealed FePt/AlN layered structure is mainly from the interface anisotropy. Therefore, for layered structures with FePt layer thickness below 5nm, although the relief of compressive stress caused by annealing will decrease the perpendicular (positive)

magnetoelastic anisotropy as discussed above, the enhanced interface anisotropy becomes dominant then K_{eff} of annealed films increases. When the FePt layer is thick, the contribution from K_S (interface anisotropy) is relatively small according to the equation of $K_{eff} = K_V + 2K_S/t$, and tensile stresses developed during annealing will result in a negative magnetoelasitc anisotropy which overwhelms the interface anisotropy, thus decreases K_{eff}. Therefore, in this work, we have proved that Fe40Pt60 alloy has positive magnetostriction coefficient, and the magnetic metal/nitride layered structures can show strong interface anisotropy. For FePt alloy, such interface anisotropy can overcome the magnetoelastic effect below a critical thickness for FePt layer.

The FePt layer thickness dependence of K_{eff} can be explain by the decrease of contribution from K_S as FePt layer thickness increases, i.e., the lowering of interface/volume atomic ratio. Moreover, the stress measurement results show that the internal stresses in the FePt layers change from compressive to tensile with the increase of FePt layer thickness. The introduction of tensile stress can give negative contribution to K_V in the form of magnetoelastic anisotropy and favor the in-plane magnetization.

The perpendicular magnetic anisotropy of FePt/AlN layered structure can also be enhanced by decreasing the AlN layer thickness. The AlN(5nm)/[FePt(2nm)/AlN (5nm)]$_5$ layered structure annealed at 500°C shows strong perpendicular magnetic anisotropy with magnetic anisotropy energy of 1.40×10^6 erg/cc. According to the results of microstructure analysis, such enhancement of perpendicular magnetic anisotropy is attributed to the decrease of interface roughness and the improvement of FePt crystallinity, as the AlN layer thickness decreases.

Publications

List of Papers

1. C. Zhang, R. Tajima, T. Sannomiya, S. Muraishi, Y. Nakamura, J. Shi, Magnetic Behavior of FePt/AlN Layered Structure, Mater. Trans., Accepted.

2. C. Zhang, T. Sannomiya, S. Muraishi, J. Shi, Y. Nakamura, Perpendicular magnetic anisotropy in FePt/AlN layered structure, Appl. Phys. A, Accepted.

3. C. Zhang, T. Sannomiya, S. Muraishi, J. Shi, Y. Nakamura, Effects of AlN layer thickness on magnetic anisotropy of FePt/AlN layered structure, in preparation.

List of Presentations

1. C. Zhang, J. Shi and Y. Nakamura. Preparation and characterization of FePt/AlN layered structure. Joint Symposium of Tokyo Institute of Technology-Dalian University of Technology, Tokyo, Japan, November 2011.

2. C. Zhang, J. Shi and Y. Nakamura. Effects of Annealing Temperature on Magnetic Anisotropy of FePt/AlN Layered Structure. The 8th International Forum on Advanced Materials Science and Technology, Fukuoka, Japan, August 2012.

3. C. Zhang, J. Shi and Y. Nakamura. Magnetic anisotropy of FePt/AlN layered structure. Joint Symposium of Tokyo Institute of Technology-Dalian University of Technology, Dalian, China, September 2012.

4. C. Zhang, J. Shi and Y. Nakamura. Perpendicular Magnetic Anisotropy in FePt/AlN Layer Structure. The First International Education Forum on Environment and Energy Science, Hawaii, USA, December 2012.

5. C. Zhang, J. Shi, Y. Nakamura, S. Muraishi, T. Sannomiya. Transition of

Magnetic Anisotropy in FePt/AlN Layered Structure. 19th International Vacuum Congress, Paris, France, September 2013.

6. C. Zhang, T. Sannomiya, S. Muraishi, Y. Nakamura, J. Shi, Magnetic Behavior of FePt/AlN Layered Structure. Annual Meeting of Japan Institute of Metals, September 2013.

Acknowledgements

This work is possible only with the help and support of lots of people during the course of my study. First of all, I would like to thank my supervisor, Professor J. Shi, for the given opportunity to join his group, and his untiring teaching and supervision throughout my study. From time to time his insight into in problems has given clues on many possible directions of progress of the project. I would also like to thank my advisor, the head of the group, Professor Y. Nakamura, for several occasions of useful discussions and giving me explanations on TEM and XRR. Moreover, His knowledge on the analysis of stress really gives me edification.

I would like to thank Assistant Professor S. Muraishi for helping me using instruments. His valuable contribution made my work possible.

I also have to thank Assistant Professor T. Sannomiya for helping me operating TEM. Without his patient explanations, I could not get used to TEM.

Thanks to Mr. R. Tajima for his cooperation on my work. The days we working together are my precious memory. Special thanks are given to Mr. Y. Tazaki for his helps at the beginning of my life in Japan. Daily laboratory work is enjoyable and yet challenging, and I would like to thank all the other members of Nakamura-Shi Laboratory for their assistance that facilitated the work.

Thanks to Mr. Y. Suzuki of the Analysis Center of Tokyo Tech for their helps in using the analysis instruments.

I greatly appreciate Professor Susa, Professor Kobayashi and Professor Fujii for being on my thesis committee.

There are three people in particular to whom I would like to express my deepest thanks and love for their endless support. My parents have been extremely

understanding and constantly supportive towards my study. Their encouragement and attention has brought me through many of the difficult times in these days. And also my fiancee. Without her understanding and encouragement, I think, my heart could not remain strong to complete my work.